



universität
wien

DISSERTATION

Titel der Dissertation

„Control of self-renewal and cell fate in *Drosophila*
neural stem cell lineages“

Verfasser

Vivien ROLLAND, MSc.

angestrebter akademischer Grad

Doktor der Naturwissenschaften (Dr.rer.nat.)

Wien, 2012

Studienkennzahl lt. Studienblatt: A 091 490

Dissertationsgebiet lt. Studienblatt: Dr.-Studium der Naturwissenschaften Molekulare Biologie

Betreuerin / Betreuer: Dr Jürgen KNOBLICH

TABLE OF CONTENTS

1. SUMMARY	5
2. ZUSAMMENFASSUNG	6
3. GENERAL INTRODUCTION	8
3.1. MODES OF ASYMMETRIC CELL DIVISION IN <i>DROSOPHILA MELANOGASTER</i>.....	8
3.1.1. Extrinsic model.....	8
3.1.2. Intrinsic model.....	10
3.2. NEUROBLAST POPULATIONS IN <i>DROSOPHILA</i>	10
3.2.1. Embryonic neuroblasts.....	10
3.2.2. Larval neuroblasts.....	10
3.3. MECHANISM OF ASYMMETRIC CELL DIVISION IN <i>DROSOPHILA</i> NEUROBLASTS	11
3.3.1. Cell fate determinants	11
3.3.2. Role of the Par complex.....	13
3.3.3. Asymmetric segregation of cell fate determinants.....	14
3.3.4. Control of spindle alignment.....	14
3.4. <i>DROSOPHILA</i> NEUROBLAST ASYMMETRIC DIVISION AND TUMORIGENESIS.....	15
3.4.1. Connection between ACD and tumor formation	15
3.4.2. The <i>Drosophila</i> larval neuroblast as a model for cancer cell biology.....	15
3.5. STRUCTURE AND AIM OF THIS STUDY	17
4. CHAPTER I – THE TUMOR SUPPRESSORS BRAT AND NUMB REGULATE TRANSIT-AMPLIFYING NEUROBLAST LINEAGES IN <i>DROSOPHILA</i>	18
4.1. CONTRIBUTIONS	18
4.2. INTRODUCTION.....	18
4.3. RESULTS.....	19
4.3.1. <i>brat</i> overgrowth originates in <i>Ase</i> ⁻ neuroblast lineages.....	19
4.3.2. PAN lineages produce intermediate progenitors	22
4.3.3. PAN lineages contain transit-amplifying secondary neuroblasts	24
4.3.4. <i>brat</i> secondary neuroblasts fail to progress beyond the immature <i>Ase</i> ⁻ state.....	30
4.3.5. Immature <i>Ase</i> ⁻ secondary neuroblasts enter mitosis in <i>brat</i>	31
4.3.6. Notch signaling regulates secondary neuroblasts in PAN lineages	32
4.3.7. Prospero acts after Brat and Numb in the PAN lineage	33
4.4. DISCUSSION	36
4.4.1. <i>Ase</i> and transit-amplifying neuroblast lineages.....	36
4.4.2. Numb, Brat, Pros, and transformation of progenitor cells	37
4.5. EXPERIMENTAL PROCEDURES.....	40
4.6. SUPPLEMENTARY DATA	41

5. CHAPTER II – CHARACTERIZATION OF BARRICADE, A NOVEL REGULATOR OF LARVAL NEUROBLAST LINEAGES	52
5.1. INTRODUCTION.....	52
5.1.1. Type 1 and type 2 neuroblast lineages	52
5.1.2. Searching for novel regulators of neuroblast lineages: Identification of <i>barricade</i>	54
5.1.3. The Barc/Tat-SF1/CUS2 family of proteins: Structure and functions.....	58
5.2. RESULTS.....	66
5.2.1. Phenotypical analysis of <i>barc</i> knock down in larval brains	66
5.2.2. Characterization of Barc expression pattern	76
5.2.3. Generation of a <i>barc</i> mutant and of rescue constructs.....	78
5.2.4. Study of the molecular function of Barc	84
5.3. DISCUSSION	96
5.3.1. Summary	96
5.3.2. Making INPs: Step by step	96
5.3.3. Loss of Barc and tumor formation	97
5.3.4. The Barc/Tat-SF1/CUS2 family of proteins: functional evolution?.....	98
5.3.5. Transcriptional elongation and regulation of neuroblast lineages	99
5.4. EXPERIMENTAL PROCEDURES.....	102
5.5. CONTRIBUTIONS	111
6. REFERENCES.....	112
7. CURRICULUM VITAE.....	125
8. ACKNOWLEDGMENTS	127

1. SUMMARY

Stem cells need to control the balance between proliferation and generation of differentiated cells in order to produce functional lineages. Studying the mechanisms that regulate this equilibrium is particularly relevant since defects in this balance can lead to tumorigenesis. We use the asymmetrically dividing *Drosophila* larval neuroblasts as a model to study how stem cells self-renew and form specific lineages.

Larval neuroblasts of the central brain were thought to form rather simple lineages composed of a single stem cell (neuroblast) and of a few differentiating cells (ganglion mother cells – GMCs – and neurons). Here, we present a previously uncharacterized type of larval neuroblast that produces transit-amplifying cells, called secondary neuroblasts or Intermediate Neural Progenitors (INPs), which then produce GMCs and neurons. Additionally, we show that the lineages formed by these rare neuroblasts are particularly important because they produce a very large amount of neurons and are very sensitive to tumor formation.

Before INPs can divide to produce GMCs, they need to mature – a process characterized by the successive expression of two transcription factors. To get a better understanding of INP biology, we made use of a genome-wide RNA interference (RNAi) screen, conducted specifically in *Drosophila* larval neuroblast lineages. In this screen, several genes led to overproliferation of progenitors upon knock down. Among them was the previously unstudied gene *CG6049/barricade (barc)*. In this study, we characterize *barc* and show that it is important in neuroblast lineages for the production of neurons. Additionally, we show that upon *barc* RNAi knock down, most INPs remain in an immature state, demonstrating that Barc is a novel regulator of INPs. Barc is a nuclear protein composed of two RNA recognition motifs (RRMs) and a Barc/Tat-SF1 motif (BTS). Here, we show that only the second RRM of Barc is dispensable for the function of the protein in larval neuroblast lineages. Additionally, we demonstrate that Barc associates with DNA *in vivo*. Barc is the homologue of human Tat-SF1 and yeast CUS2, two proteins that are involved in transcription elongation and splicing. To test whether Barc acts in a similar way, we established a cell culture system where we can efficiently knock down Barc and from which we prepared libraries of short capped RNAs and mRNAs. Analysis of these libraries will allow us to determine whether Barc acts by regulating transcription elongation and/or splicing. Finally, we generated a mutant allele and several rescue constructs that will enable us to study the effect of *barc* on cell cycle and cell fate, to identify the binding partners of Barc and to determine its binding pattern on DNA.

2. ZUSAMMENFASSUNG

Eine einzige Stammzelle ist in der Lage eine komplette Zelllinie bestehend aus mehreren differenzierten Tochterzellen zu generieren. Um dies zu ermöglichen muss die Stammzelle das Gleichgewicht zwischen Selbsterneuerung und Differenzierung bewahren. Die Regulierung dieses Gleichgewichts ist sehr komplex und unterliegt einer sehr strengen Kontrolle. Geht dieses Gleichgewicht verloren, können Tumore entstehen. Deswegen ist es wichtig, jene Mechanismen zu verstehen, welchen die komplexe Regulierung dieses Gleichgewichts unterliegt. In dieser Studie untersuchen wir neuronale Stammzellen, sogenannte Neuroblasten, aus dem larvalen zentralen Nervensystem der *Drosophila*. Neuroblasten teilen sich asymmetrisch und können sich somit selbst erneuern und gleichzeitig differenzierte Tochterzellen generieren.

Es wurde ursprünglich angenommen, dass Neuroblasten sehr „einfache“ Zelllinien generieren, welche aus einer Stammzelle (Neuroblast) und einigen wenigen differenzierten Zellen (Ganglion-Mutterzellen und Neuronen) bestehen. Diese Studie beschreibt einen bisher uncharakterisierten Neuroblastentyp, welcher zunächst intermediäre Vorläuferneuronen generiert aus denen anschließend die Ganglion-Mutterzellen und Neuronen hervorgehen. Aufgrund dieser Vorläuferneuronen, welche ebenso wie die Neuroblasten die Fähigkeit besitzen sich selbst zu erneuern, können sehr viel mehr Neuronen in kurzer Zeit generiert werden. Jedoch ist diese Art von Neuroblast genetisch instabiler und somit sehr viel sensibler in Bezug auf die Ausbildung von Tumoren.

Bevor sich intermediäre Vorläuferneuronen teilen und Ganglion-Mutterzellen generieren, durchlaufen sie eine Art Reifeprozess. Dieser Reifeprozess zeichnet sich durch die sukzessive Expression zweier Transkriptionsfaktoren aus. Um die Biologie hinter diesen Vorläuferneuronen besser zu verstehen, führten wir innerhalb der Neuroblast-Zelllinien eine genomweite Mutantenklassifizierung durch, wobei wir uns hierfür die RNA-Interferenz (RNAi) Bibliothek zu Nutzen machten. Es konnten Gene identifiziert werden, welche bei Funktionsverlust zu einer vermehrten Anzahl von Neuroblasten führten. Darunter befand sich ebenfalls das bisher unbekanntes Gen CG6049/Barricade (*barc*). Diese Studie befasst sich mit der Charakterisierung von *Barc* und zeigt dessen wichtige Bedeutung innerhalb der Neurogenese. Wird *Barc* mittels RNAi herunter reguliert, verweilen intermediäre Vorläuferzellen in einem unreifen Stadium, anstatt den Reifeprozess vollständig zu durchlaufen, um anschließend Neuronen zu generieren. Somit ist *Barc* ein neu identifizierter Regulator intermediärer Vorläuferzellen. *Barc* ist ein Kernprotein, welches zwei RNA

Erkennungsmotive und ein Barc/Tat-SF1 Motiv besitzt. Wir zeigen, dass, für die Funktion von Barc innerhalb der intermediären Vorläuferzellen, nur ein RNA Erkennungsmotiv notwendig ist. Ebenso demonstrieren wir *in vivo*, dass Barc mit der DNS interagiert. Barc ist das homologe Gen des humanen Tat-SF1 und dem CUS2 Gen aus Hefe. Beiden Genen konnte eine Rolle in der transkriptionalen Elongation und des RNA-Spleißmechanismus zugewiesen werden. Um festzustellen ob Barc eine ähnliche Funktion ausübt, etablierten wir ein Zellkultursystem, in welchem wir Barc zunächst effizient ausschalten konnten und anschließend eine Bibliothek von ‚short-capped‘ RNAs bzw. mRNAs herstellten. Die nähere Untersuchung dieser Bibliotheken wird uns Aufschluss darüber geben, ob und inwiefern Barc eine Rolle in der Regulierung der transkriptionalen Elongation und/oder des RNA-Spleißmechanismus spielt. Ebenso generierten wir ein mutantes *barc* Allel und verschiedene transgene Barc-Konstrukte, mittels welcher wir die Funktion von Barc detaillierter analysieren können. Mit Hilfe dieser Konstrukte können wir zum einen untersuchen, ob Barc einen Einfluss auf den Zellzyklus oder das Zellschicksal hat, zum anderen helfen sie uns, um Interaktionspartner von Barc zu identifizieren oder um das Barc-DNA Interaktionsmuster zu entschlüsseln.

3. GENERAL INTRODUCTION

Development is the process whereby the zygote of a multicellular organism generates and precisely organizes into tissues and organs all cells of the forming and adult being. This challenging enterprise requires the tightly regulated production of a very large number of cell types that can be as different from each other as a neuron, a spermatozoid or a muscle cell. Stem cells play an important role in generating this cellular diversity during development and maintaining it in adult organisms. They are defined by their ability to self-renew and to generate daughter cells committed to differentiation. In other words, they have the capacity to divide asymmetrically, generating two cells with different fates.

Over the last couple of decades, the fruit fly *Drosophila melanogaster* has emerged as a key model organism for studying development and has been instrumental in deciphering mechanisms of asymmetric divisions of stem cells and stem cell-like progenitors. In *Drosophila*, these cells can be found in a variety of tissues during the four successive phases of its life cycle: embryogenesis, larval stages, pupal stages – during which the larva undergoes metamorphosis, and adulthood.

The first part of this general introduction presents the different modes of asymmetric cell division (ACD) in *Drosophila*. The second one focuses on neuroblasts, one of the best-characterized models for ACD. The third one describes the basic mechanisms of ACD, while the final part summarizes evidences for the connection between defects in ACD and tumorigenesis in *Drosophila*.

3.1. MODES OF ASYMMETRIC CELL DIVISION IN *DROSOPHILA MELANOGASTER*

In *Drosophila*, ACD can be governed by either extrinsic or intrinsic cues (Fig. 1) (Knoblich, 2008). These two different modes of ACD are explained in the following paragraphs.

3.1.1. Extrinsic model

The cell-extrinsic mode relies on a signal coming from surrounding cells forming the so-called niche (Fig. 1A). This signal maintains the stem cell in a self-renewing state. Additionally, the niche signal sets up an axis of polarity ensuring that upon division the stem cell divides into a cell that remains in contact with the niche and a cell that moves away from it. While the cell remaining in contact with the niche maintains stem cell properties, the cell that moves away from the niche does no longer receive the signal and adopts a differentiating

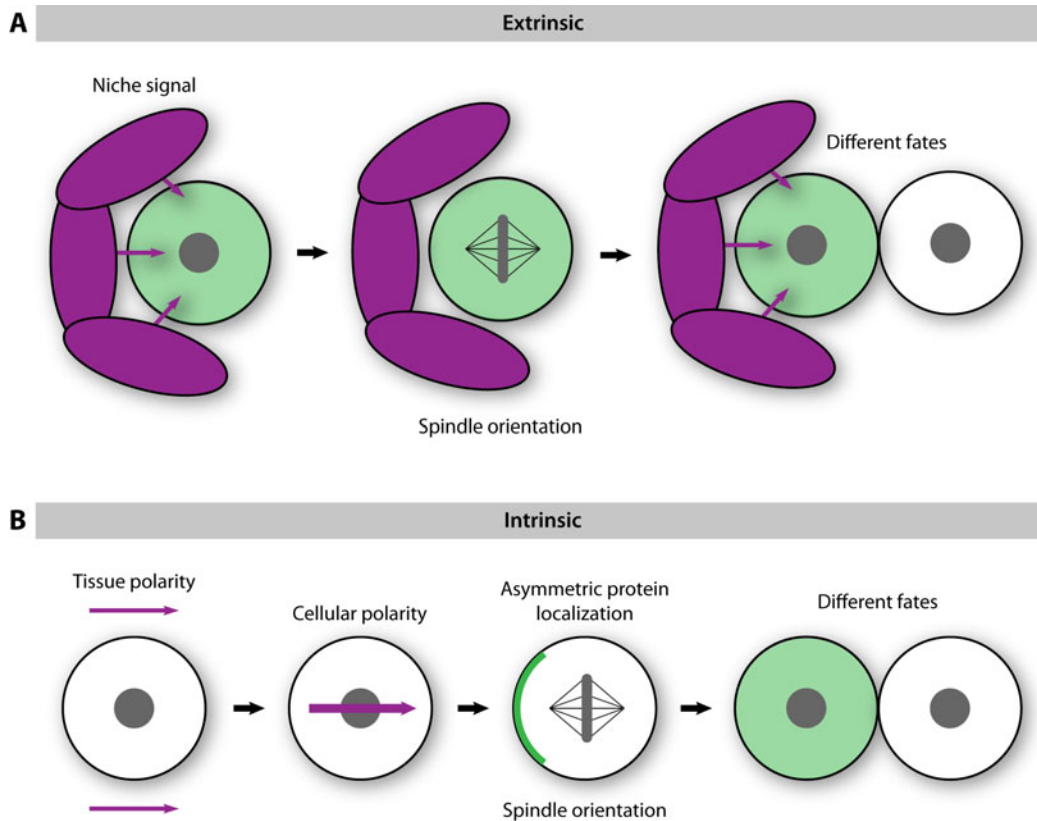


Figure 1. Modes of asymmetric cell division: cell-extrinsic versus cell-intrinsic

(A) In the cell extrinsic model, the stem cell needs a signal from the surrounding niche (purple) to maintain its self-renewing potential. Upon division, the cell dividing away from the niche (white cell) is no longer receiving this signal and differentiates, while the cell remaining in contact with the niche (green cell) retains a stem cell identity. (B) In the cell intrinsic model, a cellular axis of polarity is established prior to division by surrounding tissue. During mitosis, cell fate determinants (green) localize asymmetrically with respect to this axis of polarity. Upon cytokinesis, they segregate into one of the two daughter cells, where they act to ensure that the two daughter cells adopt different fates. Adapted from (Knoblich, 2008).

fate. This is the mode of ACD used by *Drosophila* germline stem cells for example (Knoblich, 2008).

3.1.2. Intrinsic model

The cell-intrinsic mode a cellular axis of polarity triggers asymmetric localization of specific proteins – called cell fate determinants – during mitosis and their subsequent inheritance by only one of the two daughter cells (Fig. 1B). Cell fate determinants confer a specific fate to the cell that receives them, making it different from the other daughter cell. This mode of division is used by sensory organ precursors (SOPs) and neuroblasts, the precursors of the peripheral and the central nervous system (PNS and CNS), respectively (Knoblich, 2008). SOP cells cannot be considered stem cells since they do not self-renew and only undergo a series of four divisions to produce the four cells that compose an external sensory organ (for review, see (Neumuller and Knoblich, 2009)). Neuroblasts, however, are stem cell-like progenitors that self-renew and divide asymmetrically a large number of times to give rise to all neurons and glia of the central nervous system (for review, see (Knoblich, 2010)). For these reasons, over the last years, neuroblasts have become a very attractive model to study mechanisms of ACD and more generally stem cell biology in *Drosophila*.

3.2. NEUROBLAST POPULATIONS IN DROSOPHILA

Neuroblasts proliferate in two waves: the first one during embryogenesis to generate the embryonic CNS, the second one during larval stages to produce virtually all neurons of the adult CNS (Knoblich, 2008).

3.2.1. Embryonic neuroblasts

During embryogenesis, cells of the ventral neurectoderm delaminate and adopt a neuroblast fate (Knoblich, 2008). They divide several times along the apical-basal axis into a neuroblast that continues to proliferate and a smaller ganglion mother cell (GMC) that differentiate (Ito and Hotta, 1992). GMCs only divide once and produce two terminally differentiated neurons. These neuroblasts do not regrow between each division and nearly all of them enter quiescence after about 20 cycles (Wu et al., 2008).

3.2.2. Larval neuroblasts

The second wave of proliferation takes place in larval stages. At this time, the brain is composed of a ventral nerve cord (VNC) and of two brain lobes that each consist of a central

brain (CB) and an optic lobe (OL) (Fig. 2A). Larval neuroblasts, as opposed to embryonic neuroblasts, regrow between each division and can undergo a very large number of ACDs (Truman and Bate, 1988). They can be separated into three groups depending on their origin, pattern of proliferation and localization within the larval brain. The first group comprises neuroblasts of the CB (about 85 per lobe) and of the VNC (30 per hemisegment), which correspond to embryonic neuroblasts that re-entered the cell cycle (Fig. 2A) (Ito and Hotta, 1992; Truman and Bate, 1988). They are responsible for producing the vast majority of neurons of the adult central brain, the thoracic ganglia and the abdominal ganglia (Ito and Hotta, 1992; Truman and Bate, 1988). The second group is formed by the 8 mushroom body neuroblasts (4 per brain lobe, Fig. 2A). Like CB and VNC neuroblasts they are generated in the embryo, however mushroom body neuroblasts start proliferating earlier – and stop later, forming specific neurons called kenyon cells that are involved in learning and memory (Ito and Hotta, 1992; Ito et al., 1997). Finally, the third group consists of newly born neuroblasts that originate from the OL neuroepithelium to produce the neurons of the visual processing centers of the brain (Fig. 2A) (Egger et al., 2007).

Because of their strong proliferation potential, large number and importance for brain development, CB neuroblasts have emerged as a model of choice to study ACD and self-renewal and are the main focus of this study. In this introduction they are deliberately considered to be a homogenous population (for further subdivision and characterization of this group of neuroblasts, please refer to chapter I). CB neuroblasts form lineages by dividing asymmetrically into a neuroblast and a GMC that then generates two neurons through a terminal division (Fig. 2B). The next few paragraphs describe the basic mechanisms underlying neuroblast ACD.

3.3. MECHANISM OF ASYMMETRIC CELL DIVISION IN *DROSOPHILA* NEUROBLASTS

3.3.1. Cell fate determinants

In neuroblast ACD, the generation of two daughter cells with different fates is ultimately mediated by the asymmetric segregation into the GMC of a specific set of proteins called cell fate determinants: Numb, Prospero (Pros) and Brain tumor (Brat) (Fig. 2C) (Spana et al., 1995; Hirata et al., 1995; Knoblich et al., 1995; Spana and Doe, 1995; Betschinger et al., 2006; Bello et al., 2006; Lee et al., 2006c). All three proteins are essential to specify GMC fate (see section 3.4). Numb is an endocytic protein first identified in SOPs, where it was shown to down-regulate Notch signaling via interaction with Notch and α -adapatin, a protein involved

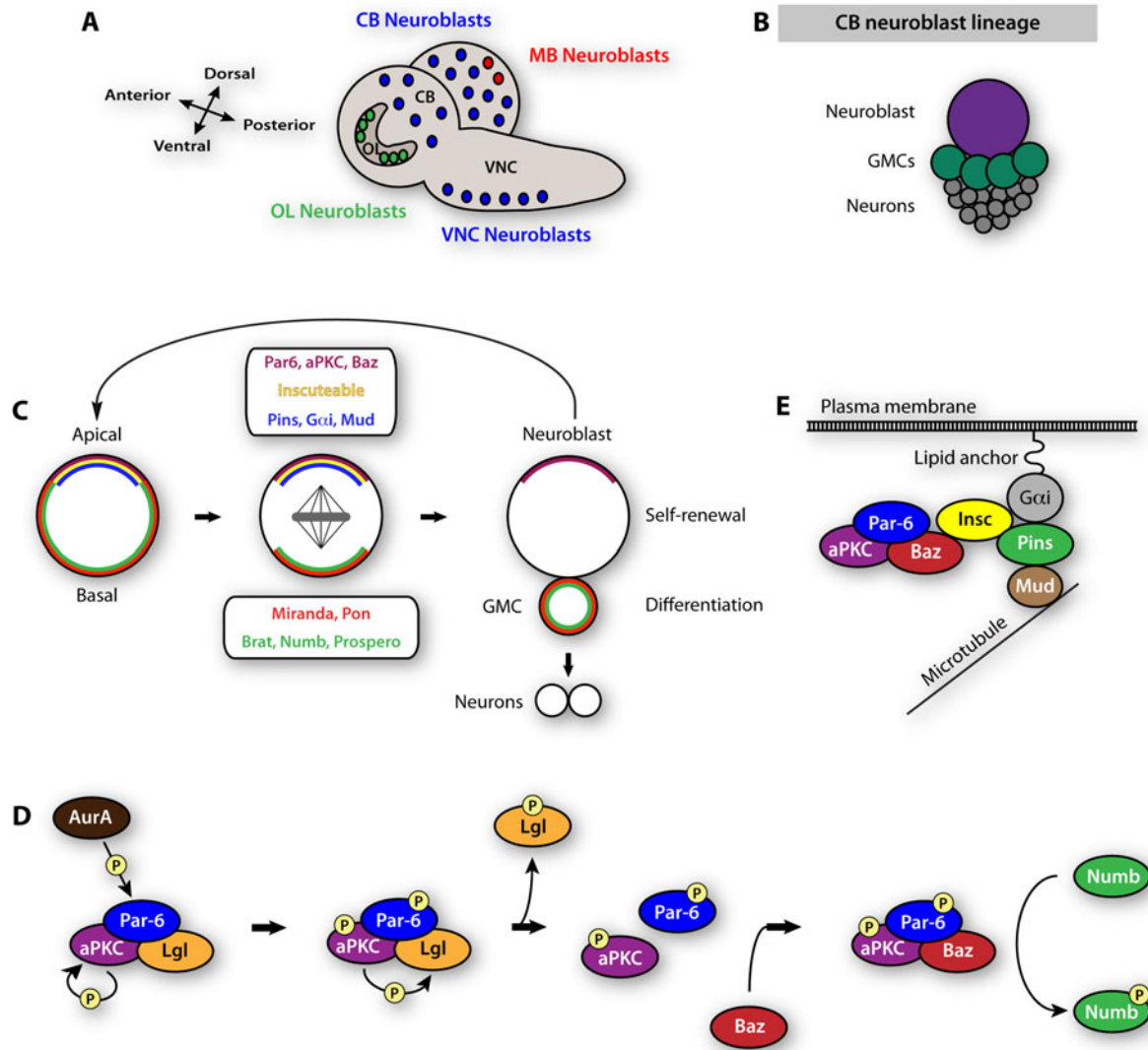


Figure 2. *Drosophila* larval neuroblast lineages and mechanism of asymmetric cell division

(A) The larval brain is composed of a ventral nerve cord (VNC) and of two brain lobes that can be further subdivided into optic lobe (OL) and central brain (CB). (B) Each CB neuroblast lineage is composed of a single large neuroblast, a few smaller GMCs and several small neurons. (C) Principle of ACD in neuroblast. In mitosis, the apical aPKC/Par6/Baz complex plays two essential roles. One is to restrict localization of Pon, Mira, Brat, Numb and Pros to the basal cortex. The other one is to control alignment of the mitotic spindle via Insc and the Gai/Pins/Mud complex. The coordination of these two events enables segregation of the determinants into the smaller GMC where they trigger differentiation, whereas the bigger cell remains a neuroblast and continues to proliferate. Adapted from (Knoblich, 2010). (D) Phosphorylation cascade that controls asymmetric localization of Numb. In interphase, aPKC forms an inactive complex with Par-6 and Lgl. In mitosis, Par6 is phosphorylated by Aur-A, which triggers autophosphorylation of aPKC. Activated aPKC phosphorylates Lgl, which leaves the complex and is replaced by Baz. This active Par complex is able to phosphorylate Numb to release it from the apical cortex, therefore limiting its localization to the basal cortex of the neuroblast. Adapted from (Wirtz-Peitz et al., 2008). (E) Control of spindle alignment. In mitosis, the Gai/Pins/Mud complex connects microtubules of the mitotic spindle to the Par complex and the apical cortex via Insc.

in receptor-mediated endocytosis (Rhyu et al., 1994; Guo et al., 1996; Santolini et al., 2000; Berdnik et al., 2002). It is thought that Numb also inhibits Notch signaling in the GMC. Pros is a homeodomain transcription factor that is cytoplasmic in the neuroblast but enters the nucleus once in the GMC (Hirata et al., 1995; Knoblich et al., 1995; Spana and Doe, 1995). In the GMC, Pros acts both as an activator and an inhibitor of transcription and regulates a large set of genes involved in neuroblast self-renewal, cell cycle control and neuronal differentiation (Choksi et al., 2006; Southall and Brand, 2009). Unlike for Numb and Pros, the precise function of Brat remains elusive (Betschinger et al., 2006; Bello et al., 2006; Lee et al., 2006c). Brat belongs to the same family of proteins than Mei-P26 and Dappled, which have both been shown to regulate cell growth and proliferation (Rodriguez et al., 1996; Page et al., 2000; Neumuller et al., 2008). Members of this family share a similar structure, containing one or more N-terminal zinc-finger like B boxes, a coiled-coil motif and a C-terminal NHL domain (Slack and Ruvkun, 1998; Betschinger et al., 2006). In the embryo, Brat is involved in establishment of the anterior-posterior axis by binding to Nanos and Pumilio and repressing translation of the posterior gene *hunchback* (Sonoda and Wharton, 2001). However, phenotypes and expression patterns of Nanos, Pumilio and Hunchback cannot explain the function of Brat in larval neuroblasts (Knoblich, 2008). Therefore, the precise mechanism by which Brat inhibits cellular growth in GMCs is currently unclear.

All three cell fate determinants are transported by adaptor proteins that also localize asymmetrically during mitosis and segregate into the GMC. Pros and Brat bind to the coiled-coil protein Miranda (Mira), whereas Numb binds to Partner of Numb (Pon) (Lee et al., 2006c; Betschinger et al., 2006; Ikeshima-Kataoka et al., 1997; Shen et al., 1997). The role of Mira in asymmetric segregation of Brat and Pros is essential, since in *mira* mutants both determinants become uniformly cytoplasmic and segregate equally into both daughter cells (Betschinger et al., 2006; Lee et al., 2006c; Shen et al., 1997; Ikeshima-Kataoka et al., 1997). The case of Pon is more complex, because in *pon* mutant neuroblasts, asymmetric localization of Numb is delayed but is then rescued by end of mitosis (Lu et al., 1998). This observation indicates that Pon facilitates Numb asymmetric segregation but is not absolutely crucial for it.

3.3.2. Role of the Par complex

Brat, Numb, Pros and their adaptor proteins Mira and Pon localize to the basal cortex during mitosis and are inherited by the GMC only (Fig. 2C). This process depends on the conserved Par complex – Par stands for “Partitioning defective mutants” – that was originally identified

in *C. elegans* and which plays a key role in cell polarity in a variety of cell types and organisms (Suzuki and Ohno, 2006; Ohno, 2001; Goldstein and Macara, 2007). The active *Drosophila* Par complex is composed of the atypical Protein Kinase C (aPKC) and the PDZ domain-containing proteins Par-6 and Bazooka (Baz, also called Par-3) (Suzuki and Ohno, 2006; Goldstein and Macara, 2007). In mitosis, these three proteins are found at the apical cortex (Wodarz et al., 1999; Schober et al., 1999; Wodarz et al., 2000; Rolls et al., 2003). In *Drosophila* neuroblasts mutant for either aPKC, Par-6 or Baz, the other two proteins are mislocalized, cell fate determinants localize uniformly around the cell cortex and mitotic spindle alignment becomes random (Knoblich, 2008). Indeed, the Par complex has two main functions during ACD of neuroblasts: to restrict localization of cell fate determinants to the basal cortex and to control spindle alignment (Fig. 2C-E).

3.3.3. Asymmetric segregation of cell fate determinants

The precise mechanism controlling basal localization of cell fate determinants remained a mystery for a long time. Recently, a phosphorylation cascade has been identified that controls this process and is summarized below (Fig. 2D) (Wirtz-Peitz et al., 2008). In interphase, aPKC forms an inactive apical complex with Par-6 and the cytoskeletal protein Lethal (2) giant larvae (Lgl). Upon entry in mitosis, the kinase Aurora A (AurA) phosphorylates Par-6, which leads to the activation of aPKC via autophosphorylation. aPKC in turn phosphorylates Lgl, which allows its release from the apical complex and its replacement by Baz. This subunit exchange triggers a modification of aPKC substrate specificity that leads to the phosphorylation of Numb and its release from the apical cortex. This model for basal localization of Numb during ACD is thought to be responsible for Brat and Pros asymmetric localization as well, since Mira is also a substrate of aPKC and that aPKC phosphorylation is important for Mira localization during neuroblast ACD (Wirtz-Peitz et al., 2008; Atwood and Prehoda, 2009).

3.3.4. Control of spindle alignment

For asymmetric determinants to be inherited by the GMC, the mitotic spindle has to be aligned with the axis of polarity (Fig. 2C&E). This is achieved by interaction of the active Par complex with the apically localized adaptor protein Inscuteable (Insc), via Baz (Kraut et al., 1996; Schober et al., 1999; Wodarz et al., 1999). This interaction has two main consequences. On the one hand Insc stabilizes the Par complex (Wodarz et al., 2000; Wodarz et al., 1999; Petronczki and Knoblich, 2001). On the other hand Insc binds to Partner of Inscuteable (Pins) and the G protein subunit α ($G\alpha i$), which form a complex with the

NuMA-related Mushroom body defect (Mud) protein (Parmentier et al., 2000; Schaefer et al., 2000; Bowman et al., 2006; Izumi et al., 2006; Siller et al., 2006). The G α i-Pins-Mud complex is anchored to the plasma membrane via N-myristoylated G α i and to microtubules of the mitotic spindle via Mud (Sprang, 1997; Bowman et al., 2006; Izumi et al., 2006; Siller et al., 2006). Interaction of the G α i-Pins-Mud complex with Insc, and therefore the Par complex, allows precise alignment of the mitotic spindle with the cellular axis of polarity to ensure that determinants are segregated into the GMC only. This is crucial for proper ACD since in neuroblasts where spindle orientation is randomized, such as in *mud* mutants, the fate of the two daughter cells is affected and ultimately dictated by the ratio of Par complex versus determinants that is inherited by each cell (Cabernard and Doe, 2009).

3.4. DROSOPHILA NEUROBLAST ASYMMETRIC DIVISION AND TUMORIGENESIS

3.4.1. Connection between ACD and tumor formation

Studies conducted in *Drosophila* in the 1960s and 1970s led to the identification of a set of five genes – *brat*, *lgl*, *discs large (dlg)*, *lethal(2)giant discs (lgd)* & *lethal(3)malignant brain tumor (l(3)mbt)* – which, when mutated, provoked tumorous overgrowth in larval brains as well as in other tissues (for review, see (Gateff, 1994)). Interestingly, when fragments of these brains were transplanted into the abdomen of wild-type flies, they continued to proliferate, failed to differentiate, showed abnormal morphologies, invaded other tissues and ultimately killed their host. Among these five tumor suppressor genes, three were recently shown to play a role in ACD: *brat*, *lgl* and *dlg* (Ohshiro et al., 2000; Peng et al., 2000; Albertson and Doe, 2003; Betschinger et al., 2006; Bello et al., 2006; Lee et al., 2006c). The discovery that defects in ACD could lead to such a dramatic phenotype first came as a surprise. Although it was not entirely clear why this could be, a simple explanation of the *brat* mutant phenotype, for example, is that the smaller cell that should normally receive Brat is unable to differentiate and instead proliferates abnormally, leading to the formation of a tumor (Fig. 3A&B).

3.4.2. The *Drosophila* larval neuroblast as a model for cancer cell biology

In addition to the tumor suppressors *lgl*, *dlg* and *brat*, many genes that play a role in ACD have been shown in recent years to prevent neuroblast overproliferation. Brains mutant for *mira*, *numb* and *pros* form transplantable tumors that can reach a 100 times their original size, invade other tissues, show centrosome alterations and become aneuploid (Caussinus and Gonzalez, 2005). Additionally, formation of tumors has been described in mutants for the mitotic kinases AurA and Polo (another kinase involved in ACD), mutants with aberrant

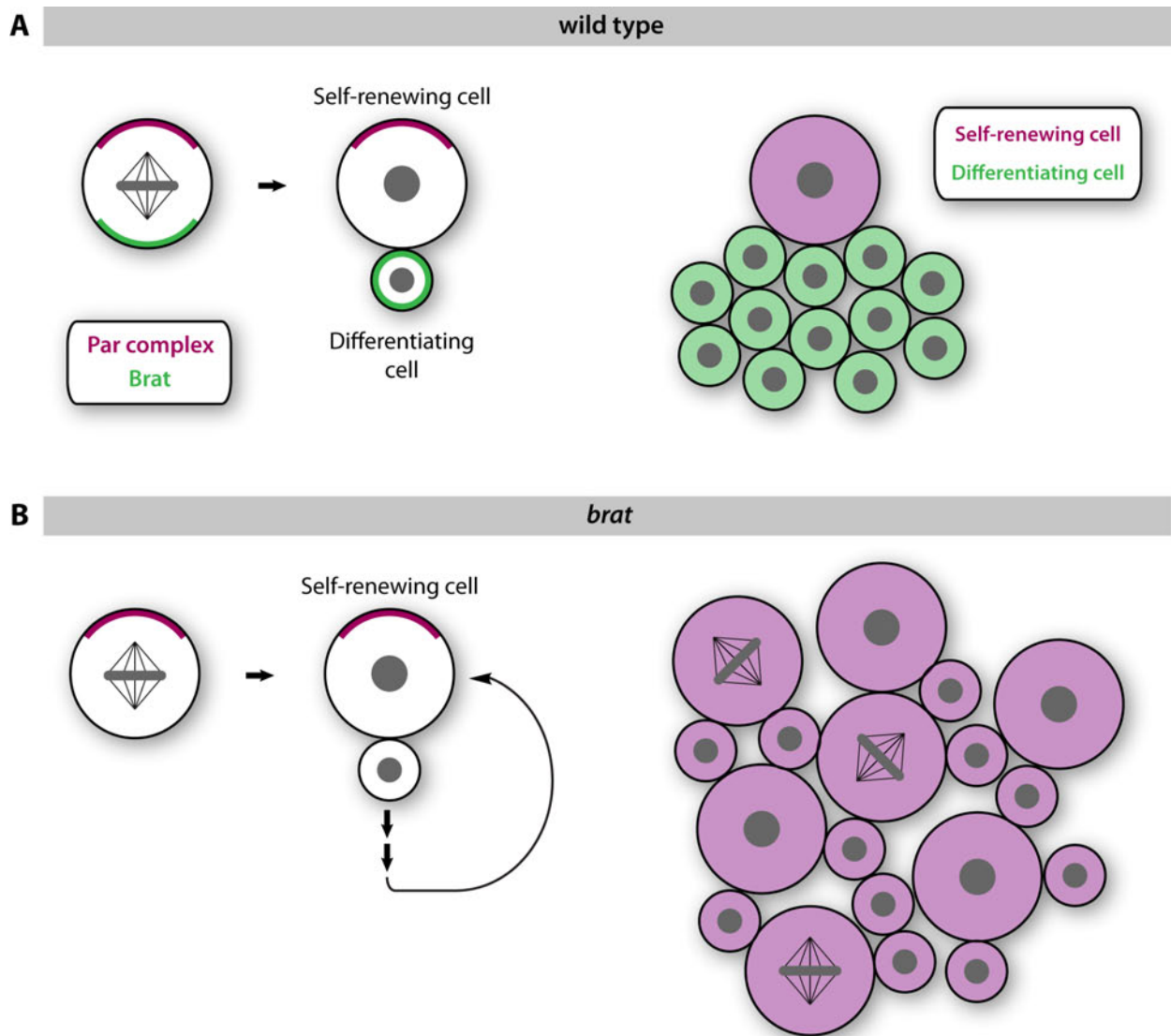


Figure 3. Defects in neuroblast ACD can lead to overproliferation and tumorigenesis

(A) In a dividing wild type neuroblast, the Par complex localizes apically whereas determinants such as Brat localize to the basal cortex. Segregation of Brat in the smaller cell triggers differentiation of this cell, whereas the bigger cell continues to proliferate. (B) In the absence of Brat, the smaller cell is unable to properly differentiate and this leads to overproliferation of self-renewing cells at the expense of differentiating cells, thereby generating a tumor.

spindle orientation and even mutants with an excess of centrosomes (Lee et al., 2006a; Wang et al., 2006; Wang et al., 2007; Bowman et al., 2006; Siller et al., 2006; Izumi et al., 2006; Cabernard and Doe, 2009; Kitajima et al., 2010; Basto et al., 2008; Castellanos et al., 2008). Conversely, mutations in the apically localized aPKC or Pins lead to fewer neuroblasts rather than overproliferation (Lee et al., 2006b).

The compelling observation that mutations in many genes involved in ACD can cause neuroblast overproliferation and formation of tumors has recently made the larval neuroblast a very potent model to study the relationship between ACD, self-renewal and tumorigenesis. Even more so in the light of the recently formulated “cancer stem cell hypothesis” which suggests that many human tumors arise from and are maintained by very small populations of stem cells (Reya et al., 2001).

3.5. STRUCTURE AND AIM OF THIS STUDY

This study is presented as two chapters introduced below.

Chapter I

It was long thought that CB neuroblasts form a homogeneous population generating rather simple lineages. The first chapter describes a previously unrecognized population of CB neuroblasts that form much more complex lineages, and their implication in tumor formation.

Chapter II

In order to identify novel genes regulating neuroblast self-renewal and lineage progression in the larval brain, a genome-wide RNAi screen was conducted in our laboratory. One of the candidate genes that caused an overproliferation phenotype is the previously unstudied gene *CG6049/barricade*. The second chapter focuses on the characterization of this gene, exploring its role in regulating neuroblast lineages.

4. CHAPTER I – THE TUMOR SUPPRESSORS BRAT AND NUMB REGULATE TRANSIT-AMPLIFYING NEUROBLAST LINEAGES IN *DROSOPHILA*

This work was published as:

Bowman SK, Rolland V, Betschinger J, Kinsey KA, Emery G and Knoblich JA. The Tumor Suppressors Brat and Numb Regulate Transit-Amplifying Neuroblast Lineages in *Drosophila*. *Developmental Cell*. 2008; 14(4): 535-46

Please note that for sake of clarity, the abstract of this paper has been removed.

4.1. CONTRIBUTIONS

The author of this thesis contributed Figure 8A to 8D and 8H to 8J – corresponding to Figure 5A to 5D and 5H to 5J of the published paper. Sarah Bowman contributed all other figures, tables and supplementary data of this chapter. Joerg Betschinger suggested the concept of a transit amplifying neuroblast lineage and made some initial observations about these neuroblasts. Gregory Emery first identified the *Igd* overproliferation phenotype. Kaolin Kinsey built the mathematical model of the type 2 lineage. Juergen Knoblich and Sarah Bowman designed experiments and wrote the manuscript.

4.2. INTRODUCTION

The development of the *Drosophila* central nervous system has become the subject of intensive investigation as a model for the regulation of self-renewal in stem cell lineages (Chia et al., 2008). Neuroblasts are specified in the embryo, and they begin dividing in a self-renewing manner to produce neurons used by the larva. In larval and pupal stages, the divisions continue and produce the neurons of the adult fly. It has long been accepted that all neuroblasts express the neural precursor gene *asense* (*ase*) (Brand et al., 1993; Jarman et al., 1993) and divide asymmetrically to self-renew and produce a small daughter cell, the ganglion mother cell (GMC). The GMC divides terminally into two neurons or glia.

During each neuroblast division, an axis of polarity is established by the activity of the Par complex, a conserved protein complex consisting of Par-3/Bazooka (Schober et al., 1999; Wodarz et al., 1999), Par-6 (Petronczki and Knoblich, 2001), and atypical Protein Kinase C (aPKC) (Rolls et al., 2003; Wodarz et al., 2000). The Par complex has two major functions. The first function is to recruit a protein called Inscuteable (*Insc*) which maintains the polarity of the Par complex and thereby the polarity of the neuroblast (Schober et al., 1999; Wodarz et al., 1999). *Insc* also directs the mitotic spindle to align along the axis of polarity (Kraut et al., 1996). The second function of the Par complex is to promote the localization of cell fate

determinants to the opposite pole of the neuroblast (Betschinger et al., 2003). The cell fate determinants segregate exclusively into the GMC at telophase and act to specify GMC fate. They include the Notch repressor Numb (Knoblich et al., 1995), the transcription factor Prospero (Pros) (Hirata et al., 1995; Knoblich et al., 1995), and the NHL-domain protein Brain tumor (Brat) (Bello et al., 2006; Betschinger et al., 2006; Lee et al., 2006c). In the GMC, Numb, Pros, and Brat are all thought to inhibit self-renewal and promote cell cycle exit and differentiation. Numb probably does this by promoting endocytosis of the Notch receptor, making levels of Notch signaling lower than in the neuroblast (Berdnik et al., 2002; Wang et al., 2006). Pros enters the GMC nucleus after degradation of its cortical anchor protein Miranda (Mira), represses expression of cell cycle genes and activates genes required for terminal differentiation (Choksi et al., 2006; Ikeshima-Kataoka et al., 1997; Li and Vaessin, 2000; Shen et al., 1997). Brat may act to prevent cell growth (Betschinger et al., 2006; Frank et al., 2002). Consistent with the functions of these genes in repressing growth and self-renewal, loss of *brat*, *numb*, or *pros* in the larva results in neuroblast lineages that escape differentiation. This causes overgrowth characterized by the overproduction of neuroblast-like cells at the expense of differentiated neurons (Bello et al., 2006; Betschinger et al., 2006; Lee et al., 2006a; Lee et al., 2006c; Wang et al., 2006). Although brain tissue mutant for *numb*, *pros*, or *brat* all share similar terminal phenotypes, the precise cellular events initiating the overgrowth are unknown. Close analysis of the *brat* phenotype indicates that the overgrowing cells arise in a specific location in the central brain (Bello et al., 2006; Betschinger et al., 2006), suggesting that some cells are particularly sensitive to loss of *brat*. In this study, we demonstrate that these cells comprise a previously uncharacterized neuroblast lineage with a transit-amplifying pool of intermediate progenitors. Unlike any known *Drosophila* neuroblasts, the neuroblasts generating this lineage repress Ase. We show that Brat and Numb act to promote maturation of intermediate progenitors. In the absence of these proteins, maturation fails to take place, immature progenitors begin to divide, and their progeny do not differentiate. Our data suggest that mitosis in an immature intermediate progenitor can initiate tumorous overgrowth.

4.3. RESULTS

4.3.1. *brat* overgrowth originates in Ase⁻ neuroblast lineages

Mutation in *brat* leads to dramatic overproduction of neuroblasts at the expense of neurons (Bello et al., 2006; Betschinger et al., 2006; Lee et al., 2006c). The phenotype is thought to arise from misregulated neuroblast division, but not all central brain neuroblasts are equally

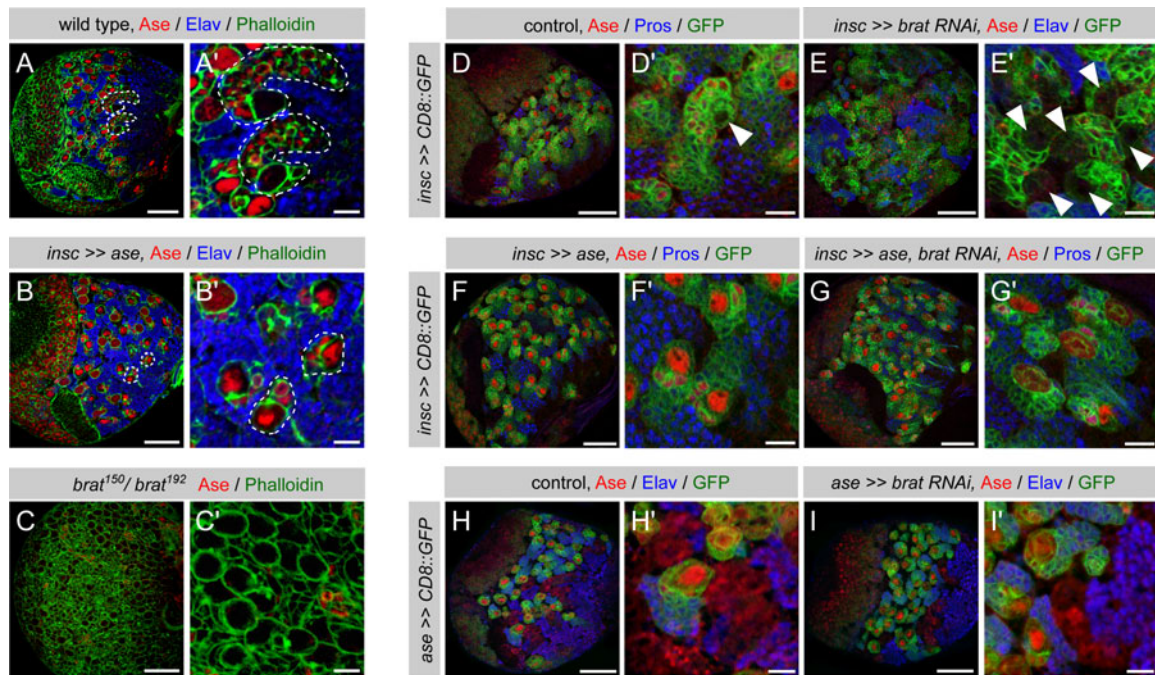


Figure 4. *brat* overgrowth originates in PAN neuroblast lineages

(A-I) Immunostainings of third instar brains labeled with indicated markers (gray boxes). For each genotype, an overview of the brain lobe and a detail of neuroblast lineages are shown. (A-B) Wild type brains contain PAN neuroblasts with long lineages of Ase⁺ progeny (A, A' outline); ectopic expression of Ase eliminates both (B, B' outline). (C, C') a *brat* zygotic mutant brain is overgrown with PAN neuroblasts. (D-G) Brains with GFP reporting *insc*-Gal4 expression. Control brains are well organized and contain PAN neuroblasts (D, D' arrowhead). Brat knockdown results in disorganized overgrowth with ectopic PAN neuroblasts (E, E' arrowheads). Expressing Ase in all neuroblasts eliminates PAN neuroblasts (F, F'). Ectopic expression of Ase prevents the overgrowth normally caused by Brat knockdown (G, G'). (H-I) Brains with GFP reporting *ase*-Gal4 expression. Neither control (H, H') nor Brat knockdown brains (I, I') show disorganized overgrowth phenotypes. Scale bars: A-I, 50 μ m; A'-I', 10 μ m.

affected by loss of Brat (Bello et al., 2006; Betschinger et al., 2006). To find molecular markers for the sensitive subpopulation, we examined known neuroblast markers and checked for differential expression among small groups of central brain neuroblasts. The expression pattern of the transcription factor Ase fit this profile and we selected it for further analysis. Ase is a member of the *achaete-scute* complex (AS-C), a quartet of genes involved in specifying neural precursor cells. Expression of Ase typically begins after the remaining three members of the AS-C have acted together with other genes to specify neural precursor fate, and it persists after the precursor starts to divide (Brand et al., 1993).

Ase protein is present in the majority of central brain neuroblast nuclei, but absent from eight neuroblasts per brain lobe (Fig. S1). Due to their position on the posterior side of the brain, we refer to these neuroblasts as Posterior Asense-Negative (PAN) neuroblasts. They may tentatively be assigned to the dorsoposterior medial group of neuroblast lineages (Pereanu and Hartenstein, 2006) because of their location. Six medial PAN neuroblasts produce long chains of Ase⁺ progeny cells with high levels of cortical actin, while Ase⁺ neuroblasts typically have a small number of closely associated Ase⁺ progeny (Fig. 4A). Two additional PAN neuroblasts generate progeny that populate more interior brain regions (Fig. S1, and data not shown). Because they are more abundant and easier to identify, we focused our analysis on the medial PAN neuroblasts.

Since Ase is thought to be expressed in all *Drosophila* neural precursor cells after their specification from the neuroepithelium (Brand et al., 1993) as well as in the neural precursors of other insects (Wheeler et al., 2003), its absence in a subset of neuroblasts is surprising. To test whether downregulation of Ase in the PAN neuroblasts allows production of the long chains of Ase⁺ progeny, we ectopically expressed Ase in all neuroblasts. For this, we used the Gal4 line 1407 inserted in the *insc* promoter (Betschinger et al., 2006), hereafter referred to as *insc*-Gal4. Ectopic Ase expression eliminates all Ase⁻ neuroblasts and all lineages with long chains of Ase⁺ progeny containing high levels of cortical actin (Fig. 4B). Since high levels of Ase could potentially interfere with specification of neuroblast identity during embryogenesis, we prevented this by using the temperature sensitive Gal4 inhibitor Gal80^{ts} to limit Ase overexpression to the larval stages. This also eliminated PAN neuroblast lineages (PAN lineages; data not shown). We conclude from these experiments that ectopic expression of Ase eliminates PAN lineages, perhaps by transforming PAN neuroblasts to Ase⁺ neuroblasts that produce fewer progeny.

PAN neuroblasts are found on the dorsal-posterior central brain, the region thought to cause the *brat* overgrowth phenotype (Bello et al., 2006; Betschinger et al., 2006). To investigate whether the *brat* phenotype originates in PAN lineages, we tested whether *brat* loss of function could cause brain overgrowth in their absence. For this, we overexpressed Ase with *insc*-Gal4 and simultaneously knocked down *brat* using transgenic RNAi. In control brains, PAN lineages are clearly visible in the posterior medial region (Fig. 4D, 4D'). Brat knockdown significantly reduces the amount of Brat protein (Fig. S2), causing disorganized overgrowth with many ectopic PAN neuroblasts (45.6 ± 6.0 PAN neuroblasts, $n=5$ brain lobes; Fig. 4E, 4E'). As described above, overexpression of Ase eliminates the PAN lineages (Fig. 4F, 4F'). Simultaneous overexpression of Ase and *brat* knockdown does not generate either the overgrowth or the ectopic PAN neuroblasts seen with *brat* RNAi alone (0.0 ± 0.0 PAN neuroblasts, $n=6$ brain lobes; Fig. 4G, 4G'), even though Brat protein is reduced to similar levels (Fig. S2). This indicates that PAN lineages are required for the *brat* overgrowth phenotype. If the *brat* phenotype arises in the PAN lineages only, *brat* knockdown in Ase⁺ neuroblasts should have no effect. To test this, we knocked down *brat* using *ase*-Gal4. *ase*-Gal4 is expressed in all central brain neuroblasts except for the eight PAN neuroblasts (Fig. S1, 4H, 4H'). Notably, the Ase⁺ progeny of the PAN lineage express *ase*-Gal4 at low or undetectable levels; this may be because transcriptional control of *ase* in these cells lies outside the 2kb genomic fragment used to make *ase*-Gal4. While knockdown of Brat with *ase*-Gal4 significantly reduces Brat protein levels (Fig. S2), it does not cause overgrowth of Ase⁺ neuroblasts (Fig. 4I, 4I'). We conclude from these data that PAN neuroblasts are the neuroblast subpopulation affected by mutation in *brat*, and the PAN lineages produce the neoplastic transformation seen in *brat* mutants. Correspondingly, overgrown *brat* mutant brains consist almost entirely of Ase⁻ neuroblasts (Fig. 4C).

4.3.2. PAN lineages produce intermediate progenitors

To investigate why *brat* affects Ase⁻ neuroblasts specifically, we analyzed PAN lineages in greater detail using the MARCM system (Lee et al., 1999). This method allows the generation of wild type or mutant neuroblast clones that express membrane-bound GFP in an otherwise wild type, GFP-negative background. For this analysis, we induced clones at 48 hours after larval hatching (ALH), and examined them either 24 or 48 hours later. Ase⁺ neuroblast clones always contain one Ase⁺ neuroblast, several Ase⁺ daughter cells, and many Elav⁺ neurons (Fig. 5A, 5B). The major difference between clones that have been developing for 24 hours (24-hr clones) and clones that have been developing for 48 hours (48-hr clones) is an increase in Elav⁺ neurons (Table 1B). Occasionally, we observed a single Ase⁺ progeny cell dividing

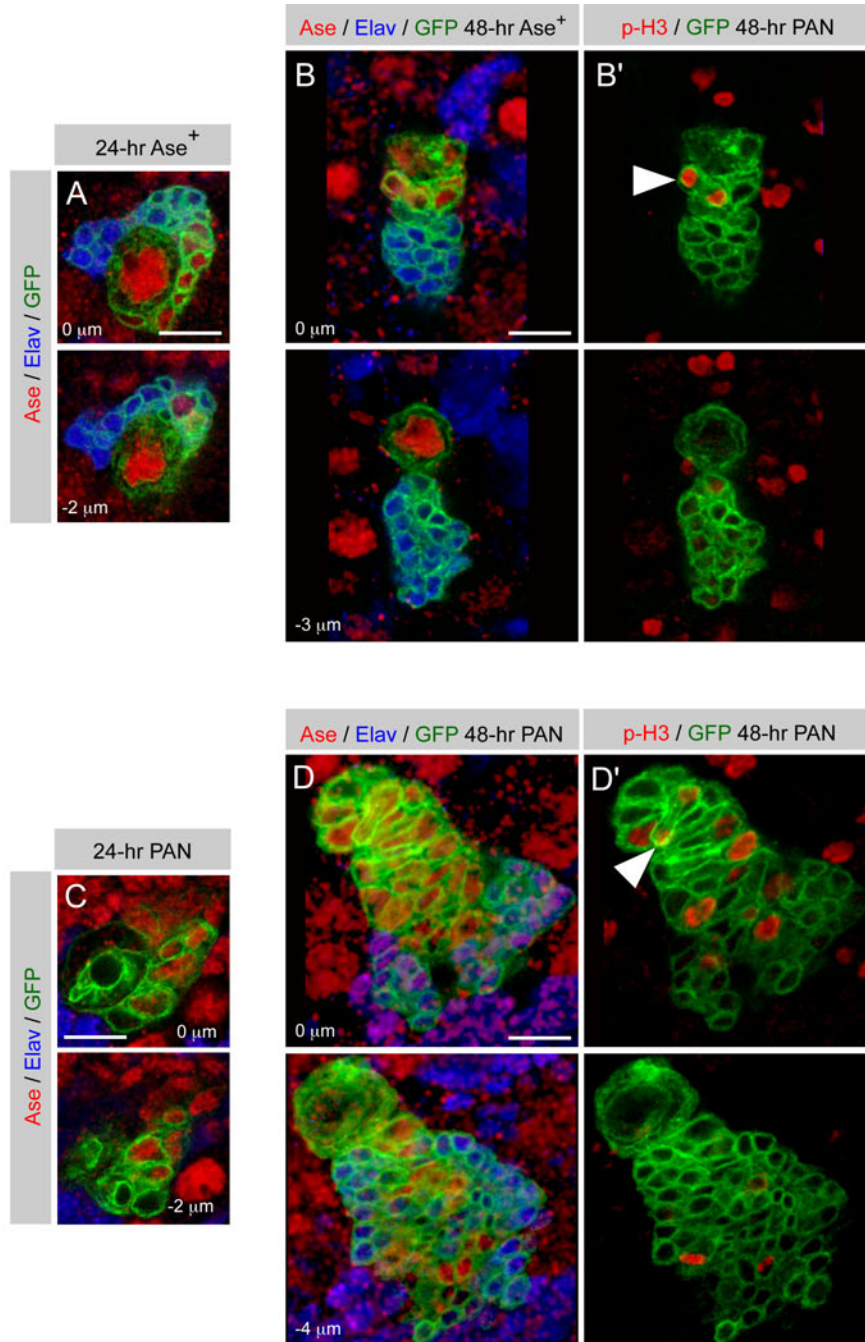


Figure 5. PAN lineages produce intermediate progenitors

(A-D) Immunostainings of MARCM clones in central brain neuroblasts labeled with indicated markers (gray boxes). p-H3: phospho histone H3. Neuroblast clones are three-dimensional structures, so two separate optical sections from a Z-stack through each clone are shown. The most superficial section is labeled 0 μm. (A-D) Neuroblast clones are reported by GFP expression. In 24-hr (A) and 48-hr clones (B), Ase⁺ neuroblasts produce Ase⁺ and Elav⁺ progeny. A single Ase⁺ cell divides symmetrically in size and adjacent to the neuroblast (B', arrowhead). In 24-hr PAN clones, the neuroblast produces Ase⁻ progeny and Ase⁺ progeny, but almost no Elav⁺ progeny (C). 48-hr PAN clones contain a small number of Ase⁻ cells, and large numbers of Ase⁺ and Elav⁺ cells (D). All mitotic cells are Ase⁺, several are far away from the neuroblast, and one divides asymmetrically in size (D', arrowhead). Scale bars: 10 μm.

symmetrically in size, always closely associated with the neuroblast (Fig. 5B'). These observations are consistent with a standard neuroblast lineage, where an Ase⁺ neuroblast produces an Ase⁺ GMC that divides terminally to produce 2 Elav⁺ neurons.

By contrast, in 24-hr PAN neuroblast clones (PAN clones), the neuroblast produces almost exclusively Elav⁻ progeny (Fig. 5C, Table 1B). Some daughter cells are Ase⁻, but most are Ase⁺. In 48-hr clones, the PAN neuroblast produces more than twice as many cells as an Ase⁺ neuroblast (48-hr Ase⁺ clones 57.6 ± 3.8 progeny, n=5 clones; 48-hr Ase⁻ clones 131.4 ± 2.6 progeny, n=5 clones). Ase⁻ progeny are never in mitosis, but there are around 9 mitotic Ase⁺ progeny per clone (9.2 ± 0.6 cells per Ase⁻ clone, n=4 clones) – some dividing as many as 11 cell diameters away from the neuroblast (Fig. 5D, 5D'). These observations show that a PAN neuroblast can produce more progeny than an Ase⁺ neuroblast in the same time period, and in contrast to an Ase⁺ lineage, the progeny of the PAN neuroblast will enter mitosis far away from their mother.

The increased number of progeny in the PAN neuroblast clones could be produced either by more frequent divisions of the PAN neuroblasts, or by multiple rounds of mitosis in the Ase⁺ daughter cells. To distinguish these possibilities, we calculated the mitotic index of PAN neuroblasts. We reasoned that an increased rate of PAN neuroblast division would result in an observable increase in the fraction of mitotic PAN neuroblasts. Throughout larval development, the mitotic index of PAN neuroblasts and Ase⁺ neuroblasts are similar (Table 1A), so the increased number of progeny is unlikely to arise from more frequent PAN neuroblast division. These results, together with the large number of mitotic Ase⁺ daughters, suggest that the Ase⁺ progeny divide multiple times to produce the large numbers of cells observed in PAN neuroblast clones. This contrasts sharply with a standard neuroblast lineage, where neuroblast daughters always divide terminally. The presence of intermediate progenitors in the medial central brain would explain why this region contains high numbers of small, BrdU-incorporating cells (Ito and Hotta, 1992).

4.3.3. PAN lineages contain transit-amplifying secondary neuroblasts

How does an Ase⁻ neuroblast produce Ase⁺ intermediate progenitors? To test whether PAN neuroblasts stochastically produce Ase⁻ and Ase⁺ daughters, we examined PAN clones with telophase neuroblasts. All PAN neuroblasts observed generate Ase⁻ daughters (n=7 telophase neuroblasts, Fig. S3A). This indicates that the Ase⁺ progeny in the clone must arise from these

A: Mitotic index of central brain neuroblasts

stage	Ase ⁺			PAN		
	total NB	mitotic NB	mitotic index	total NB	mitotic NB	mitotic index
48 hr ALH	260	71	27%	84	18	21%
72 hr ALH	276	66	24%	81	23	28%
96 hr ALH	491	139	28%	94	20	22%

B: Composition of wild type neuroblast clones

clone type	n	Ase ⁻ Elav ⁻ (2° NB)	Ase ⁺ Elav ⁻ (2° NB and GMC)	Ase ⁻ Elav ⁺ (neuron)	divisions (GMC+neuron/2)
Ase ⁺ 24-hr	13	0	7.5 ± 0.6	20.3 ± 1.2	17.7 ± 0.7
Ase ⁺ 48-hr	5	0	5.4 ± 0.5	52.2 ± 3.6	31.5 ± 2.0
PAN 24-hr	9	3.4 ± 0.2	21.0 ± 1.6	2.1 ± 0.7	ND
PAN 48-hr	5	2.2 ± 0.2	47.0 ± 3.1	82.2 ± 4.8	ND

clone type	n	Ase ⁻ nPros ⁻ (2° NB)	Ase ⁺ nPros ⁻ (2° NB)	Ase ⁺ Pros ⁺ (GMC)	Ase ⁻ Pros ⁺ (neuron)
PAN 24-hr	5	4.0 ± 0.3	9.4 ± 0.5	7.8 ± 1.2	2.2 ± 0.6
PAN 48-hr	4	3.3 ± 0.3	27.5 ± 1.7	22.8 ± 2.7	90.3 ± 3.8

C: Composition of 24-hr *brat192* or *numb15* neuroblast clones

clone type	n	Elav ⁻	Elav ⁺	divisions (GMC+neuron/2)
<i>brat</i> , Ase ⁺	10	8.3 ± 0.6	14.3 ± 2.3	15.5 ± 1.1
<i>brat</i> , PAN	10	10.0 ± 0.7	0.0 ± 0.0	ND
<i>numb</i> , PAN	11	11.5 ± 1.5	0.0 ± 0.0	ND

Table 1. (A) Staged larvae were stained for Ase, phalloidin, and phospho histone H3 to quantify the mitotic index. (B) Cell composition of MARCM clones stained for Ase and Elav (upper part) or Ase and Pros (lower part). All cells in the clone were counted and then tabulated according to the indicated marker profile. For PAN neuroblasts, we focused on the medial population. nPros: nuclear Pros. (C) Cell composition of MARCM clones stained for Ase and Elav. Error here and above is standard error of the mean. ND: not determined because GMCs and/or neurons are not specifically detected.

Ase⁻ cells. We next tested whether the Ase⁻ daughters become quiescent or remain Ase⁻ for a long time. For this, we made use of the observation that daughter cell position correlates with time of birth: recently born daughters are near the primary neuroblast, while daughters born 1 or 2 days ago (or descendents of those daughters) tend to be several cell diameters away (compare figure 5C and 5D). If Ase⁻ daughters remain Ase⁻ for longer than 24 hours, we would expect to see them far from the PAN neuroblast in 48-hr clones. We quantified this distance and found that 20% of Ase⁻ daughters are one cell diameter away from the PAN neuroblast, and 80% of them directly contact it (n=9 48-hr clones and 20 Ase⁻ daughters). The position near the PAN neuroblast suggests that all Ase⁻ daughters were born relatively recently, and the absence of Ase⁻ daughters in positions occupied by older progeny indicates that Ase⁻ status is not maintained. The most likely possibility is that these cells become Ase⁺. This data does not directly rule out the possibility that Ase⁻ daughters are quiescent. We therefore stained PAN clones with anti-Cyclin E (CycE). CycE marks some Ase⁻ daughter nuclei, indicating they are cycling cells (Fig. S3B). We conclude that the PAN neuroblast produces Ase⁻ daughters that remain Ase⁻ for a limited period of time before becoming Ase⁺ intermediate progenitors.

To determine the identity of the Ase⁺ intermediate progenitors, we stained 48-hr neuroblast clones with anti-Pros and anti-Ase antibodies. Pros is present in the nuclei of GMCs and neurons but never nuclear in neuroblasts (Bello et al., 2006; Betschinger et al., 2006). Correspondingly, in Ase⁺ neuroblast clones, neuroblasts appear Ase⁺Pros⁻, GMCs appear Ase⁺Pros⁺ and neurons Ase⁻Pros⁺ (Fig. 6A). Unlike the daughters of Ase⁺ neuroblasts, many daughters of PAN neuroblasts do not import Pros to the nucleus. Of these daughters, 2 or 3 are Ase⁻, and many more are Ase⁺ (Fig. 6B at 0 μm, Table 1B). There are also Ase⁺Pros⁺ GMCs (Fig. 6B at -1 μm, Table 1B). Absence of nuclear Pros is consistent with a neuroblast-like cell type. To investigate this further, we checked the expression of neuroblast markers Deadpan (Dpn) and CycE in the PAN lineage. Dpn and CycE are typically confined to one or two adjacent daughters in Ase⁺ neuroblast lineages (data not shown, (Bello et al., 2006; Betschinger et al., 2006; Lee et al., 2006c)). In PAN lineages, Dpn and CycE maintain high levels of expression in large numbers of progeny (Fig. 6C, 6D). This implies that many of these daughters could be secondary neuroblasts.

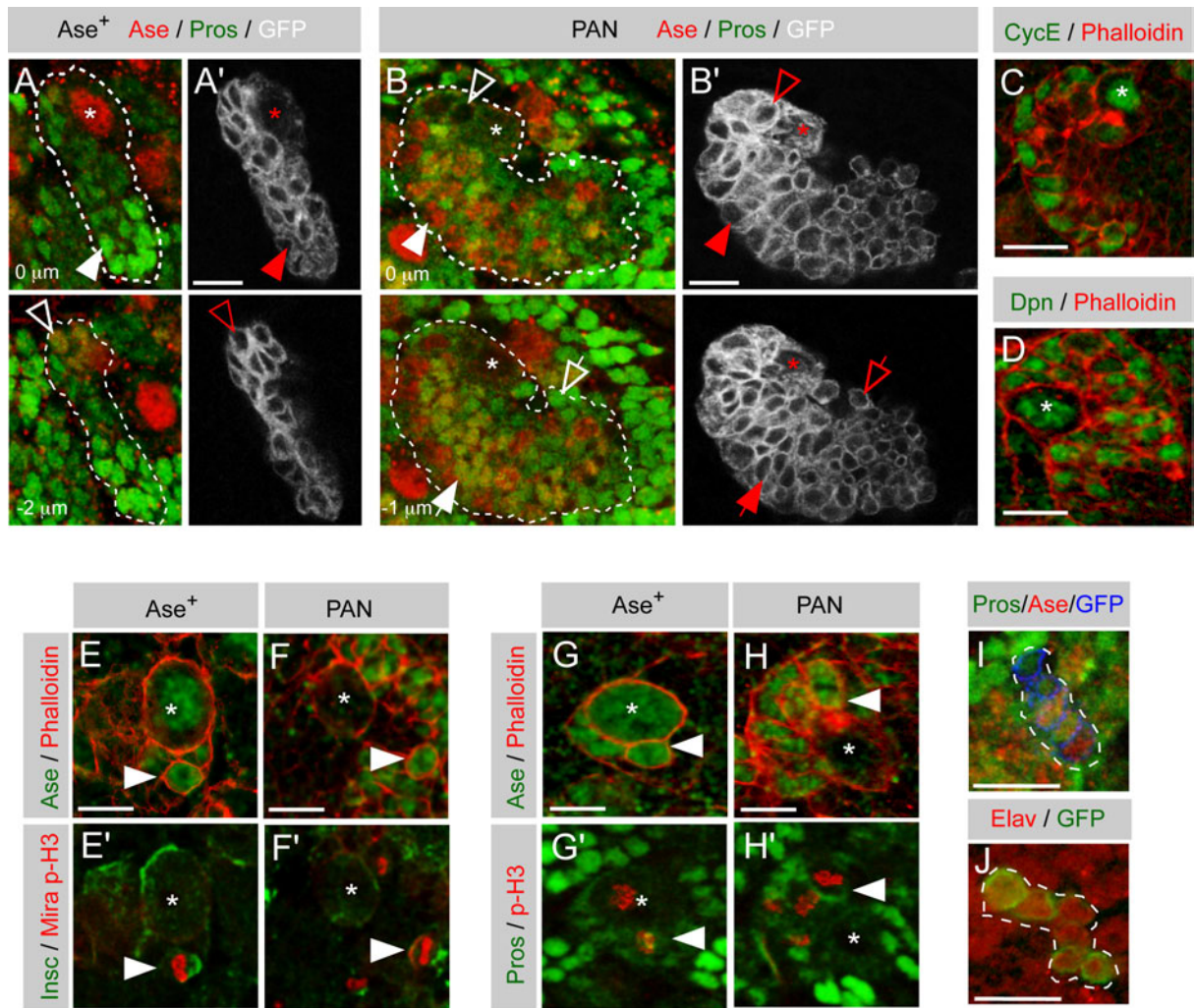


Figure 6. PAN lineages contain secondary neuroblasts

Immunostainings of larval brains labeled with indicated markers (gray boxes). Primary neuroblasts are marked with a star. **(A-B)** 48-hr MARCM clones in central brain neuroblasts. Two separate optical sections from a Z-stack through each clone are shown. Neuroblast clones are reported by GFP expression. **(A, A')** *Ase*⁺ neuroblasts exclude *Pros* from the nucleus, and generate *Ase*⁺*Pros*⁺ GMCs (open arrowhead) and *Ase*⁻*Pros*⁺ neurons (closed arrowhead). **(B, B')** PAN neuroblasts do not have nuclear *Pros*. All *Ase*⁻ (open arrowhead) and many *Ase*⁺ (closed arrowhead) daughters do not have nuclear *Pros*. GMCs are *Ase*⁺*Pros*⁺ (closed arrow) and neurons are *Ase*⁻*Pros*⁺ (open arrow). **(C-D)** Many PAN neuroblast progeny express the neuroblast markers *CycE* **(C)** and *Dpn* **(D)**. **(E-H)** Neuroblast daughter cells in mitosis (arrowheads). *Mira* is not present in mitotic GMCs **(E')** but segregates asymmetrically in some progeny of the PAN neuroblast **(F')**. Similarly, *Pros* is cytoplasmic in mitotic GMCs **(G')** but asymmetric cortical in some PAN progeny **(H')**. **(I-J)** 24-hr **(I)** and 48-hr **(J)** secondary neuroblast clones contain multiple *Ase*⁺ cells **(I)** and multiple neurons **(J)**. Scale bars: 10 μm.

To find out if the presumptive secondary neuroblasts divide asymmetrically, we analyzed the localization of several proteins known to regulate asymmetric divisions in embryonic and larval neuroblasts. Mitotic GMCs localize Insc to a cortical crescent but not Mira because Mira is degraded after GMC birth (Fig. 6E, E', (Ikeshima-Kataoka et al., 1997; Matsuzaki et al., 1998; Schuldt et al., 1998; Shen et al., 1997)). In the PAN lineages, some daughters maintain cortical Mira (Fig. S4B) and, like neuroblasts, localize Insc and Mira to opposing crescents in mitosis (Fig. 6F'). Similar observations were made for Pros, which is dispersed in the cytoplasm of mitotic GMCs, but forms a crescent in some mitotic progeny of the PAN lineage (Fig. 6G', 6H'). Furthermore, Brat, Numb, and aPKC all show asymmetric localization in the presumptive secondary neuroblasts (Fig. S4C-E), and asymmetrically sized divisions occur in these cells as well (Fig. 5D, arrowhead). All of these observations strongly suggest that the Ase⁺ cells without nuclear Pros are indeed asymmetrically dividing secondary neuroblasts.

If the secondary neuroblasts divide in a self-renewing manner, they should generate MARCM clones with greater than 4 neurons. We therefore searched for these clones in the posterior medial brain. Besides the PAN clones, many clones in this region consist of 1 or 2 Elav⁺ cells (data not shown), the clone type predicted by an origin in GMCs. It is also possible to observe clones in this region with multiple Ase⁺ cells (Fig. 6I) or clones with more than 4 Elav⁺ cells (Fig. 6J). Due to the low frequency of MARCM clone induction, it is unlikely that these multi-cell clones are overlapping GMC clones. Instead, they probably arise from sequential, GMC-producing divisions of the small neuroblast-like cells. Since some clones consist exclusively of multiple Elav⁺ cells, secondary neuroblasts may eventually divide terminally or die. These findings indicate that a PAN neuroblast divides asymmetrically to produce a secondary neuroblast. The secondary neuroblast is initially Ase⁻, but it eventually upregulates Ase and divides asymmetrically to self-renew and generate a GMC.

To test whether such a lineage could produce the observed cell types in PAN clones, we made a computational model of the PAN lineage. The program tracked the numbers of the various cell types over time, starting with an initial division of the PAN neuroblast at time $t = 0$. This was done by looping simple, partially-recursive population functions according to division rate and latency time parameters (see supplementary methods for additional details). Using the model, we were able to determine a limited range of time for each event in the proposed PAN neuroblast lineage that returned values in good agreement with the observed cell populations at 24 and 48 hours (Fig. 9). We conclude from this that the proposed lineage

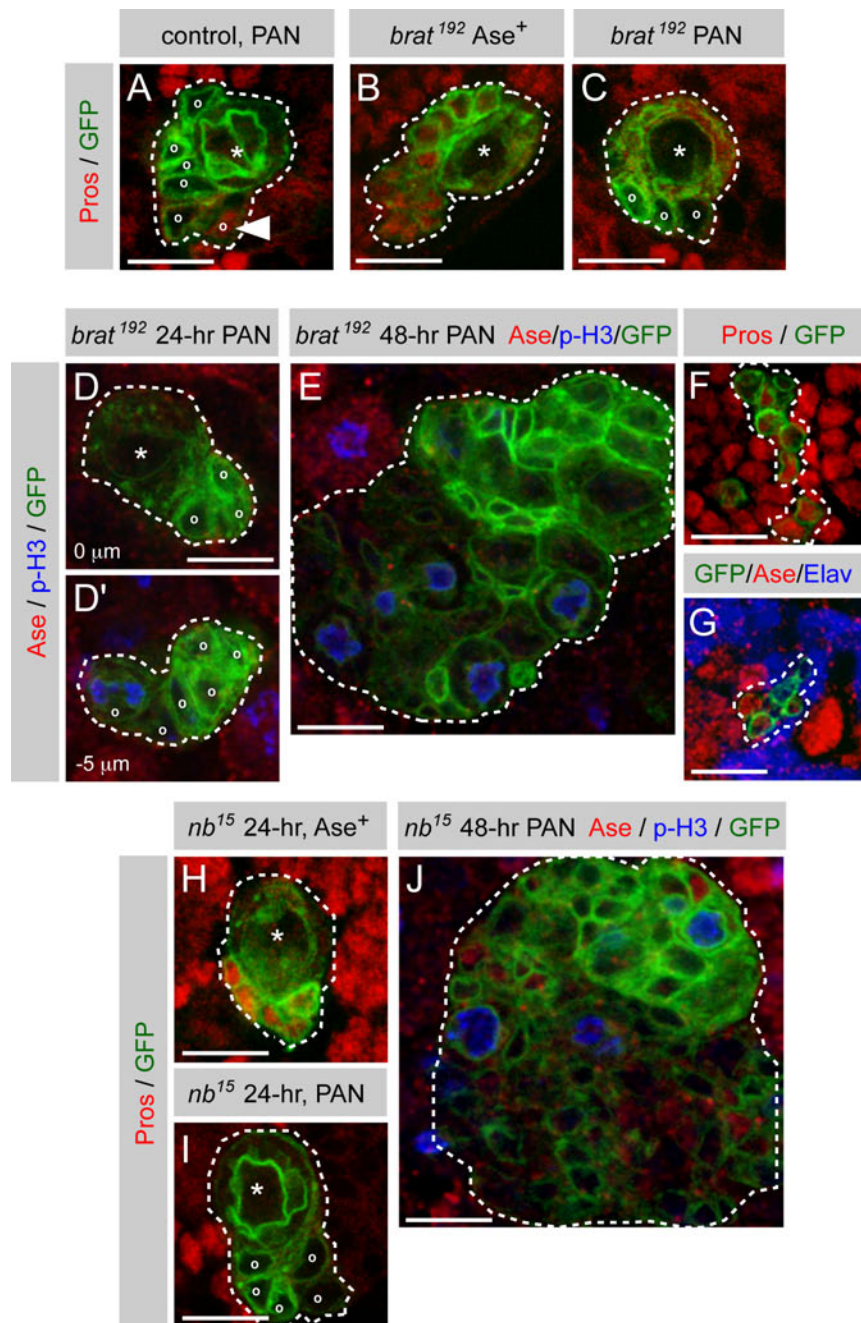


Figure 7. Immature Ase⁻ secondary neuroblasts enter mitosis in *brat*

Immunostainings of MARCM clones reported by GFP expression and labeled with indicated markers (gray boxes). Stars indicate primary neuroblasts and circles indicate daughter cells. (A-C) Pros in 24-hr clones. In wild type PAN clones, Pros is nuclear in some daughters (A, arrowhead). In *brat* Ase⁺ clones, Pros is nuclear in all daughters (B), but in *brat* PAN clones, no daughters have nuclear Pros (C). (D, E) Mitotic Ase⁻ cells in *brat* PAN clones. In 24-hr clones, Ase⁻ secondary neuroblasts enter mitosis (D'). In 48-hr clones, mitotic Ase⁻ cells increase in size and number (E). (F-G) *brat* secondary neuroblast clones. Differentiated Pros⁺ (F) Ase⁺ and Elav⁺ (G) cells are created in the absence of *brat*. (H-J) *numb* clones. In 24-hr *numb* Ase⁺ clones, all daughters have nuclear Pros (H). Pros is not nuclear in daughters of *numb* PAN neuroblasts (I). Ase⁻ daughters enter mitosis in *numb* 48-hr PAN clones. Scale bars: 10 μm.

can plausibly generate the numbers of secondary neuroblasts, GMCs, and neurons observed in PAN clones.

4.3.4. *brat* secondary neuroblasts fail to progress beyond the immature Ase^- state

To investigate the initial events leading to overgrowth in *brat* PAN lineages, we analyzed 24-hr *brat* MARCM clones. *brat* clones in Ase^+ neuroblast lineages do not overgrow (Fig. 7B, Table 1C), confirming that these lineages are unaffected by loss of Brat. Surprisingly, *brat* clones in PAN lineages show an undergrowth phenotype at 24 hours – they contain about half the number of progeny as wild type clones (Fig. 7C, Table 1C). We determined the identity of the *brat* daughters by staining with anti-Pros. In wild type PAN clones, some cells import Pros into the nucleus (Fig. 7A, Table 1B), showing that after 24 hours secondary neuroblasts divide and give rise to $Pros^+$ GMCs and neurons. In *brat* PAN clones, no progeny have nuclear Pros, suggesting all are secondary neuroblasts (Fig. 7C). While other groups report similar findings on the absence of nuclear Pros in *brat* (Bello et al., 2006; Lee et al., 2006c), we use Pros staining simply to discriminate neuroblasts from more differentiated cells. If the *brat* secondary neuroblasts entered mitosis, we would expect to see far more than the 10 progeny produced in 24 hr-clones. This implies a cell cycle block in *brat* secondary neuroblasts. In agreement with this, previous work shows that *brat* neuroblasts generate progeny that are cell cycle delayed (Lee et al., 2006c).

To investigate the nature of the cell cycle block, we checked the expression of cell cycle markers in the larval brain. Mitotic central brain neuroblasts express the G1-S transition markers CycE and E2F1, and these proteins associate with segregating DNA in late telophase (Fig. S5A-B). This should cause the larval neuroblast and its daughter to enter S phase shortly after cytokinesis, similar to embryonic neuroblasts (Weigmann and Lehner, 1995). To analyze the kinetics of this in greater detail, we stained clones containing telophase PAN neuroblasts with anti-E2F1, which does not label S-phase cells, and with anti-CyclinA (CycA), a marker for S and G2 phases (Reis and Edgar, 2004). In wild-type clones, the E2F1-positive daughter being born is located near other daughters with low or undetectable levels of E2F1 (Fig. S5C). Since the PAN neuroblast always directs the birth of its daughter towards a group of Ase^- secondary neuroblasts (Fig. S3, n=7 telophase PAN neuroblasts), it is likely that the daughters with low E2F1 are both Ase^- and recently born. The low E2F1 indicates a rapid entry into S phase by the Ase^- secondary neuroblast shortly after its birth. This is followed by accumulation of CycA and re-expression of E2F1, indicating progression to G2 (Fig. S5C and

S5C'). Importantly, we observe the same events in *brat* secondary neuroblasts, so they must also progress through S phase (Fig. S5D). Therefore, we conclude that the cell cycle delay in *brat* secondary neuroblasts occurs in G2. Since the number of progeny in the 24-hr *brat* clone is small (Table 1C), the block could be maintained for around 24 hours.

In order to find out why the cell cycle is blocked in *brat* secondary neuroblasts, we analyzed other regulators of cell proliferation. The pro-growth and proliferation protein dMyc is present in both wild-type and *brat* secondary neuroblasts (Fig. S6), indicating the delay is not due to lack of growth stimulus. The Cdk inhibitor Dacapo (Dap) could potentially slow the cell cycle, but we did not detect Dap in *brat* secondary neuroblasts (data not shown). To test whether the delay is caused by a defect in the differentiation of secondary neuroblasts, we checked the expression of Ase. In wild type PAN clones, Ase is upregulated some time after daughter cell birth (Fig. 5C). In *brat* mutant PAN clones, upregulation of Ase never occurs (Fig. 7D). This suggests that the *brat* mutant secondary neuroblasts have not fully matured. Collectively, these observations show that loss of Brat does not impede secondary neuroblast entry into S phase, but it does prevent upregulation of Ase. This triggers a G2 block in the Ase⁻ secondary neuroblast.

4.3.5. Immature Ase⁻ secondary neuroblasts enter mitosis in *brat*

A terminal cell cycle delay in an immature secondary neuroblast would not produce overgrowth in *brat*. Therefore, we checked whether the Ase⁻ secondary neuroblasts ever entered mitosis in *brat* clones. In wild type PAN lineages, Ase⁻ secondary neuroblasts are never positive for phospho-histone H3 (Fig. 5D, 5D', and data not shown). In 24-hr clones in *brat* PAN lineages, we occasionally observe Ase⁻ secondary neuroblasts in mitosis (Fig. 7D'). Although all cells in the clone are Ase⁻, it is possible to distinguish secondary neuroblasts from PAN neuroblasts by size: the PAN neuroblast has a cell diameter greater than 10 μm , while secondary neuroblasts have a diameter of around 5-7 μm . Mitosis in an immature secondary neuroblast with a deregulated cell cycle may be the event that initiates *brat* mutant overgrowth. By the 48-hr time point, mitotic Ase⁻ cells have increased in size and number (Fig. 7E). Most cells in the *brat* clone remain Ase⁻, showing that the daughters of the mitotic Ase⁻ cells also fail to upregulate Ase and differentiate.

Could the mitotic immature secondary neuroblast be solely responsible for the *brat* overgrowth? The *brat* PAN neuroblast cannot generate the bulk of the cells, since it produces

only 10 cells in 24 hours (Table 1C) and the 48-hr *brat* clone contains over 100 cells (124 ± 14 cells, $n=5$ clones). If *brat* mutant Ase^+ secondary neuroblasts or GMCs cause overgrowth, we should be unable to detect MARCM clones with more than 1 neuron. However, we regularly observe *brat* clones containing multiple $Elav^+$, $Pros^+$, and Ase^+ cells in the medial central brain (Fig. 7F, 7G). This leaves the Ase^- secondary neuroblast as the likely origin of the overgrowth. We conclude from these observations that the earliest events in *brat* overgrowth are failure to achieve Ase^+ secondary neuroblast status and cell cycle block in G2. Escape from the block and completion of mitosis in the immature Ase^- secondary neuroblast establishes a lineage that is unable to produce differentiated daughter cells (Fig. 7E). We propose that these events are the source of the overgrowing neuroblasts characteristic of *brat* mutant brains.

4.3.6. Notch signaling regulates secondary neuroblasts in PAN lineages

We have shown that loss of *Brat* causes defective differentiation in transit-amplifying secondary neuroblasts and this leads to overgrowth. It is therefore critical to understand how this transit-amplifying lineage is specified and regulated. In some mammalian transit-amplifying stem cells lineages, Notch controls proliferation and differentiation (Wilson and Radtke, 2006). Furthermore, in *Drosophila* larval brains, mutation in *numb*, an antagonist of Notch, causes overgrowth and production of ectopic neuroblasts (Lee et al., 2006a; Wang et al., 2006). To test whether misregulation of Notch signaling causes defects in the transit-amplifying PAN lineages, we generated *numb* MARCM clones. In Ase^+ neuroblast lineages, *numb* loss of function does not affect production of differentiated GMCs and neurons (Fig. 7H and S7A). By contrast, *numb* mutant 24-hr PAN clones contain secondary neuroblasts delayed in G2 (Fig. 7I, Table 1C, and Fig. S5E). This phenotype is identical to that caused by loss of *Brat*. Similarly, 48-hr PAN clones mutant for *numb* are filled with undifferentiated Ase^- cells (Fig. 7J, Fig. S7B). This indicates that *Numb* is required to promote the maturation of Ase^- secondary neuroblasts, perhaps by downregulating Notch signaling. To check whether ectopic activation of Notch generally causes overgrowth of the PAN lineage, we expressed the Notch intracellular domain (N^{intra}) in all neuroblasts using *insc-Gal4*. Because it is lethal at embryonic stages, we restricted N^{intra} expression to the larval stages using *Gal80^{ts}*. Consistent with previous results (Wang et al., 2006), we observed that upon N^{intra} overexpression, the brain becomes filled with PAN neuroblasts (Fig. S7D). A similar phenotype is observed when Notch is hyperactivated through loss of function of *lgd* (Fig. S7E), a gene required for protein trafficking of the Notch receptor and downregulation of Notch signaling (Gallagher and

Knoblich, 2006; Jaekel and Klein, 2006). These results show that overactivation of Notch leads to the production of ectopic PAN neuroblasts, probably by interfering with differentiation in the PAN lineages.

Since Notch overactivation results in ectopic PAN neuroblasts, we tested whether Notch loss of function would result in too few PAN neuroblasts. For this, we used *insc-Gal4*, *Gal80^{ts}*, and transgenic Notch RNAi to deplete Notch in all neuroblasts (Fig. S8). Knockdown of Notch has two different effects on PAN lineages: it either eliminates them entirely or reduces the number of associated *Ase*⁺ progeny (Fig. S7G). Similarly, we observe complete absence of PAN lineages when Notch signaling is inhibited by expressing *Numb* in all neuroblasts (Fig. S7H). We conclude from these results that Notch signaling must be active in the PAN neuroblast and the secondary neuroblasts to produce a wild type lineage, but overactivation of Notch causes uncontrolled division of *Ase*⁻ secondary neuroblasts.

4.3.7. Prospero acts after Brat and Numb in the PAN lineage

Since loss of *Brat* or *Numb* causes defects only in PAN lineages, we investigated whether this is also true for the cell fate determinant *Pros*. The absence of nuclear *Pros* in *brat* clones has led to a model where *Brat* exerts its effects on cell fate by regulating *Pros* (Bello et al., 2006; Lee et al., 2006c). If this is true, then loss of *Brat* and loss of *Pros* should have comparable consequences. We tested this by generating *pros* MARCM clones. In *Ase*⁺ lineages, *pros* clones fail to produce significant numbers of *Elav*⁺ neurons in 77% of clones examined (n=26 *Ase*⁺ clones; Fig. 8A, 8B), a phenotype distinct from *brat* or *numb*. In the PAN lineages, loss of *Pros* results in production of many *Ase*⁺ progeny but almost no *Elav*⁺ cells (Fig. 8C, 8D). These results confirm that *Pros* is required to make differentiated neurons (Bello et al., 2006; Betschinger et al., 2006; Choksi et al., 2006; Lee et al., 2006c). The presence of *Ase*⁺ progeny in the *pros* mutant PAN lineage indicates a requirement for *Pros* only after the transition from *Ase*⁻ to *Ase*⁺ secondary neuroblast status. We conclude that *Pros* acts at a later time point in the PAN lineage than *Brat*. Consistent with this, *pros-Gal4* is not detectably expressed in PAN neuroblasts or *Ase*⁻ secondary neuroblasts, and it becomes visible only in *Ase*⁺ secondary neuroblasts (Fig. 8E, 8F). We cannot exclude that *pros* transcription in the PAN neuroblasts and *Ase*⁻ secondary neuroblasts requires a promoter not contained in *pros-Gal4*. Still, since loss of *Brat* and loss of *Pros* cause fate misspecification in different cell types, these results demonstrate that *Brat* does not act exclusively by regulating *Pros*.

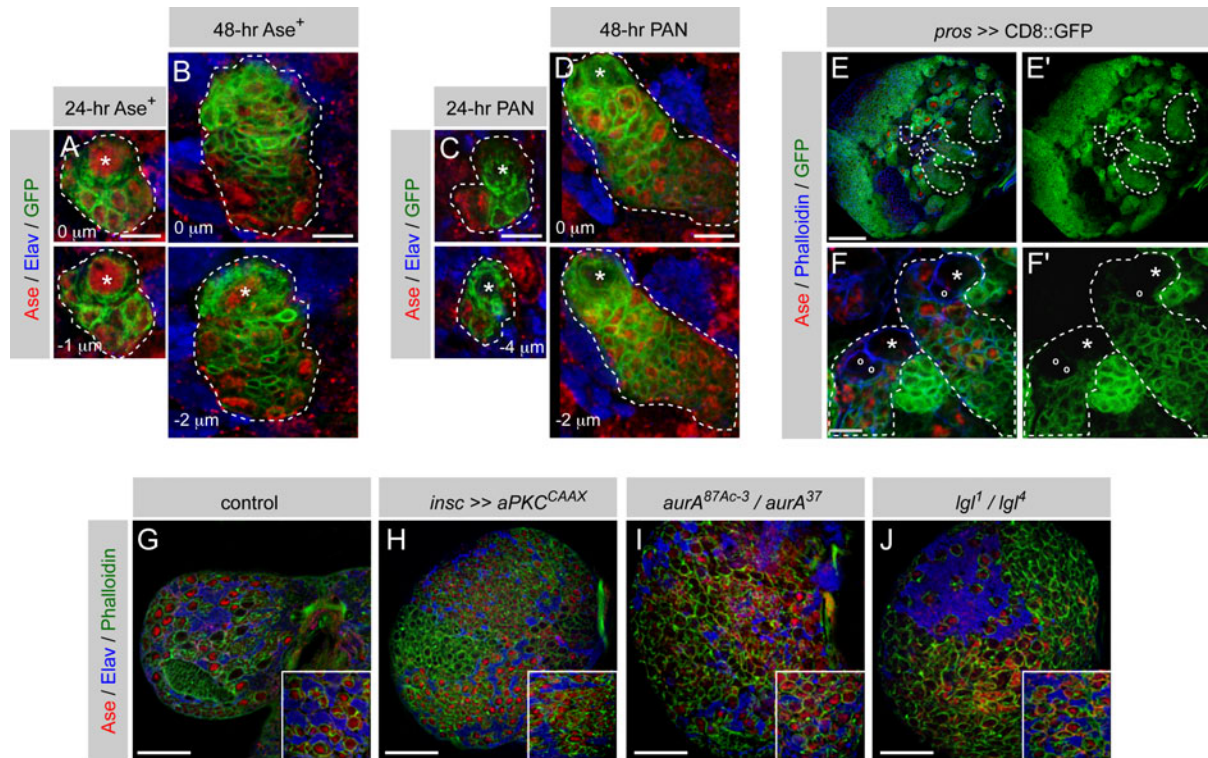


Figure 8. Pros is not required for maturation of secondary neuroblasts

Immunostainings labeled with indicated markers (gray boxes). (A-D) *pros* MARCM clones reported by GFP expression. Stars indicate primary neuroblasts. Two separate optical sections from a Z-stack through each clone are shown. Loss of Pros in *Ase*⁺ lineages results in failure to generate neurons (A, B). In PAN lineages, Pros is not required to generate *Ase*⁺ daughters, but neurons fail to differentiate (C, D). (E-F) *pros*-Gal4 expression reported by GFP. *pros*-Gal4 is not expressed in the PAN neuroblasts (E) or their *Ase*⁻ daughters (circles, F). (G-J) PAN lineage behavior in other tumor models. Early third instar larval brains. Insets: *Ase*⁺ neuroblasts of the ventral nerve cord. Expression of membrane-targeted aPKC (H) or loss of AurA (I) results in overgrowth in both *Ase*⁺ and PAN lineages, but loss of Lgl affects PAN lineages more strongly (J). Scale bars: (A-D, F) 10 μm; (E, G-J) 50 μm.

The different sensitivities of Ase⁺ and PAN neuroblasts to loss of cell fate determinants prompted us to analyze whether brain overgrowth caused by other genetic lesions begin in PAN lineages. Overexpression of membrane-targeted aPKC (aPKC^{CAAX}) (Lee et al., 2006b) and loss of the mitotic kinase *aurora-A* (AurA) (Lee et al., 2006a; Wang et al., 2006) cause overgrowth in both Ase⁺ and PAN lineages (Fig. 8I, 8J), but loss of *lgf* (Betschinger et al., 2006) affects PAN lineages much more strongly than Ase⁺ lineages (Fig. 8K). This may be because aPKC^{CAAX} and *aurA* affect the function of proteins that promote the differentiation of GMCs and secondary neuroblasts, while *lgf* misregulates proteins required for differentiation of secondary neuroblasts more severely. We conclude that while PAN lineages contribute to a general neuroblast overgrowth phenotype in the aPKC^{CAAX} and *aurA* brains, they are primarily responsible for the overgrowth in *lgf* mutants.

4.4. DISCUSSION

It was previously thought that all daughters of *Drosophila* neuroblasts are GMCs. We show that several neuroblasts in the *Drosophila* larval brain repress Ase and produce daughters that behave like secondary neuroblasts. The proteins Brat and Numb act to promote the progression of recently born secondary neuroblasts from an Ase⁻ to an Ase⁺ status. Once the secondary neuroblast becomes Ase⁺, it begins to divide and produce GMCs. In the absence of Brat or Numb, the transition from Ase⁻ to Ase⁺ secondary neuroblast fails to occur, and the Ase⁻ secondary neuroblast enters mitosis. This incorrectly specified mutant daughter cell is unable to make differentiated progeny, and it initiates overgrowth of neuroblast-like cells in the larval brain.

4.4.1. Ase and transit-amplifying neuroblast lineages

Ase is best known for its role as a neural precursor gene, so its absence from any neuroblast is surprising. Three mechanisms are known to downregulate expression of Ase. One is transcriptional repression mediated by Pros (Choksi et al., 2006). Since Pros is not nuclear in neuroblast nuclei, it is unlikely to repress *ase* in the PAN neuroblasts. The transcription factor Tramtrack (Ttk) also represses *ase* transcription (Badenhorst et al., 2002), and we analyzed the reporter line *ttk0219* to see if *ttk* expression correlated with the PAN lineage. Although the *ttk* reporter is active in some PAN neuroblasts, it is also active in many Ase⁺ neuroblasts, suggesting that *ttk* transcription is not sufficient for specifying PAN identity (data not shown). Finally, Notch signaling can indirectly repress Ase by downregulating expression of two *ase* activators, the transcription factors Achaete and Scute (Oellers et al., 1994; Heitzler et al., 1996). We favor the idea that Notch signaling mediates Ase repression because inhibiting signaling results in elimination of PAN neuroblast lineages (Fig. S7G, S7H). Since all central brain neuroblasts appear to express equal levels of Notch receptor (Fig. S8) and report equal levels of signaling through the reporter construct *gbe+Su(H) lacZ* (data not shown, (Almeida and Bray, 2005)), other factors must undetectably enhance Notch signaling levels in the PAN neuroblast or otherwise act together with Notch to specify PAN identity.

It is unclear why PAN neuroblasts downregulate Ase because there are few known Ase target genes. The three neural precursor cell types known to generate neuroblasts – the embryonic neuroepithelium (Jarman et al., 1993), the optic lobe neuroepithelium (Egger et al., 2007), and now the PAN neuroblast – do not express Ase, although the PAN neuroblast is unique in this group for expressing most other neuroblast markers. In the optic lobe, Ase expression is

correlated with upregulation of Dap and cell cycle exit (Wallace et al., 2000). This probably does not play a role in the central brain since most of the cycling neuroblasts are Ase⁺. Ectopic expression of Ase in imaginal discs upregulates *achaete* and the E3 ubiquitin ligase *neuralized* (Brand et al., 1993), but at first glance, neither of these gene products seem like they would conflict with secondary neuroblast fate. Still, Ase expression is clearly not compatible with the production of transit-amplifying lineages because ectopic Ase abolishes them (Fig. 4B, 4B'). To test whether the inverse is true and downregulating Ase generates supernumerary transit-amplifying neuroblast lineages, we analyzed *ase¹* mutants. Ase protein was gone but additional neuroblasts producing daughters without nuclear Pros were not observed (data not shown). We interpret these results to mean that downregulation of Ase is not an instructive signal for specification of PAN neuroblast identity, but rather a consequence of specification. While failure to express Ase in the secondary neuroblasts might be predicted to lead to overgrowth, as in *numb* or *brat*, we could detect no overgrowth in the *ase* mutant brains. This implies that once the PAN neuroblast daughter is born, Ase is not required to promote the transition from immature to mature secondary neuroblast. Nevertheless, Ase expression is a useful reporter of this cell fate transition.

4.4.2. Numb, Brat, Pros, and transformation of progenitor cells

In the PAN lineage, the most recently born daughter cells are Ase⁻ secondary neuroblasts. This immature state is normally quickly bypassed when the cell becomes an Ase⁺ secondary neuroblast (Fig. 9). Our data indicate that Brat and Numb promote this transition, because in the absence of either protein, the progeny of the PAN neuroblast fail to become Ase⁺. Numb inhibits Notch signaling, so this phenotype shows that downregulation of Notch allows the secondary neuroblast to mature and become Ase⁺. Since loss of Brat and loss of Numb have identical phenotypes in 24-hr clones, does this mean that Brat is also an antagonist of Notch? Two points argue against this hypothesis. First, although Brat is expressed in the *Drosophila* sensory organ precursor and segregates asymmetrically (Betschinger et al., 2006), its loss does not cause any change in daughter cell identity (A. Hutterer and J.A.K., unpublished results). This system is sensitive to levels of Notch signaling, so the result is inconsistent with a role for Brat in the regulation of Notch. Second, unlike overexpression of Numb, overexpression of Brat can not silence reporting through the Notch sensor *gbe+Su(H) lacZ* in the larval brain (data not shown). Thus, Brat does not seem to regulate cell fate by acting through Notch. While we cannot exclude that Brat regulates Notch signaling in a Su(H)-independent manner, the exact molecular function of Brat in this context remains to be discovered.

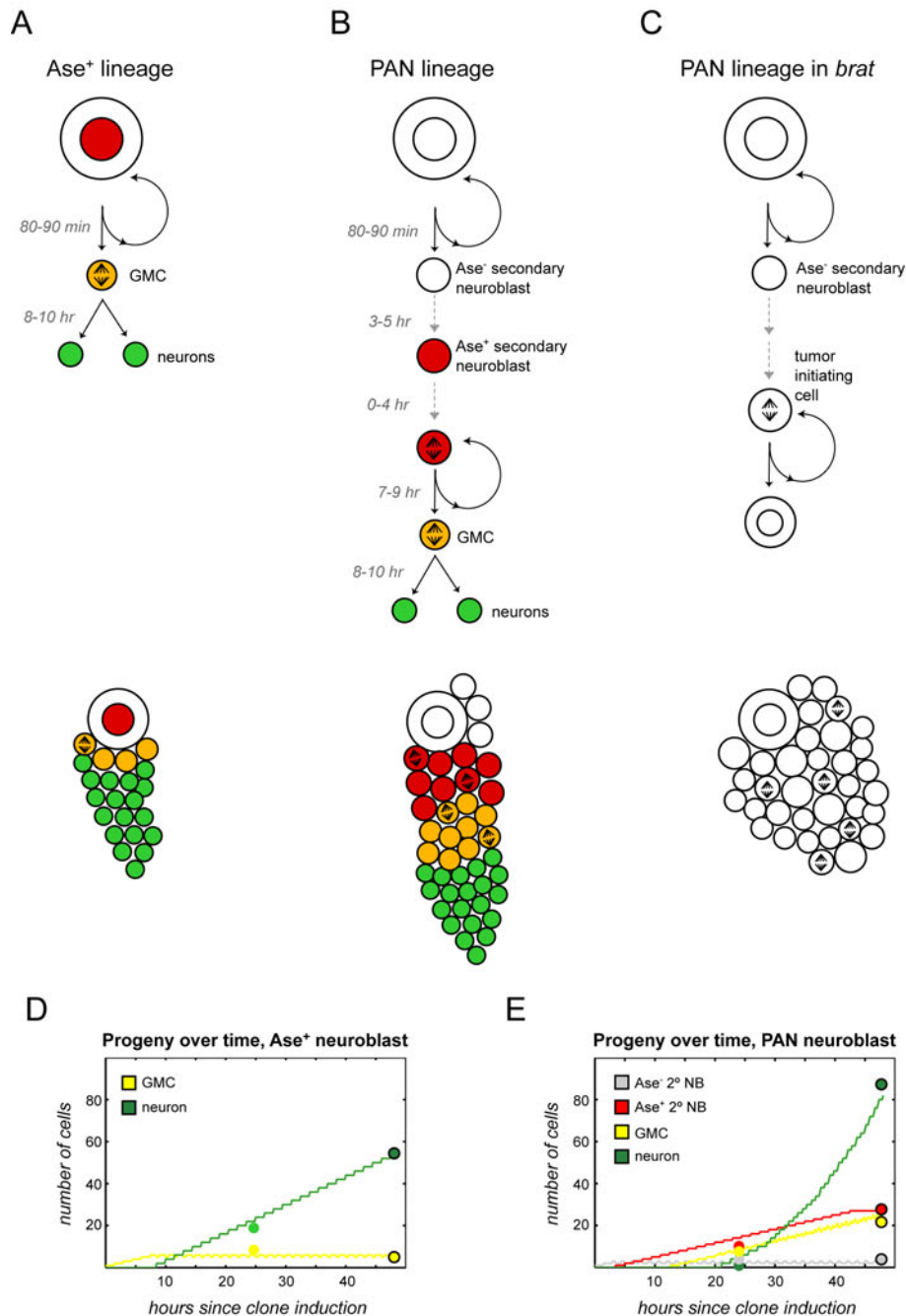


Figure 9. Models of neuroblast lineages in the central brain

(A-C) Lineage diagrams with estimated time for each stage and cartoons of corresponding neuroblast clones. (A) Self-renewing Ase⁺ neuroblasts produce progeny that follow the standard GMC-neuron progression. (B) PAN neuroblasts generate Ase⁻ secondary neuroblasts that mature into self-renewing Ase⁺ secondary neuroblasts. These transit-amplifying cells produce GMCs, which divide terminally to produce two neurons. (C) In the absence of Brat, Ase⁻ secondary neuroblasts are unable to become Ase⁺. Upon mitotic entry, they become tumor-initiating cells. (D-E) Plots showing production of neuroblast progeny over time. Production of neurons in Ase⁺ lineages is linear (D), while production of neurons in PAN lineages is exponential (E). Plots were created using Matlab and computer-modeled neuroblast lineages (see supplemental methods for details). Colored circles correspond the cell numbers recorded in Table 1B.

Loss of Brat and Numb may cause identical phenotypes in the PAN lineage not because they have identical functions, but because of the nature of the Ase⁻ secondary neuroblast. In the Ase⁺ neuroblast lineage, Pros is imported into the nucleus of the neuroblast daughter. One cell fate determinant in addition to Pros is enough to establish GMC fate, because loss of Brat or Numb alone does not prevent neural differentiation (Fig. 4G, 4I, 7B, 7H, S7A). In the PAN lineage, the Ase⁻ secondary neuroblast does not have nuclear Pros, so it uses only Brat and Numb to make it different from its mother. For this reason it may be more sensitive to loss of either cell fate determinant. Additionally, besides small size and increased levels of Brat and Numb inherited at the time of its birth, we did not find a single molecular marker that makes the Ase⁻ secondary neuroblasts different from PAN neuroblasts. This suggests the Ase⁻ secondary neuroblast may not yet be strongly committed to its fate. While this unstable state is normally bypassed when the cell becomes an Ase⁺ secondary neuroblast, in the absence of Brat or Numb, the weak commitment of the Ase⁻ secondary neuroblast may ensure that no matter which protein is lost, the result will be identical: it reverts to a fate similar to its mother's. Instead of becoming a transient-amplifying progenitor, the Ase⁻ secondary neuroblast commits to unlimited self-renewal. Because this occurs in a cell that may not express Pros (Fig. 8F), mitosis therefore begins the production of cells unable to differentiate (Fig. 9). This could explain why *brat* neuroblasts do not appear to express Pros or segregate it asymmetrically (Bello et al., 2006; Betschinger et al., 2006), and could also explain why expressing Pros rescues *brat* tumors. The defect in the lineage caused by *brat* – mitosis in cells not expressing Pros – is now repaired. We propose that blocking full commitment to the intermediate progenitor fate and allowing mitosis in a mis-specified daughter may be a general mechanism for causing overgrowth in a transit-amplifying lineage. While transit-amplifying lineages offer the possibility to produce differentiated cells at a faster rate than stem cell lineages without intermediate progenitors (Fig. 9D, 9E), this may always come with a higher risk of tumorigenesis. Our data suggest that specification of secondary neuroblast fate is a genetic weak point.

4.5. EXPERIMENTAL PROCEDURES

Fly Strains

Fly strains used were 1407-Gal4 inserted in the *insc* promoter (Betschinger et al., 2006); UAS *ase* (Brand et al., 1993); UAS *brat* RNAi (Dietzl et al., 2007); *ase*-Gal4 (Zhu et al., 2006); FRT40A, *brat*¹⁹² (Betschinger et al., 2006); FRT40A, *brat*¹⁵⁰ (Betschinger et al., 2006); FRT40A, *numb*¹⁵ (Berdnik et al., 2002; Bhalerao et al., 2005); FRT82B, *pros*¹⁷ (Doe et al., 1991); UAS CD8::GFP (Bloomington stock center); MARCM stocks using C155-Gal4 (Lee et al., 1999); *pros*-Gal4 (a gift from F. Matsuzaki); FRT40A, *Igl*^I and FRT40A, *Igl*^d (from F. Matsuzaki); FRT82B, *aurA*^{87Ac-3} and FRT82B, *aurA*³⁷ (Berdnik and Knoblich, 2002); UAS *aPKC*^{CAAXWT} (Sotillos et al., 2004). To prevent embryonic lethality some UAS constructs were expressed with 1407-Gal4 and Gal80^{ts} (Bloomington stock center 7018) and reared at 18 degrees until larval stages. Then larvae were incubated at 29 degrees for 3 days to allow expression of the transgene. All other transgenes were expressed at 25 degrees.

Antibodies

Antibodies used were guinea pig anti-Ase (affinity purified, 1:100, (Bhalerao et al., 2005)), mouse anti-Elav (1:100, Developmental Studies Hybridoma Bank, University of Iowa [DSHB]), rat anti-Elav (1:300, DSHB), mouse anti-Pros (1:10, DSHB), guinea pig anti-Dpn (1:1000, gift from J. Skeath), mouse anti-CycE (1:100, H. Richardson), rabbit anti-Mira (1:100, (Betschinger et al., 2006)), rabbit anti-phospho histone H3 (1:1000, Upstate), mouse anti-Insc (1:100, (Schaefer et al., 2001)).

Immunohistochemistry

To generate MARCM clones, larvae were heat shocked in Eppendorf tubes for 90 min at 37 degrees, then allowed to recover for 24 or 48 hours on fly food at 25 degrees. Other genotypes were dissected as wandering third instar larvae unless otherwise noted. Larval brains were dissected in PBS, fixed in 5% paraformaldehyde in PBS for 20 minutes, and blocked using 2% normal donkey serum in PBS with 0.05% Triton-X-100. Brains were incubated with primary antibody overnight and labeled using standard methods, then mounted in Vectashield or (Vector Laboratories). To visualize cortical actin, we used rhodamine Phalloidin (Molecular Probes) or Alexa 488 Phalloidin (Molecular Probes). Secondary antibodies were conjugated to Alexa 405, Alexa 488, Alexa 568 (all from Molecular Probes) or Cy5 (Jackson Immunofluorescence). Images were recorded on a Zeiss LSM510 confocal microscope.

4.6. SUPPLEMENTARY DATA

Supplementary figures

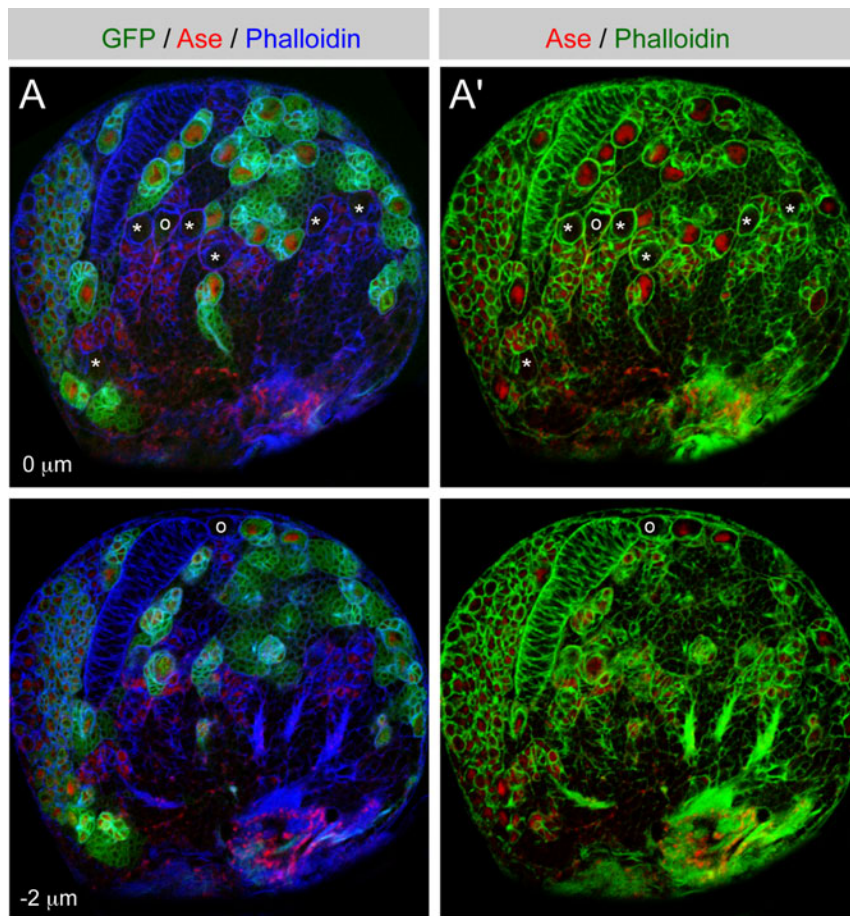


Figure S1. 8 neuroblasts per brain lobe are Ase⁻

Immunostainings of a third instar brain. Two Z-sections from a Z-stack are shown. **(A)** GFP reporting ase-Gal4 expression (green) stained for Ase (red) and Phalloidin (blue). Medial Ase⁻ neuroblasts with surface-level progeny are indicated with a star, Ase⁻ neuroblasts with progeny located in interior brain regions are indicated with a circle. Note that ase-Gal4 is not expressed in the Ase⁺ progeny of the Ase⁻ neuroblasts. **(A')** The same brain, with Ase (red) and Phalloidin (green) only.

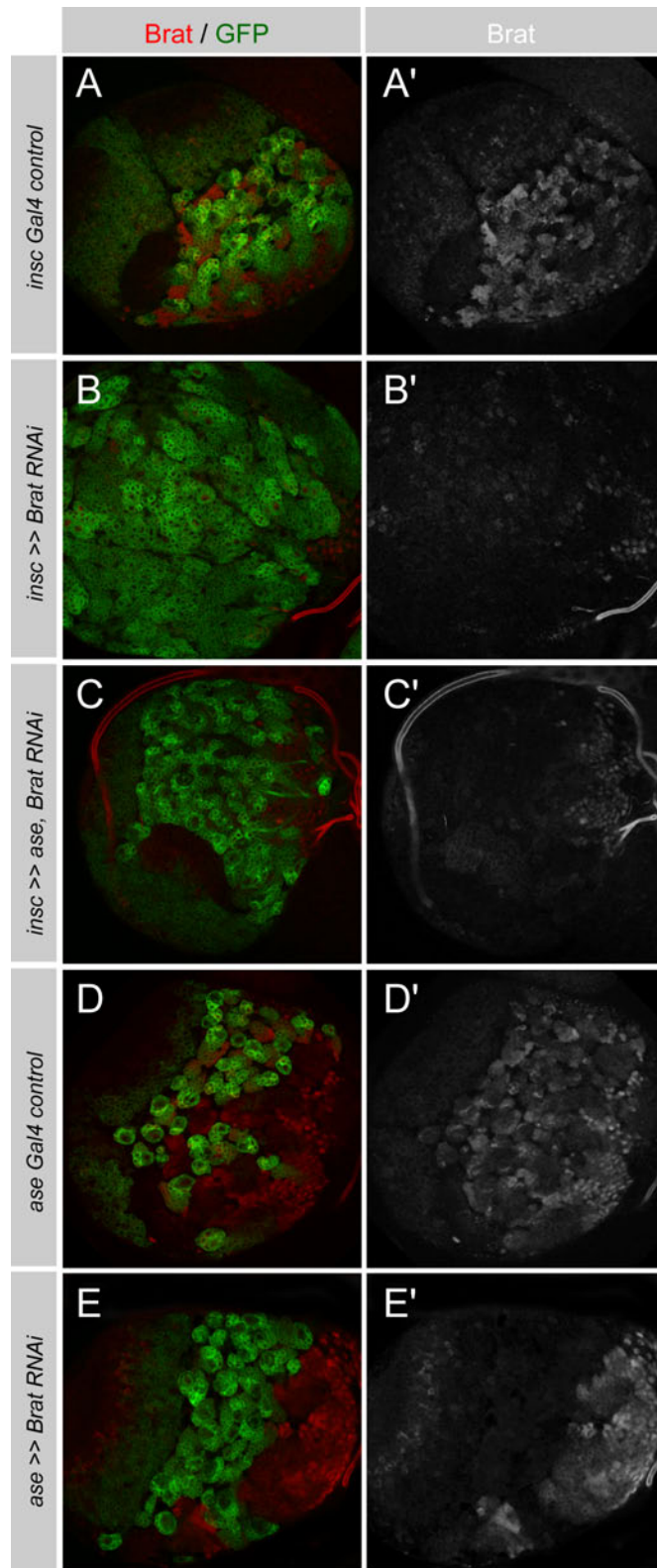


Figure S2. Reduction of Brat protein by knockdown with transgenic RNAi

(A-E) Third instar brains with GFP reporting Gal4 expression (green) stained for Brat (red). Brat staining is also shown alone (gray). (A-C) *insc*-Gal4 is expressed in all neuroblasts. Brat protein is present in control brains (A, A') but depleted with Brat RNAi alone (B, B') or Brat RNAi plus UAS *ase* (C, C'). (D-E) *ase*-Gal4 is expressed in *Ase*⁺ neuroblasts. Brat protein is present in control brains (D, D') but depleted in the *Ase*⁺ neuroblasts where Brat RNAi is expressed (E, E').

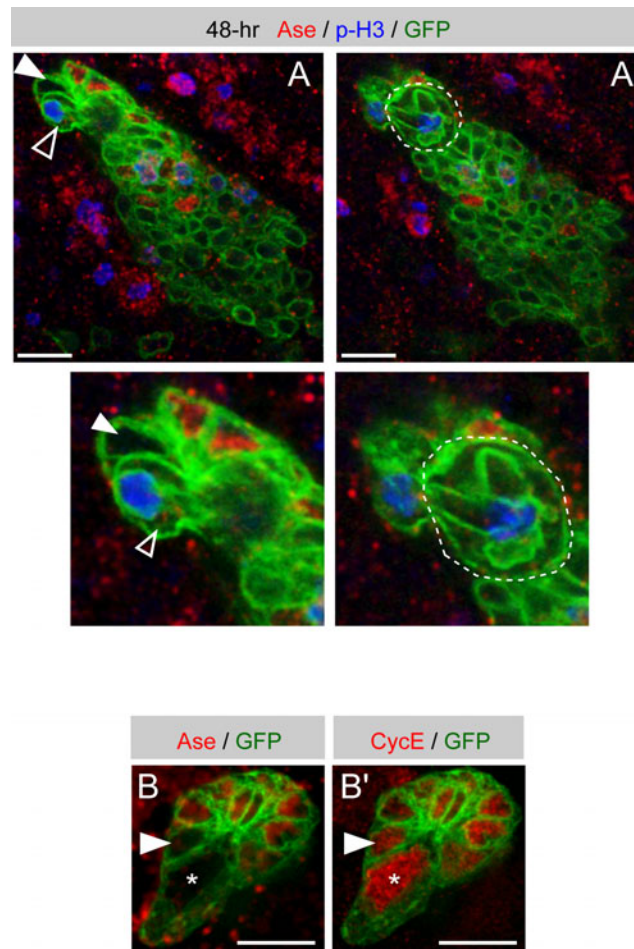


Figure S3. Characteristics of Ase⁻ secondary neuroblasts

(A) Above: 48-hr MARCM clone reported by GFP (green) with staining of Ase (red) and phospho-histone H3 (blue). The Ase⁻ daughter being born (open arrowhead) from the telophase PAN neuroblast (star, outline) is situated near another Ase⁻ daughter (closed arrowhead). Below: higher magnification. **(B)** 48-hr MARCM clone reported by GFP (green) with staining of Ase (red in **B**) and CycE (red in **B'**). An Ase⁻ secondary neuroblast is positive for CycE (arrowhead).

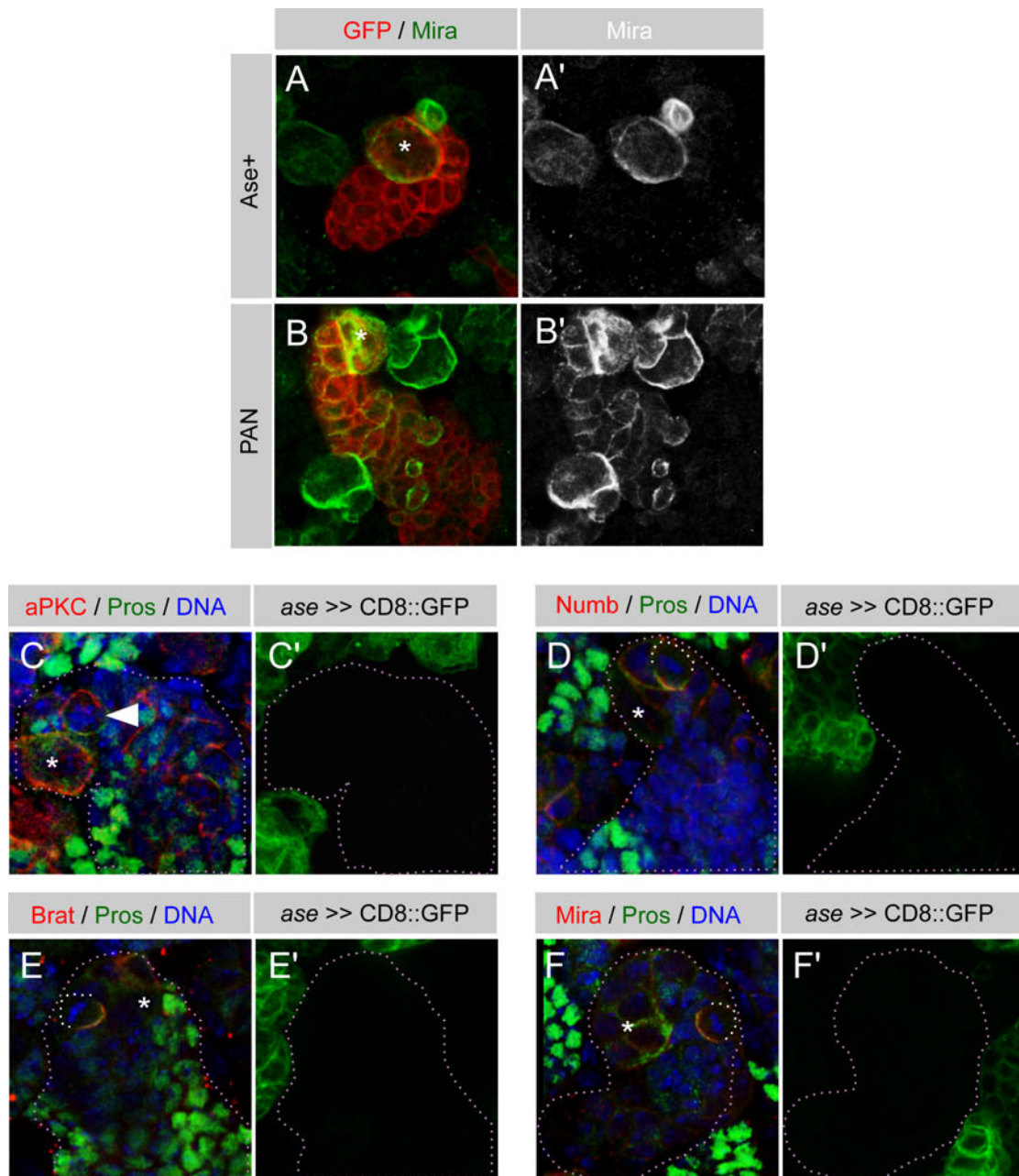


Figure S4. Asymmetric protein localization in secondary neuroblasts.

(A-B) 48-hr MARCM clones reported by GFP (green) with staining of Mira (green in **A** and **B** white in **A'** and **B'**). Star indicates primary neuroblasts. In Ase⁺ lineages, few progeny retain cortical Mira (**A**), but many daughters of PAN neuroblasts do (**B**). (C-F) PAN lineages (lavender dotted line) identified by absence of ase-Gal4 expression and mitotic secondary neuroblasts (arrowhead and white dotted line) identified by segregation of Pros (green). Star indicates approximate position of the primary neuroblast, which is below the plane shown in **E** and **F**. Secondary neuroblasts asymmetrically segregate aPKC (red in **C**, arrowhead), Numb (red, **D**), Brat (red, **E**), and Mira (red, **F**).

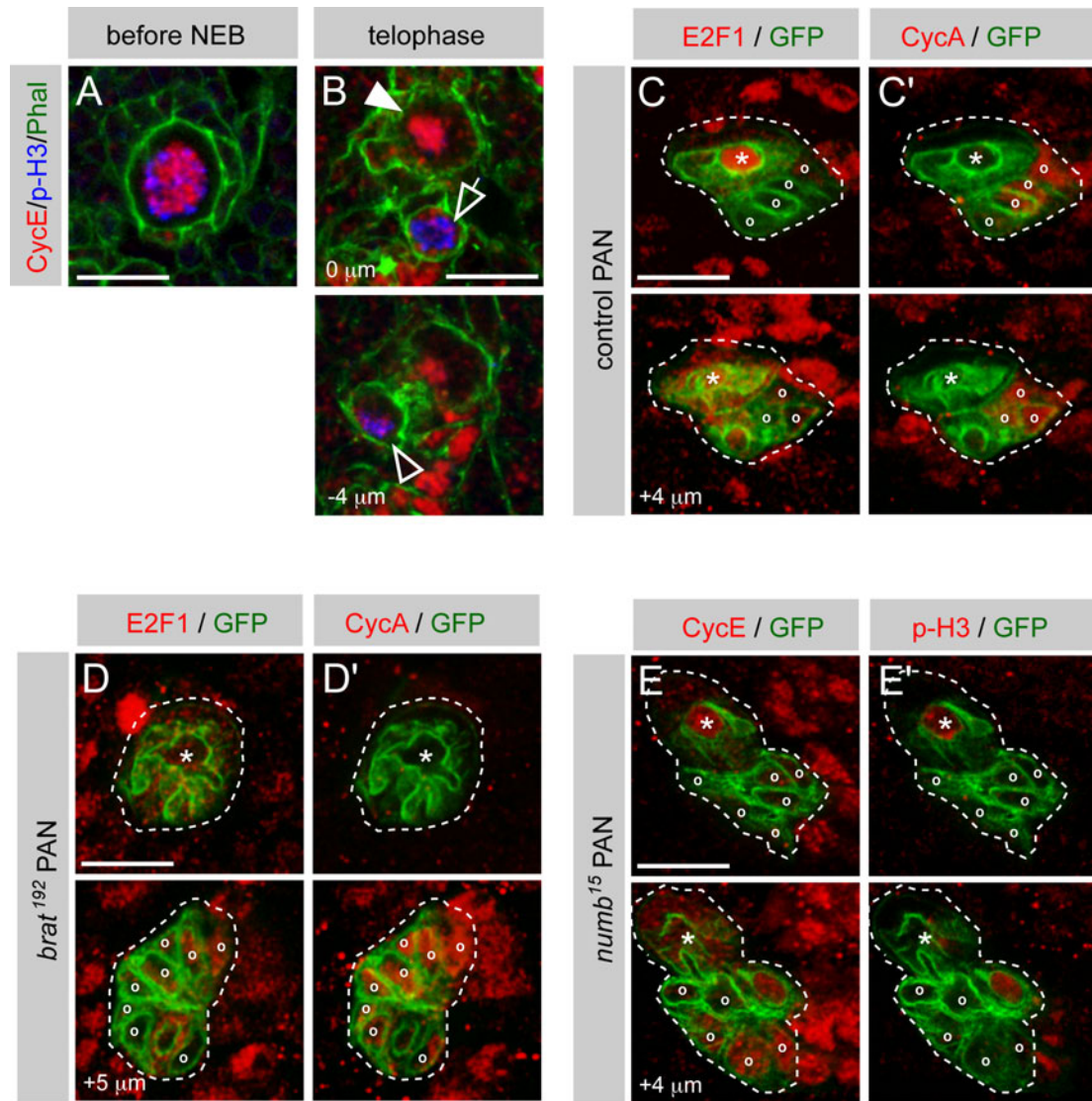


Figure S5. Cell cycle delay in *brat* secondary neuroblasts occurs in G2

(A-B) wild type central brain neuroblasts stained with phalloidin (green), CycE (red) and p-H3 (blue). The expression of CycE in mitotic neuroblasts is clearly visible before nuclear envelope breakdown (A). In PAN neuroblasts, CycE associates with DNA in late telophase (B, arrowheads). It is also expressed in mitotic secondary neuroblasts (B, arrow). (C-E) Cell cycle profiling in 24-hr MARCM clones with telophase PAN neuroblasts. The clone is reported by expression of GFP (green). Stars indicate primary neuroblasts, and circles indicate progeny. The daughter being born is unmarked, but has a distinctive ring of GFP around the nucleus. In wild-type clones (C) and in *brat* clones (D), E2F1 is present in the cells being born but not in the nearest neighbors of the newly born daughter. Cyclin A is absent from the dividing cells but upregulated in the daughters near the site of birth (C', D'). In *numb* clones, CycE associates with DNA in the daughter being born, but it is absent from the newest daughter's neighbors (E, E').

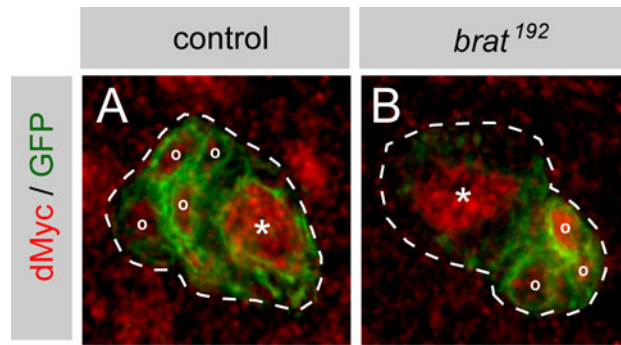


Figure S6. dMyc is expressed in the progeny of control and brat PAN neuroblasts

(A-B) 24-hr MARCM clones reported by GFP (green) with staining of dMyc (red). Neuroblasts are indicated with a star and progeny are indicated with a circle. Both wild type (A) and brat (B) neuroblasts produce daughter cells that express dMyc.

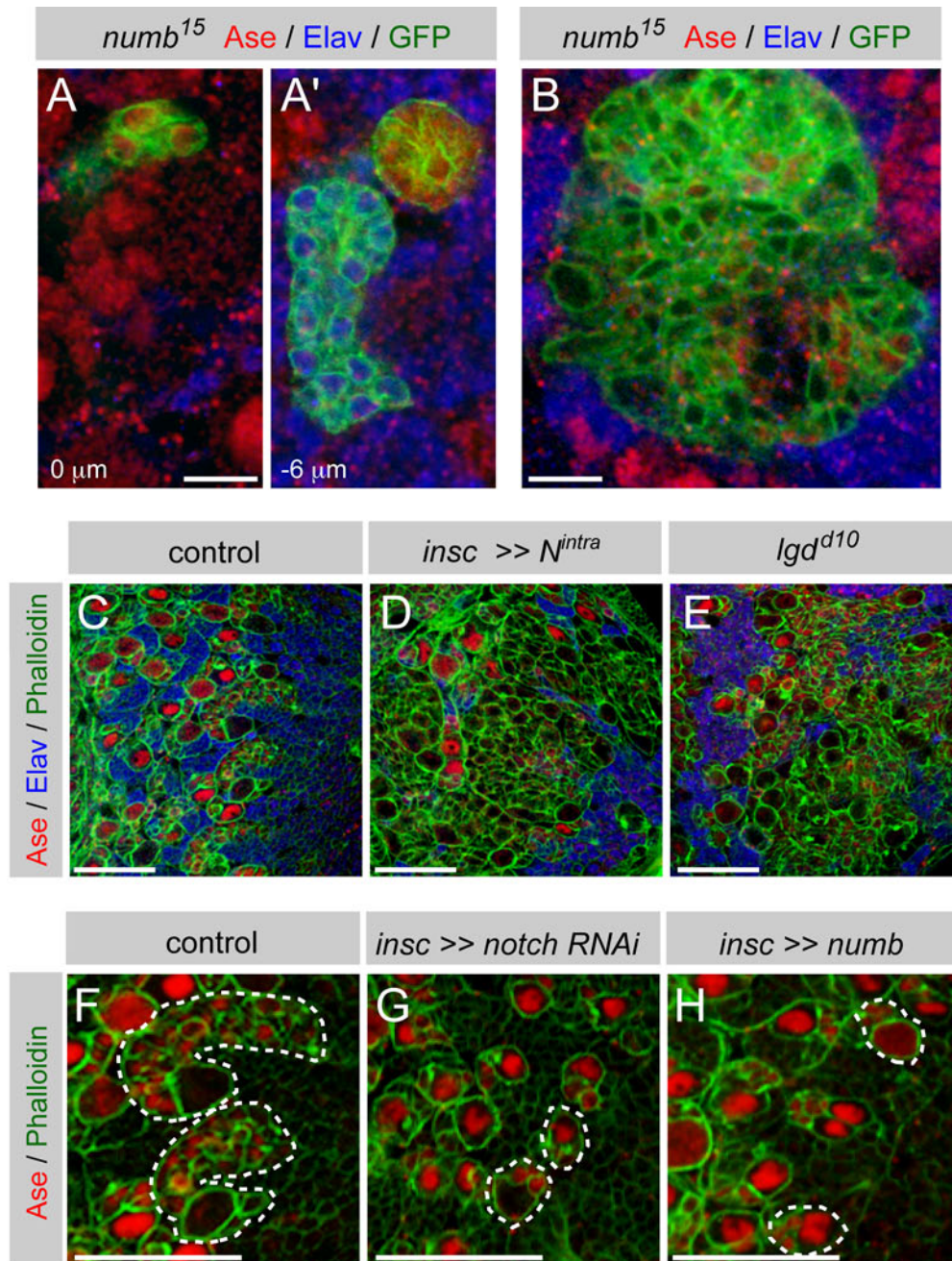


Figure S7. Notch signaling regulates the PAN lineage

(A-B) 48-hr *numb* MARCM clones reported by GFP (green) stained for Ase (red) and Elav (blue). Loss of *numb* does not affect differentiation in Ase⁺ neuroblasts (A, A'). In PAN neuroblasts, loss of *numb* results in overgrowth of Ase⁻ progeny (B). (C-E) Third instar brains stained for Ase (red), Elav (blue), and Phalloidin (green). Control brains (C) have a small number of PAN neuroblasts. Overactivating Notch by expressing Notch intracellular domain (*N^{intra}*, D) or removing *Igd* (E) generates ectopic PAN neuroblasts. (F-H) Medial neuroblast lineages (outline) stained for Ase (red) and Phalloidin (green). Control brains have PAN neuroblasts with many Ase⁺ progeny (F). Notch knockdown eliminates PAN neuroblasts or reduces the number of Ase⁺ progeny (G). Inhibiting Notch by overexpressing *Numb* eliminates PAN lineages (H). Scale bars: (A-B) 10 μm; (C-H) 40μm.

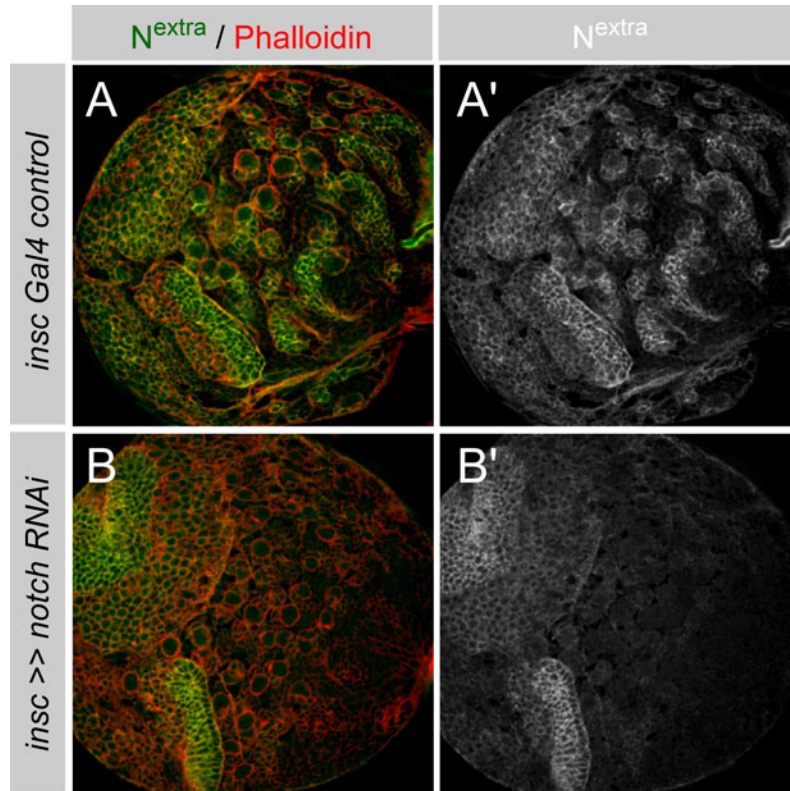


Figure S8. Reduction of Notch protein by knockdown with transgenic RNAi

(A-B) Third instar brains with staining of Phalloidin (red) and Notch extracellular domain (Nextra, green). Nextra staining is also shown alone (gray). In control brains, Nextra is present on the cell surface of neuroblasts and some of their progeny **(A)**. In brains expressing Notch RNAi under the control of *insc-Gal4*, Notch protein is depleted **(B)**.

Fly strains and antibodies

Additional fly strains used were: UAS N^{intra} (a gift from S. Bray); UAS *notch* RNAi (Dietzl et al., 2007); UAS *numb* (Chien et al., 1998); *Igd^{d10}* (Gallagher and Knoblich, 2006; Jaekel and Klein, 2006); *gbe+Su(H) lacZ* (Furriols and Bray, 2001); *ttk⁰²⁷⁹* (Lai et al., 1996); *ase¹* (Dominguez and Campuzano, 1993).

Additional antibodies used were: mouse anti-dMyc (1:5, B. Edgar); mouse anti- N^{extra} (1:200, DSHB); rabbit anti-Brat (1:100, (Betschinger et al., 2006)); rabbit anti-PKCz/aPKC (1:200, Santa Cruz); rabbit anti-Numb (1:200); guinea pig anti-dE2F1 (1:1000, T. Orr-Weaver); rabbit anti-CyclinA (1:1000, D. Glover).

Computer modeling of neuroblast lineages

We propose that the PAN neuroblast produces an Ase^- intermediate progenitor. This Ase^- cell becomes Ase^+ before dividing to make a GMC, and the GMC will divide terminally to produce two neurons. Such a lineage is not conducive to modeling as analytical expressions because of the recursive nature of the cell populations, the varying cell identities within a single cell cycle, and the treatment of divisions as discrete events in time. Instead, we used computer routines to determine if the proposed lineage could theoretically produce the numbers of cell types observed in 24- and 48-hr clones, and what cell division rates and latency periods would be required to produce those numbers. We developed three versions of the routines using the Matlab v7 software package (Mathworks Inc., New York, NY). Code is available upon request. The results of this analysis are presented in Fig. 9.

The first routine is a simulation of the Ase^+ neuroblast lineage, which we used to validate our computational approach. In this lineage, the Ase^+ neuroblast produces a GMC, and the GMC divides terminally to produce two neurons. Input parameters for this model are:

Rnb, the rate of neuroblast division

Rgmc, the time between creation and division of the GMC

Rnb and Rgmc are determined empirically from the clonal analysis in Table 1B. Each GMC and each pair of neurons is assumed to represent one neuroblast division. Therefore, $Rnb = t / (GMC + neurons/2)$, where t = time elapsed since clone induction. Rgmc is calculated to be $GMC \times Rnb$. Total number of GMCs ($Ngmc$) at a given time sample was determined as the sum of $Ngmc$ at the previous time sample, plus the number of new GMCs (i.e. number of neuroblast divisions) created since the previous sample, minus the number of GMCs that divided to create neurons. The number of neurons at a given time sample was calculated as the number at the previous sample plus twice the number of GMCs that divided since the

previous sample. Our empirically determined R_{nb} and R_{gmc} , when used as inputs in this routine, produced total numbers of GMCs and neurons in close agreement with the observed numbers in 24- and 48-hr Ase^+ neuroblast clones (see below). This provided proof of concept for similar modeling of the more complicated PAN lineage.

Our second routine simulated a model of the PAN lineage. In this routine, we assumed that the secondary neuroblasts have unlimited cell divisions. Input parameters for this model are:

R_{nb} (see above),

L_{snb-} , a latency period between the creation of the Ase^- secondary neuroblast and when it becomes Ase^+ ,

L_{snb+} , a second latency period between when the secondary neuroblast becomes Ase^+ and the first division of the secondary neuroblast,

R_{snb} , the rate of secondary neuroblast division

R_{gmc} (see above).

We assumed that R_{nb} and R_{gmc} are identical for Ase^+ and PAN neuroblast lineages, and varied L_{snb-} , L_{snb+} , and R_{snb} until we reached output in good agreement with the observed numbers of secondary neuroblasts, GMCs, and neurons in PAN clones. An important limitation placed on the values of L_{snb-} , L_{snb+} , and R_{snb} was the observation that it takes about 24 hours to create two neurons (see Table 1B); therefore $R_{nb} + L_{snb-} + L_{snb+} + R_{snb} + R_{gmc}$ must be less than 24 hours. A new Ase^- secondary neuroblast (snb^-) was created every R_{nb} hours. The total number of Ase^- secondary neuroblasts (N_{snb-}) at a given time sample is the sum of N_{snb-} at the previous time sample, plus the number of new snb^- , minus the number of snb^- that start expressing Ase after latency period L_{snb-} . The total number of Ase^+ secondary neuroblasts (N_{snb+}) at a given time sample is the sum of N_{snb+} at the previous time sample, plus the number of snb^- starting to express Ase . The number of GMCs (N_{gmc}) is the sum of the previous N_{gmc} , plus the number of new GMCs, minus the number of GMCs that divided to create neurons. The number of new GMCs is created from either snb^+ just finishing the latency period L_{snb+} , or snb^+ that last divided R_{snb+} hours before. The total number of neurons (N_n) is the sum of the previous N_n , plus twice the number of GMCs that divided since the previous sample.

The third routine simulated a model of the PAN lineage similar to the previous model, but with the Ase^+ secondary neuroblast 'dying' after a specified number of divisions (X_{snb+}). The total number of Ase^+ secondary neuroblasts (N_{ase+}) at a given time sample is subsequently calculated as the sum of the previous N_{ase+} , plus the number of snb^- starting to express Ase ,

minus the number of snb^+ older than $Xsnb^+ \times Rsnb^+$ hours. Limiting the Ase^+ secondary neuroblasts to either 4 or 5 divisions could produce outputs in agreement with the observed numbers of progeny in PAN clones.

Values used to generate the plots in Figure 9:

Input, Ase^+ neuroblast lineage, first routine:

$Rnb = 1.5$ hours

$Rgmc = 8.5$ hours

Input, PAN neuroblast lineage, third routine:

$Rnb = 1.5$ hours

$Lsnb^- = 3.5$ hours

$Lsnb^+ = 1$ hour

$Rsnb = 8.1$ hours

$Rgmc = 8.5$ hours

$Xsnb^+ = 5$ divisions

5. CHAPTER II – CHARACTERIZATION OF BARRICADE, A NOVEL REGULATOR OF LARVAL NEUROBLAST LINEAGES

5.1. INTRODUCTION

The identification and characterization of PAN lineages described in chapter I has been confirmed by two other studies that were published concomitantly to ours (Bello et al., 2008; Boone and Doe, 2008). Each study originally used different terms to describe same cell types and for sake of clarity a common nomenclature has been adopted. In this chapter, we are using the common terminology and changes are summarized below:

Bowman and al. 2008	Common nomenclature
Ase ⁺ lineage	Type 1 lineage
PAN lineage	Type 2 lineage
Primary neuroblast (in PAN lineage)	Neuroblast
Secondary neuroblast (in PAN lineage)	Intermediate Neural Progenitor (INP)

Since this chapter strongly focuses on type 2 lineages, the next few paragraphs briefly summarize current knowledge about type 1 and type 2 lineages.

5.1.1. Type 1 and type 2 neuroblast lineages

Type 1 neuroblasts are the most common population of neuroblasts in the CB and they form relatively simple lineages (Fig. 10A&B). These neuroblasts express the cortical protein Mira and the nuclear transcription factors Ase and Dpn (Boone and Doe, 2008; Bowman et al., 2008). Upon division they segregate Mira, Brat, Numb and Pros into the smaller GMC (Fig. 10D) (Bowman et al., 2008; Boone and Doe, 2008; Bello et al., 2008). In the GMC, Mira and Dpn are degraded while Pros enters the nucleus and together with Brat and Numb, triggers differentiation. Each GMC divides symmetrically into two neurons.

Type 2 neuroblasts are rare – eight per lobe – and are located on the posterior side of the brain (Fig. 10A) (Bowman et al., 2008). However, these lineages are highly relevant for two main reasons. Firstly, they form complex and long lineages that produce about one quarter of all neurons of the brain (Fig. 10C) (Bello et al., 2008; Izergina et al., 2009). Secondly, they are more prone to overproliferation and tumor formation (Bowman et al., 2008; Weng et al., 2010; Neumuller et al., 2011). Type 2 neuroblasts can be distinguished from type 1 neuroblasts by the fact that they express Dpn but lack Ase (Bowman et al., 2008; Boone and Doe, 2008). They divide asymmetrically into another neuroblast and an INP, which inherits Mira, Brat and Numb, but not Pros which is not expressed in type 2 neuroblasts (Fig. 10E) (Bowman et al., 2008; Boone and Doe, 2008; Bello et al., 2008). INPs are transit-amplifying

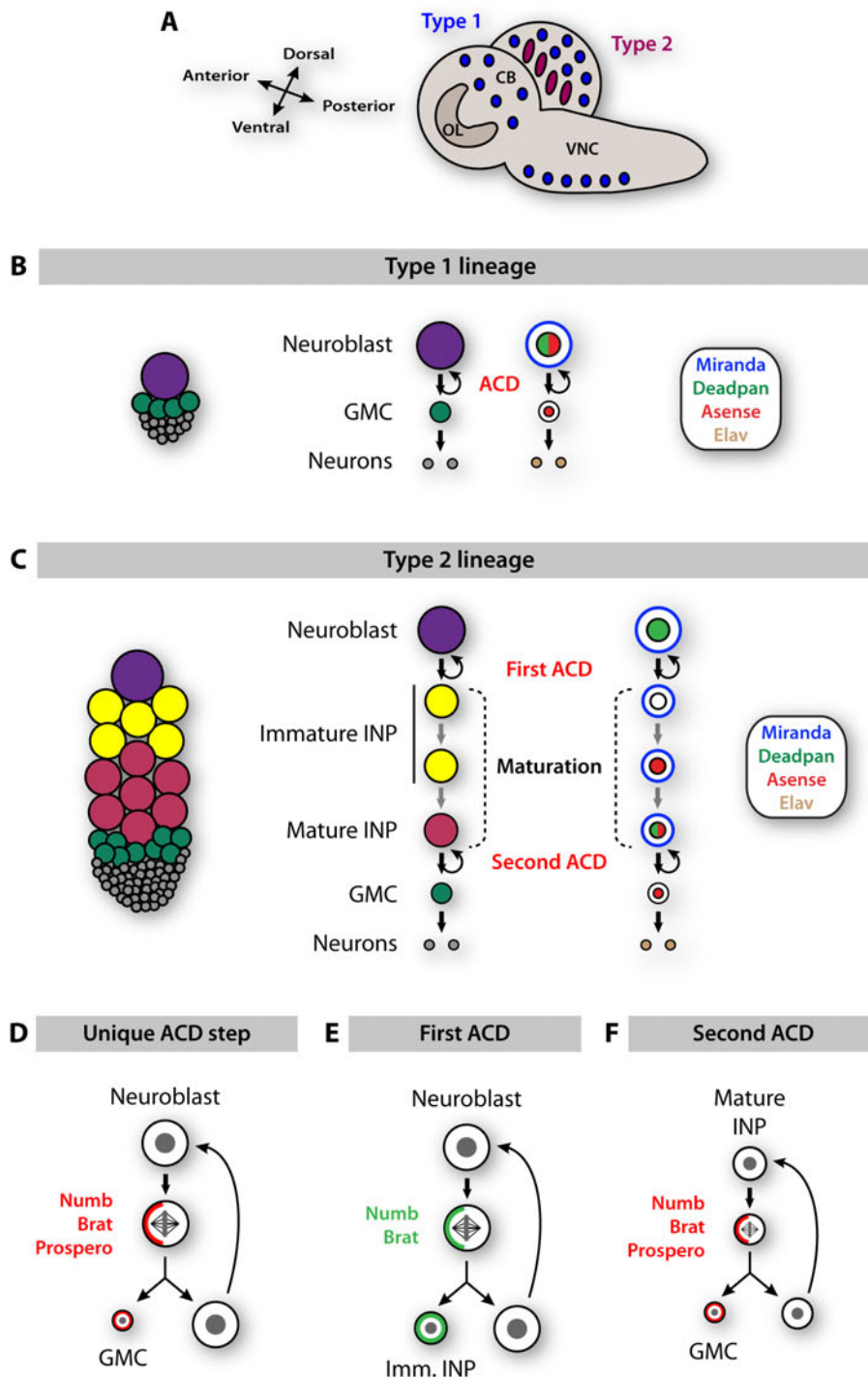


Figure 10. Type 1 and type 2 larval neuroblast lineages

(A) Type 1 lineages are found in the CB and the VNC of larval brains. Type 2 lineages are localized on the posterior side of each brain lobe. (B) Each type 1 lineage is composed of a single $Mira^+Ase^+Dpn^+$ neuroblast that divides asymmetrically into another neuroblast and an Ase^+ GMC. Each GMC produces two $Elav^+$ neurons. (C) Each type 2 lineage is composed of a single $Mira^+Ase^+Dpn^+$ neuroblast that divides into another neuroblast and an immature intermediate neural progenitor (imm. INP). Imm. INPs are first $Mira^+Ase^-Dpn^-$, then $Mira^+Ase^+Dpn^-$ and become mature when reaching the $Mira^+Ase^+Dpn^+$ stage (this process is called maturation). Mature INPs divide several times into an INP and a GMC. Each GMC produces two $Elav^+$ neurons. (D) In type 1 neuroblast ACD, Numb, Brat and Prospero segregate into the GMC. (E) In type 2 neuroblast ACD, Numb and Brat segregate into the imm. INP. (F) In mature INP ACD, Numb, Brat and Prospero segregate into the GMC.

cells that have the potential to produce several GMCs each. However, newly born INPs, which express Mira but lack Dpn and Ase, are mitotically inactive and called immature INPs (imm. INPs) (Bowman et al., 2008; Boone and Doe, 2008). In order to produce GMCs, they need to undergo a process called maturation, to sequentially express Ase, then Dpn (Bowman et al., 2008; Boone and Doe, 2008; Bayraktar et al., 2010). Once INPs express both nuclear proteins, they are called mature INPs and divide several times into another INP and a GMC, which this time inherits Mira, Brat, Numb and Pros (Fig. 10F) (Bowman et al., 2008; Boone and Doe, 2008; Bello et al., 2008; Bayraktar et al., 2010). Similarly to type 1 GMCs, type 2 GMCs divide symmetrically into two neurons.

As explained here, a set of markers (Mira, Ase, Dpn and Elav) is available to clearly identify all cells types that constitute type 2 lineages. However, the mechanisms that control type 2 lineage progression, and especially INP maturation, remain unclear.

5.1.2. Searching for novel regulators of neuroblast lineages: Identification of *barricade*

In order to identify novel regulators of neuroblast lineage progression, we made use of a neuroblast genome-wide RNAi (RNA interference) screen that was recently conducted in our laboratory (for more details about the screen, see (Neumuller et al., 2011)).

5.1.2.1. Genome-wide RNAi screen in neuroblasts: principle, workflow and phenotypic categories

In this screen, the function of individual genes was assessed by RNAi-mediated knock down, in neuroblast lineages only. This tissue specificity was made possible by the use of the Gal4/UAS system (Fig. 11A).

The Gal4/UAS system is widely used in *Drosophila* and relies on transgenic expression of the yeast transcription activator GAL4, that can bind UAS motifs to stimulate transcription of a sequence fused to it (Brand and Perrimon, 1993). For example, tissue specific expression of GAL4 combined with a UAS-RNAi construct, allows knocking down a chosen gene in a desired tissue. In the case of this screen, *insc*-Gal4 was used to express UAS constructs in neuroblast lineages, specifically. To optimize screening conditions, *insc*-Gal4 was combined with UAS-*CD8::GFP* (membrane tethered GFP), which enables the visualization of cells within neuroblast lineages, and with UAS-*Dicer-2*, which enhances RNAi (Dietzl et al., 2007). This fly line is referred to as “driver line” because GAL4 drives expression of UAS constructs. To test the function of single genes on a genome-wide level, the GD RNAi library

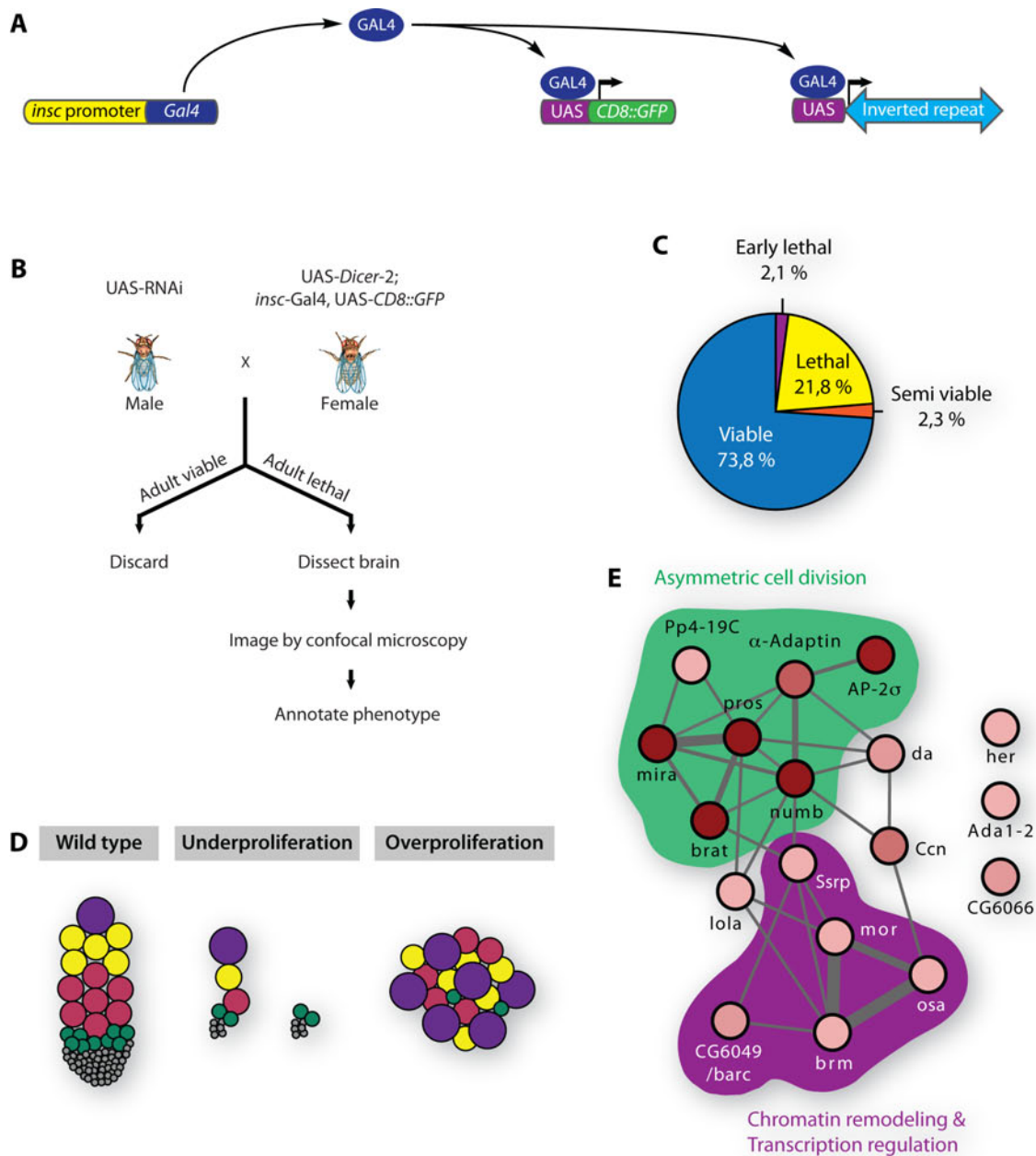


Figure 11. Genome-wide *in vivo* RNAi screen to identify novel regulators of self-renewal and neuroblast lineage progression

(A) Principle of the GAL4/UAS system used in the screen. GAL4 is fused to the promoter of *insc* (*insc-Gal4*), allowing GAL4 expression in neuroblast lineages. GAL4 activates transcription of a membrane tethered GFP (*UAS-CD8::GFP*), and of an inverted repeat sequence that drives RNAi against a chosen gene (*UAS-RNAi*), leading to its knock-down in neuroblast lineages. (B) Workflow of the genome-wide RNAi screen. (C) Viability and lethality rates of crosses in the primary genome-wide screen. Lethal and semi-viable crosses were chosen for further analysis. Early lethal crosses could not be analyzed further because individuals died before the third instar larvae stage. (D) Most interesting phenotype categories observed in the screen: underproliferation (shorter lineages and/or less neuroblasts) and overproliferation (more neuroblasts/INPs). (E) Interaction network of genes causing overproliferation. Genes are represented as nodes and their color intensity reflects the strength of their RNAi phenotype. Lines that connect nodes represent known interactions or associations of the nodes (Genetic/Biochemical interaction and/or literature association). Line thickness reflects the amount of evidence for interaction between two nodes. (B,C,E) are adapted from (Neumuller et al., 2011).

of the Vienna *Drosophila* RNAi collection (VDRC) was used. Each one of the GD RNAi lines contains a short gene fragment cloned as an inverted repeat and fused to a UAS (Dietzl et al., 2007). Upon transcription in neuroblast lineages, this fragment forms a hairpin that ultimately drives RNAi against this gene and knocks it down.

The rationale of the screen was that if a gene is required in neuroblast lineages, its knock down with *insc*-Gal4 should result in lethality prior to adult stages. For that, females of the driver line were crossed to males of the GD RNAi library (Fig. 11B). When a cross was viable, the GD RNAi line was discarded. When a cross was lethal prior to adulthood or semi viable, third instar larvae were dissected, their brains were imaged (GFP signal) and potential phenotypes were annotated. A total of 17362 GD lines were tested in the primary screen (12314 genes), therefore covering about 89% of all annotated *Drosophila* protein coding genes. Among crosses of the primary screen, 4182 were lethal or semi viable (24.1%, 3412 genes), and larval brain imaging revealed phenotypes in 832 lines (687 genes) (Fig. 11C). These 832 lines were then filtered using a quality criterion. Indeed, RNAi mediated by double stranded RNA (dsRNA) can potentially target several genes – off-target – and this is evaluated by the so-called “S19” score, where 0 reflects absence of specificity and 1, complete specificity (Kulkarni et al., 2006; Dietzl et al., 2007). Lines with S19>0,85 were considered for final phenotypical analysis, hence generating a list of 620 candidate lines, corresponding to about 4.5% of all *Drosophila* protein coding genes.

Larval brain phenotypes observed in these 620 lines were very diverse. To precisely describe the phenotype of each line, criteria such as number, size and shape of neuroblasts/INPs/GMCs or formation of GFP aggregates were scored from 0 to 10 to reflect phenotypical strength. Most of these 620 lines could then be grouped in two separate categories, depending on their phenotype: “underproliferation” when then showed fewer neuroblasts and “overproliferation” when then showed too many neuroblasts or GMCs (Fig. 11D).

The underproliferation category is very likely to contain genes required for maintaining stem cell renewal, as one would expect that their knock down results in fewer neuroblasts. However, this category is also expected to contain a large number of housekeeping genes, which should also result in fewer cells. Indeed, the underproliferation category is very large and contains 538 genes.

The overproliferation category, however, should contain genes required for differentiation and lineage progression, since their knock down would result in more neuroblasts or INPs. This category is therefore the one we became interested in. Surprisingly, this group only contains 29 lines and after staining with Mira (neuroblast/INP) and Pros (GMCs/neurons), 18 genes were confirmed to generate more neuroblasts/INPs upon knock down.

5.1.2.2. Overproliferation network

Interestingly, most of these 18 genes are known to interact with each other in a genetic and/or biochemical way. Together with information from the published literature, these data allowed to constitute an interaction network of the overproliferation genes (Fig. 11E). This network can be divided into two main sub networks: one containing genes involved in ACD and one containing genes involved in chromatin remodeling and transcription regulation.

The ACD sub network is composed of 7 genes. This group contains the cell fate determinants Numb, Brat and Pros, and the adaptor protein Mira, which have all been shown to generate overproliferation upon knock down. Additionally, this group contains α -adapatin and AP-2 σ , two members of the AP-2 complex that interacts with Numb, and the protein phosphatase PP4, which plays a role in Mira, Brat and Numb localization (Santolini et al., 2000; Berdnik et al., 2002; Sousa-Nunes et al., 2009). These genes were expected to give such phenotypes and validate the screening procedure.

The chromatin remodeling and transcription regulation sub network is composed of *brahma* (*brm*), *osa*, *moira* (*mor*), *ssrp* and *CG6049*. Brm, Osa and Mor are members of the chromatin remodeling Brm complex, which is related to the SWI/SNF complex (Papoulas et al., 1998). The mammalian SWI/SNF complex has been involved in tumor suppression and in regulating proliferation of neural stem cells (Reisman et al., 2009; Yoo and Crabtree, 2009). Ssrp is a subunit of the FACT complex, which promotes transcription elongation by destabilizing nucleosomes to allow for RNA polymerase II (RNA Pol II) to proceed (Belotserkovskaya et al., 2004). The last member of this sub network is *CG6049*, a previously uncharacterized gene that was renamed *barricade* (*barc*), because of its role in preventing overproliferation (Neumuller et al., 2011). We therefore decided to study *barc* in order to determine how it regulates neuroblast lineages. Barc belongs to a conserved family of proteins that have been involved in transcription elongation and splicing. The structure of these genes and the function of its homologues are presented below.

5.1.3. The Barc/Tat-SF1/CUS2 family of proteins: Structure and functions

Barc is the homologue of human Tat stimulating factor 1 (Tat-SF1) and yeast CUS2 (Yan et al., 1998; Zhou and Sharp, 1996). The Barc/Tat-SF1/CUS2 family of genes is conserved in eukaryotes (Fig. 12).

5.1.3.1. The Barc/Tat-SF1/CUS2 family of proteins

The common structure to all members of this family is composed of a nuclear localization signal (NLS) and two RNA recognition motifs (RRMs). RRM, also called ribonucleoprotein domains (RNPs) or RNA-binding domains (RBDs), are the most common eukaryotic RNA binding domains (for reviews, see (Kielkopf et al., 2004) and (Maris et al., 2005)). These domains of about 90 amino acids can bind single stranded RNA, DNA and in some cases proteins. RRM are found alone or in several copies and are typically present in proteins that play a role in RNA-dependant processes. RRM of both Tat-SF1 and CUS2 have been described as being very similar to RRM found in the human proteins Ewing's sarcoma (EWS) and Fused in sarcoma (FUS/TLS), two proteins associated with various solid human tumors (Yan et al., 1998; Zhou and Sharp, 1996; Rabbitts, 1994; Ladanyi, 1995; Rabbitts et al., 1993; Crozat et al., 1993; Sorensen et al., 1994; Delattre et al., 1992).

CUS2 is mainly composed of the NLS and the two RRM. All other proteins of this family, however, are longer and extend either on their N- or C-terminus. Proteins of *A. thaliana*, *C. elegans* and *D. melanogaster* extend on their N-terminus, whereas the mouse and human proteins have a rather short N-terminus extension but a very long acidic C-terminus. Apart from CUS2, all members of this family possess a short conserved region called Barc/Tat-SF1 motif (BTS) (Neumuller et al., 2011). This motif has been shown to bind FF domains, which are present in several transcription and splicing factors (Smith et al., 2004).

Our understanding about the function of this family of proteins comes from the study of human Tat-SF1, and to a lesser extend of yeast CUS2. This knowledge is summarized below.

5.1.3.2. Functions of human Tat-SF1 and yeast CUS2

Tat-SF1 was originally identified for its role in Human immunodeficiency virus type 1 (HIV-1) transcription (Zhou and Sharp, 1996). Tat-SF1 was then shown to play a general role in transcription elongation (Li and Green, 1998). Additionally, Tat-SF1 and CUS2 have been involved in splicing (Yan et al., 1998; Miller et al., 2011; Miller et al., 2009; Fong and Zhou, 2001; Zhou and Sharp, 1996). The next few paragraphs briefly explain mechanisms

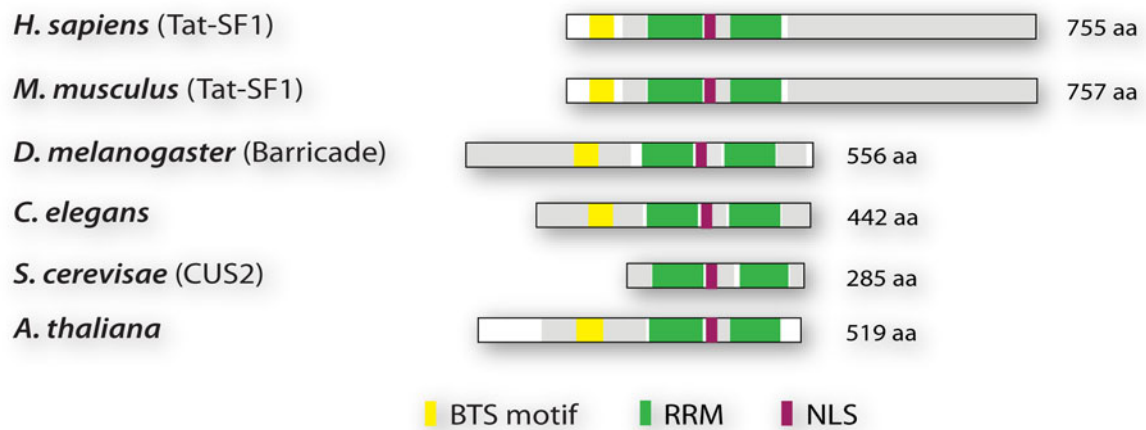


Figure 12. The Barc/Tat-SF1/CUS2 family of proteins

These proteins all contain two RNA Recognition Motifs (RRMs) and an Nuclear Localization Signal (NLS). Additionally, most of them possess a Barc/Tat-SF1 (BTS) motif. Grey boxes represent low complexity regions. Adapted from (Neumuller et al., 2011).

regulating transcription elongation of both HIV and endogenous genes, as well as splicing and summarized knowledge about the role of Tat-SF1 and CUS2 in these processes.

- **Tat-SF1 stimulates HIV-1 transcription**

The HIV-1 retrovirus is the most virulent virus responsible for the deadly Autoimmune Deficiency Syndrome (AIDS). Following entry in a CD4⁺ lymphocyte or a macrophage, viral HIV-1 RNA undergoes reverse transcription and integrates into the cellular genome. To be able to propagate and infect other cells, multiple copies of HIV-1 RNA have to be produced. To achieve that, the provirus uses host RNA Pol II to transcribe its genome from its 5' long terminal repeat (LTR) promoter. Upon transcription initiation, the 5' end of the nascent RNA forms a stem-loop structure called Transactivation Response Element (TAR element). If not further stimulated, polymerase can only produce short transcripts that do not allow viral replication (Kao et al., 1987). Synthesis of full-length transcripts requires the viral protein Tat to interact with the TAR element and to recruit several cellular factors that drive processive elongation and allow HIV-1 replication (Fig. 13, for review see (Ott et al., 2011)). Two of these essential cellular factors are the Positive Transcription Elongation Factor b (P-TEFb) and Tat-SF1 (Mancebo et al., 1997; Wei et al., 1998; Zhu et al., 1997; Zhou et al., 1998; Zhou and Sharp, 1996). Depletion of either P-TEFb or Tat-SF1 is sufficient to inhibit HIV-1 Tat transactivation (Zhou and Sharp, 1996; Zhou et al., 1998; Zhu et al., 1997; Zhou et al., 1998).

The function of P-TEFb – whose main subunits are Cyclin T (CycT) and Cyclin Dependant Kinase 9 (CDK9) – in promoting HIV RNA elongation is dual and relies on a series of phosphorylations. On the one hand, P-TEFb phosphorylates the Negative Elongation Factor (NELF), which detaches from Pol II. On the other hand, it phosphorylates the DRB Sensitivity Inducing Factor (DSIF) and the carboxyterminal domain (CTD) of RNA pol II to promote processive elongation (Fig. 13, (Zhou and Yik, 2006; Ott et al., 2011)). The kinase activity of P-TEFb is essential for HIV-1 Tat transactivation since CDK9 depleted nuclear extracts are unable to trigger productive elongation (Zhu et al., 1997; Zhou et al., 1998).

The mechanism by which Tat-SF1 regulates HIV-1 RNA elongation remains unclear. Tat-SF1 has been shown to associate with P-TEFb via its subunit CDK9 (Zhou et al., 1998). Additionally, P-TEFb can phosphorylate Tat-SF1 in a CDK9-independent manner, suggesting that P-TEFb could regulate Tat-SF1 activity (Zhou et al., 1998). However, the importance of Tat-SF1 phosphorylation in regulating elongation has not been demonstrated so far.

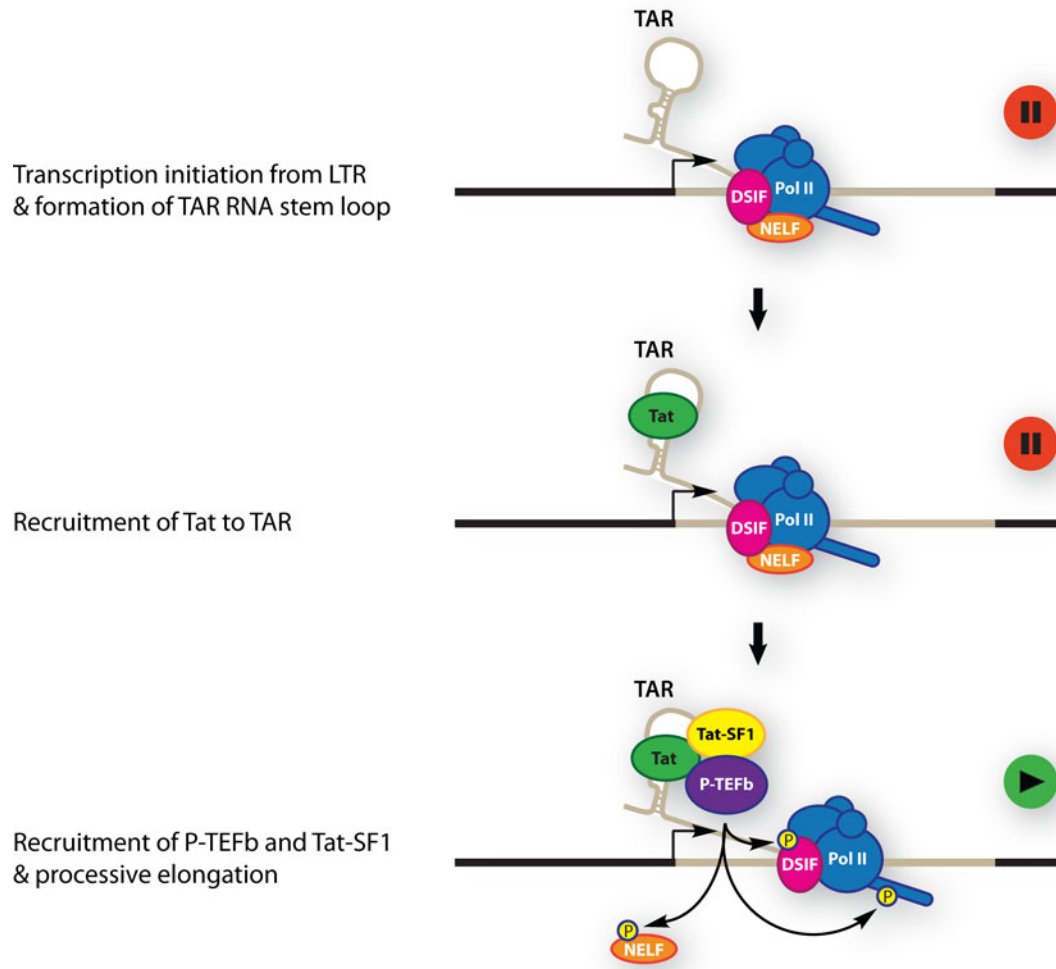


Figure 13. Model for HIV-1 transcription elongation

Upon transcription initiation, the nascent HIV-1 mRNA forms a stem-loop structure (TAR element). In the absence of the viral protein Tat, polymerase is paused and no full-length transcript is produced. In the presence of Tat and upon its binding to the TAR element, Tat recruits Tat-SF1 and P-TEFb. P-TEFb carries out a series of phosphorylation (NELF, DSIF, RNA Polymerase II carboxyterminal domain) and, together with Tat-SF1, stimulates processive elongation and production of full length HIV-1 mRNAs.

- **Tat-SF1 promotes RNA Pol II elongation**

Interestingly, although Tat-SF1 was originally identified as a Tat-dependent activator of transcription, Tat-SF1 was later shown to activate transcription in a Tat-independent manner and is now considered a general elongation factor (Li and Green, 1998). Transcription elongation of endogenous protein coding genes was long thought to be mainly regulated at the level of RNA Pol II recruitment and transcription initiation. However, observations made at the promoter of *Drosophila* heat shock and mammalian *c-myc* genes, revealed that although Pol II was engaged in transcription, it was paused after synthesizing around 25-50 nucleotides (Gilmour and Lis, 1986; Bentley and Groudine, 1986; Rougvie and Lis, 1988; Krumm et al., 1992; Strobl and Eick, 1992; Rasmussen and Lis, 1993). This phenomenon is referred to as Pol II promoter-proximal pausing (PPP) and was initially considered to be happening at very few genes. However, over the last couple of years Pol II PPP was observed at a very large number of *Drosophila* and mouse *loci*, and pausing release is now considered a critical step in the regulation of elongation (Muse et al., 2007; Zeitlinger et al., 2007; Core et al., 2008; Lee et al., 2008; Nechaev et al., 2010). Interestingly, control of Pol II PPP-release seems to be particularly important for genes involved in development and stimulus-response (for review, see (Nechaev and Adelman, 2010) and (Levine, 2011)).

When paused after having transcribed 25-50 nucleotides, RNA Pol II is associated with NELF and DSIF, which at this point inhibit productive elongation (Fig. 14). In a similar way to HIV-1 transcription, productive elongation requires intervention of P-TEFb, which phosphorylates NELF, DSIF and the CTD of Pol II to allow for PPP-release. Additionally, different complexes associate with Pol II to stimulate productive elongation. Among them are the Paf1 complex (Paf1C) and Tat-SF1 (Zhu et al., 2005; Kim et al., 1999). Paf1C acts at least partially through modifying histones during elongation both in *Drosophila* and humans (Zhu et al., 2005; Adelman et al., 2006). Tat-SF1 binds to Pol II, Paf1C and DSIF, and its activity depends on Paf1C and DSIF (Kim et al., 1999; Chen et al., 2009). Although Tat-SF1 associates with all these proteins to stimulate elongation, its precise mechanism of action remains unclear.

- **Tat-SF1, CUS2 and precursor mRNA splicing**

A few observations suggest that Tat-SF1 and CUS2 are involved in splicing, the process of removing introns from precursor mRNAs. With the rare exception of self-splicing introns, splicing requires both a series of specific intronic sequences and a conserved machinery called the spliceosome (for reviews, see (Will and Luhrmann, 2011; Burge et al., 1999)).

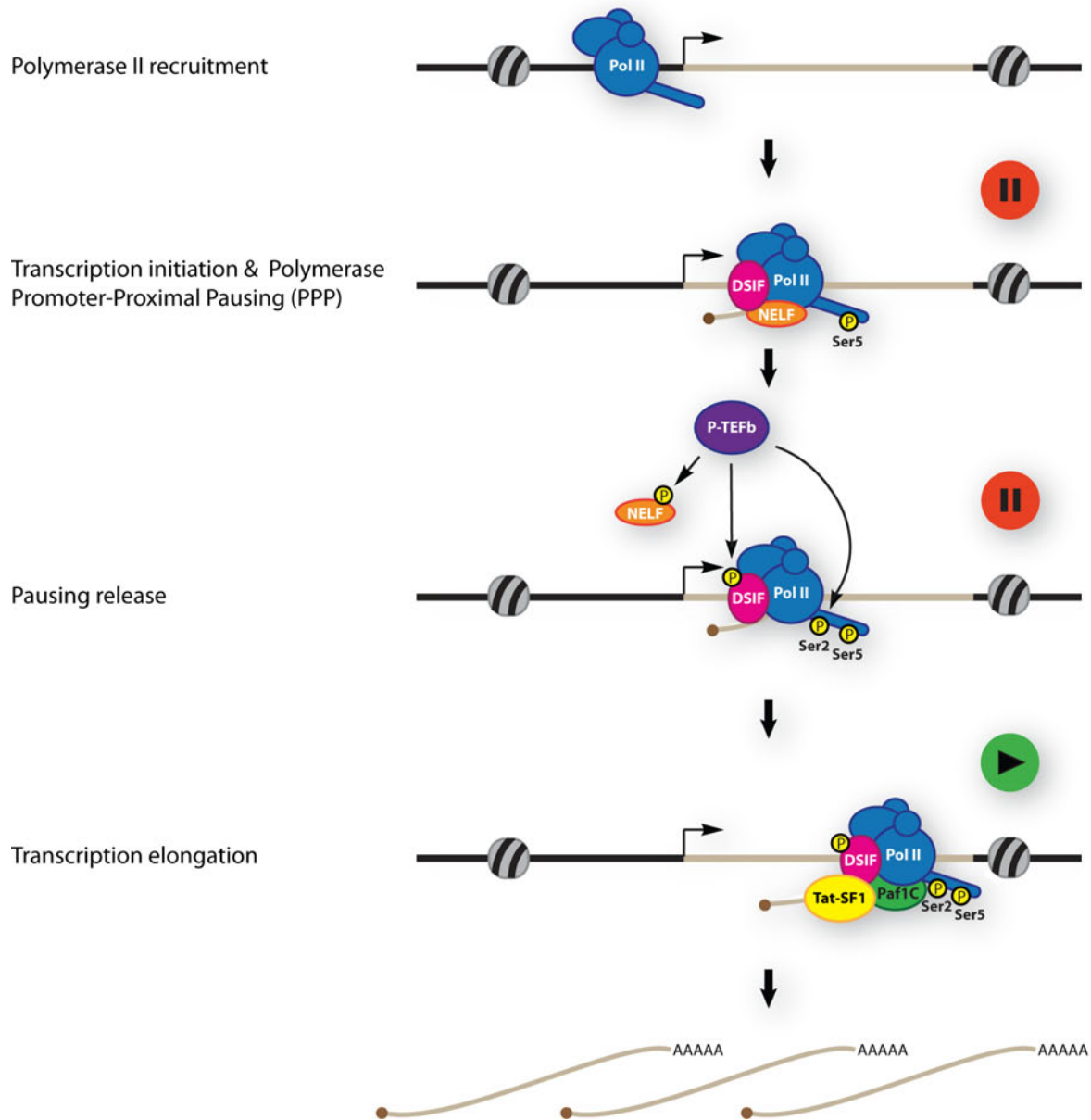


Figure 14. Model for the regulation of Polymerase Promoter-Proximal Pausing (PPP) and transcription elongation

RNA polymerase II is recruited to the promoter of a gene and initiates transcription. Shortly after transcription initiation, polymerase pauses. At this point, polymerase is phosphorylated on Serine 5 of its carboxyterminal domain (CTD) and associated with NELF and DSIF. Release from this paused state is mediated by P-TEFb, which phosphorylates NELF (to inhibit it), DSIF (to activate it) and Serine 2 of the polymerase CTD. Together with the recruitment of elongation factors such as Tat-SF1 and Paf1C, polymerase can resume processive elongation to produce full-length mRNAs.

Each intron is defined by several motifs required for its excision: a 5' splice site (ss), a 3'ss and a branch point. 5' and 3'ss are sequences found on each end of the intron and serve as intronic boundaries. The branch point sequence is usually located 18 to 40 nucleotides upstream of the 3'ss and contains an adenosine residue that is essential for splicing to take place (Fig. 15A).

The spliceosome is a large machinery composed of several small nuclear ribonucleoproteins (snRNPs). Each snRNP is composed of a small nuclear RNA (snRNA) and of several proteins. In Eukaryotes, the vast majority of splicing events are carried out in the nucleus by the so-called U2-dependant or major spliceosome, which is composed of the U1, U2, U5 and U4/6 snRNPs (Will and Luhrmann, 2011). UsnRNPs recognize intronic sequences and, through a series of rearrangements, they carry out two successive transesterifications that ultimately lead to excision of the intron as a lariat, and junction of the two flanking exons (Fig. 15B).

CUS2 was proposed to be a splicing factor based on two main observations. First, CUS2 was shown to bind RNA via its first RRM and to interact with U2snRNA (Yan et al., 1998). Second, a yeast two-hybrid experiment revealed that it binds to PRP11, a subunit of the U2snRNP complex (Yan et al., 1998). However, absence of CUS2 does not seem to impair splicing under normal condition and seems to be required in challenging environments (Yan et al., 1998).

Tat-SF1 was shown to interact with all five UsnRNAs of the spliceosome via its first RRM and with SF3a66/SAP62, the human homologue of PRP11 (Fong and Zhou, 2001; Zhou and Sharp, 1996). Knock down of Tat-SF1 has been shown to increase the unspliced/spliced ratio of HIV transcripts and to have an effect on cellular genes both at the level of transcription and splicing (Miller et al., 2009; Miller et al., 2011).

In summary, proteins of the Barc/Tat-SF1/CUS2 family have been implicated in regulating transcription elongation and/or splicing through mechanisms that remain elusive. Although control of elongation is considered to be particularly important for genes involved in development, there are very few examples of genes regulating this process and causing developmental defects. The *Drosophila* member of this family, *barc*, was identified in a genome wide RNAi screen for defects in larval brain development. A preliminary analysis of its phenotype, conducted together with the screen, revealed that it mainly affects INPs of type

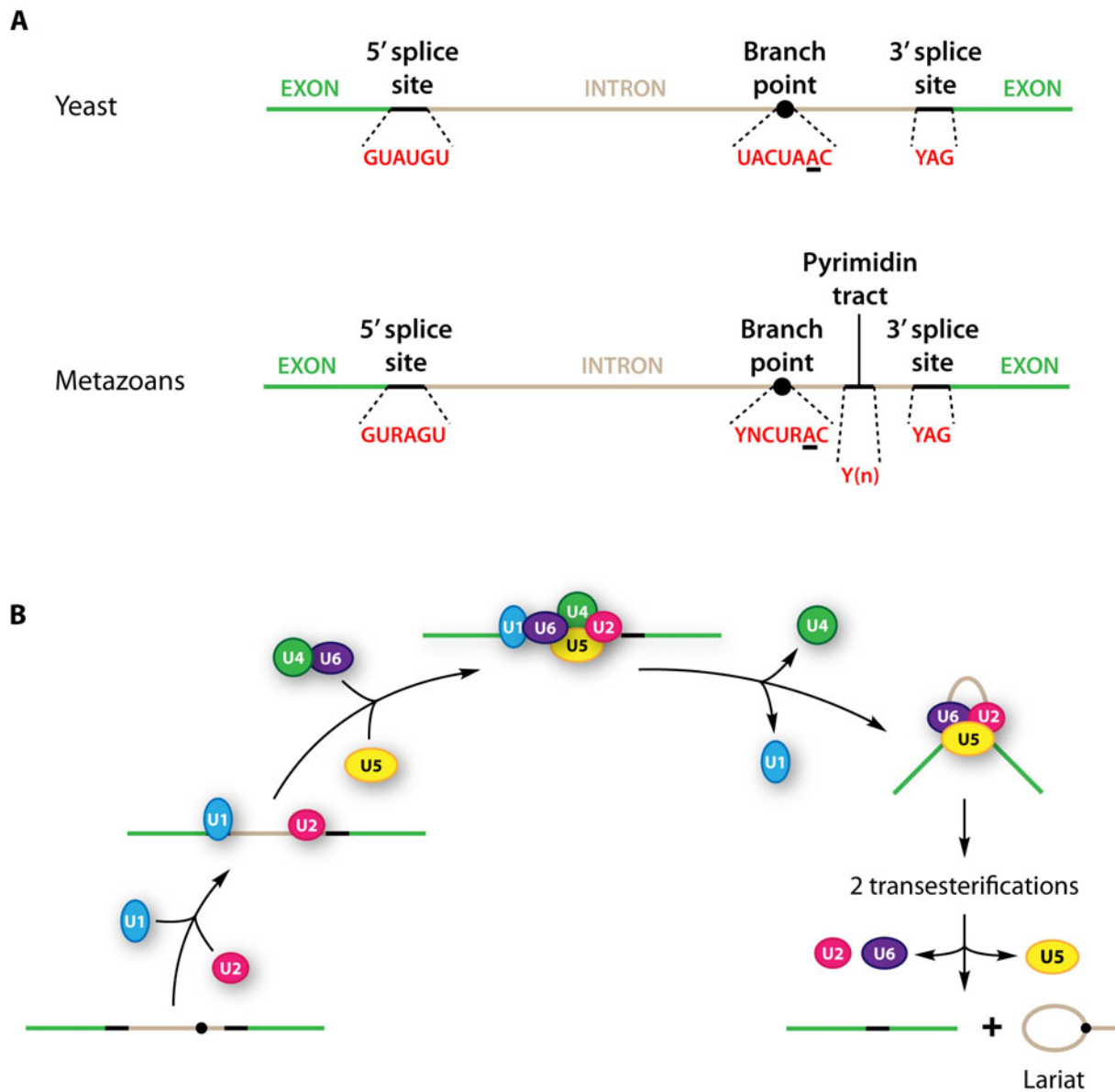


Figure 15. Splicing in yeast and metazoans: intronic sequences and basic mechanism

(A) Eukaryotic introns contain three sequences required for splicing: a 5' splicing site (ss), a 3' ss and a branch point. Introns of higher eukaryotes additionally contain a pyrimidin tract. (B) Basic mechanism of splicing by the U2 spliceosome. First, U1 and U2 snRNPs bind to the 5'ss and the branch point, respectively. Then, they recruit U5 and U4/U6 snRNPs to the intron. At this point, a series of rearrangements takes place between intronic sequences and snRNPs that lead to the release of U1 and U4 snRNPs. U2, U5 and U6 snRNPs then carry out 2 transesterifications that lead to the junction of the two flanking exons and the release of the intron as a lariat. Adapted from (Will and Luhrmann, 2011).

2 lineages (Neumuller et al., 2011). Our study confirms and largely extends beyond this finding, characterizing *barc* and aiming at understanding how it regulates neuroblast lineages.

5.2. RESULTS

5.2.1. Phenotypical analysis of *barc* knock down in larval brains

In the genome wide screen, RNAi-mediated knock down of *barc* using *insc*-Gal4 resulted in lethality and generation of more neuroblast/INPs in larval brains. The GD RNAi line that generated this phenotype is called “Transformant ID 25497” in the VDRC collection. Since it is the only GD RNAi line designed against *barc*, in this chapter we will call it UAS-*barc*RNAi^{GD} or simply *barc* GD RNAi. Our first aim was to precisely describe the *barc* RNAi phenotype in order to determine how it affects neuroblast lineages.

5.2.1.1. The *barc* RNAi phenotype is specific

We first looked at the effect of *barc* knock down in both type 1 and type 2 lineages, using *insc*-Gal4, and staining for the neuroblast/INP marker Mira (Fig. 16). Our first observation was that *barc* GD RNAi brains have an increased number of Mira⁺ cells on the posterior side of the brain lobe, compared to wild type controls (Fig. 16A-A'' & 16B-B''). This result suggests that knock down of *barc* generates more neuroblasts or INPs. The s19 score of the *barc* GD RNAi construct is 1, which means that it is predicted to be completely specific. However, to rule out that the phenotype is caused by an RNAi off-target effect, we used a second RNAi line (UAS-*barc*RNAi^{Custom}) that targets a non-overlapping fragment of the *barc* mRNA (Fig. 16C-C'' & 16F). Using this line, we observed the same phenotype than we did with UAS-*barc*RNAi^{GD}, confirming that *barc* is indeed responsible for the observed phenotype. We then wanted to test whether the RNAi phenotype could be rescued by re-expressing Barc. For that, we co-expressed *barricade*^{Res-FL}, an RNAi resistant full-length *barc* construct, together with the GD RNAi construct (Fig. 16F) (Neumuller et al., 2011). Interestingly, these flies survived until adulthood and their larval brains did not show a phenotype (Fig. 16D-D''). One could argue that this rescue comes from a weaker RNAi knock down of *barc* caused by the fact that *insc*-Gal4 has to drive one more UAS construct (UAS-*barc*^{Res-FL}). To rule this out, we tried to rescue the RNAi phenotype with UAS-*CD8::GFP*. As expected, these flies died before adulthood, indicating that the rescue indeed comes from re-expression of Barc, and not weaker knock down. Additionally, a version of Barc lacking its two RRM and its NLS (*barricade*^{Res-ΔRRM1&2}) was also unable to rescue the RNAi phenotype and showed an accumulation of Mira⁺ cells

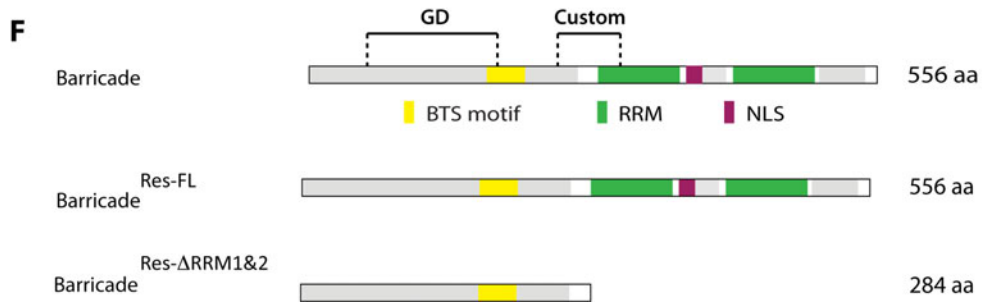
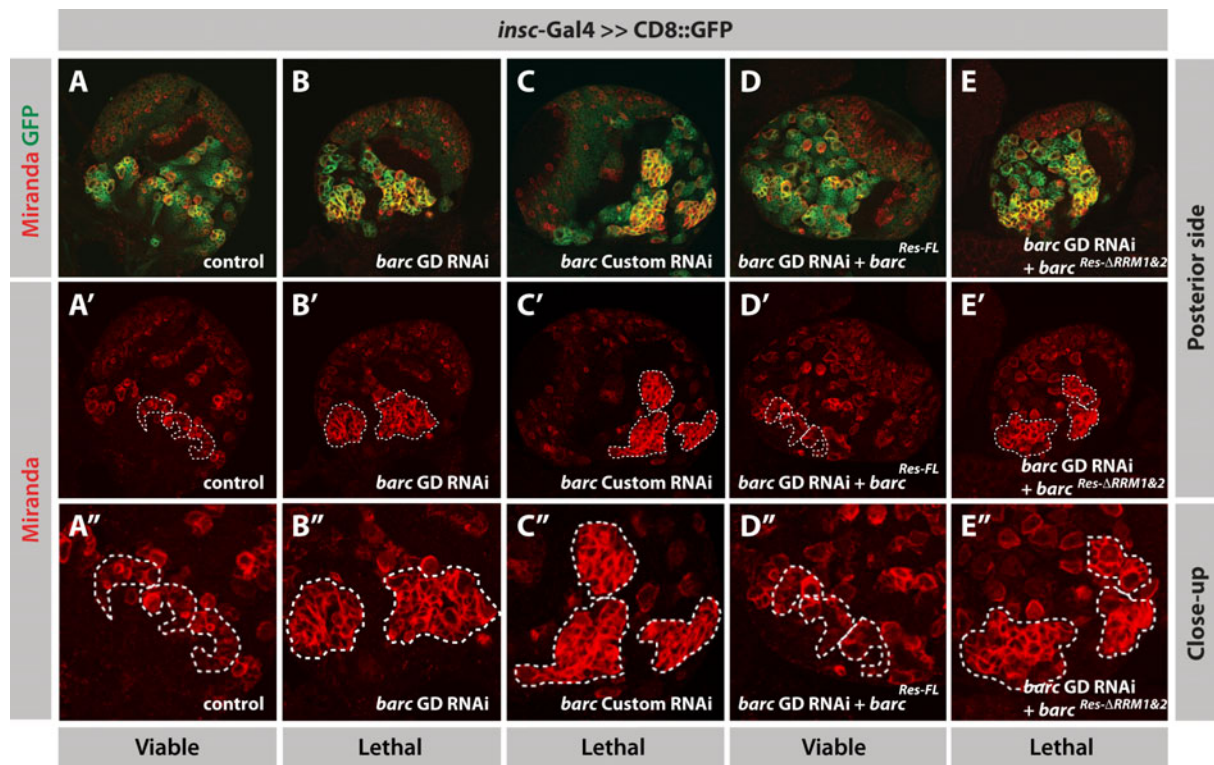


Figure 16. *barc* knock down leads to an accumulation of Mira⁺ cells in larval brains

(A-E'') Third instar brains expressing *insc-Gal4 >> CD8::GFP* and labeled with indicated markers. Brains expressing either *barc* GD RNAi (B-B'') or *barc* Custom RNAi (C-C'') show an accumulation of progenitors (Neuroblasts/INPs, Mira⁺) in the dorsomedial part of the brain, compared to brains expressing no RNAi (A-A''). This phenotype can be rescued by co-expression of *barc* GD RNAi and *barc^{Res-FL}* (D-D'') but not *barc* GD RNAi and *barc^{Res-ΔRRM1&2}* (E-E''). Progenitors of type 2 lineages (Mira⁺) are highlighted (dashed line). Adult survival/lethality of each genotype is indicated in the lower grey boxes. (F) Schematic representing *barc^{Res-FL}*, *barc^{Res-ΔRRM1&2}* and the regions targeted by the GD and the Custom *barc* RNAi lines.

on the posterior side, indicating that the function of *Barc* is carried out by its RRM domains and/or its nuclear localization (Fig. 16 E-E'' & 16F).

Taken together, these results indicate that the accumulation of *Mira*⁺ cells observed upon RNAi knock down is specific to *barc*.

5.2.1.2. *barc* RNAi strongly affects type 2 neuroblast lineages

Interestingly, these groups of *Mira*⁺ cells are found precisely where type 2 lineages are located, which prompted us to examine whether this phenotype originates in these lineages. To test that, we knocked down *barc* in all lineages using *insc*-Gal4 and stained larval brains with *Ase*. As mentioned earlier, *Ase* is expressed in type 1 neuroblasts but is absent in all eight type 2 neuroblasts (Fig. 17A-A'). Stainings of *barc* RNAi knock down brains revealed that the severe *Mira* phenotype indeed originates in type 2 lineages (Fig. 17B-B' & C-C'). Careful analysis of these stainings unraveled that these large groups of *Mira*⁺ cells are composed of two to three type 2 lineages, that each possess a single *Mira*⁺*Ase*⁻ neuroblast and a large number of *Mira*⁺*Ase*⁺ cells of intermediate size. The fact that the majority of the cells that accumulate in *barc* RNAi type 2 lineages express both *Mira* and *Ase* suggests that they are in fact INPs (for detailed analysis, see below).

Taken together, these data indicate that *barc* is important in type 2 neuroblast lineages where it prevents from accumulation of INPs.

5.2.1.3. *barc* RNAi leads to an accumulation of INPs at the expense of neurons

We next wanted to determine whether *barc* deficient type 2 lineages are able to produce terminally differentiated neurons. To test this, we co-stained these lineages with *Mira* (neuroblasts/INPs) and *Elav* (neurons) (Fig. 18A). A wild type lineage (traceable with *UAS-CD8::GFP*) contains a single large *Mira*⁺*Elav*⁻ neuroblast, a curved chain of *Mira*⁺*Elav*⁻ INPs, a few *Mira*⁻*Elav*⁻ GMCs and a large number of *Mira*⁻*Elav*⁺ neurons (Fig. 18B). In lineages expressing *barc* GD or Custom RNAi, however, virtually all cells are *Mira*⁺*Elav*⁻, indicating that these lineages are unable to produce neurons (Fig. 18C&D). As expected, lineages rescued by expression of *UAS-barc*^{Res-FL} are able to produce neurons just like in a wild type situation (Fig. 18E).

These data indicate that *barc* RNAi type 2 lineages accumulate INPs that are unable to produce neurons.

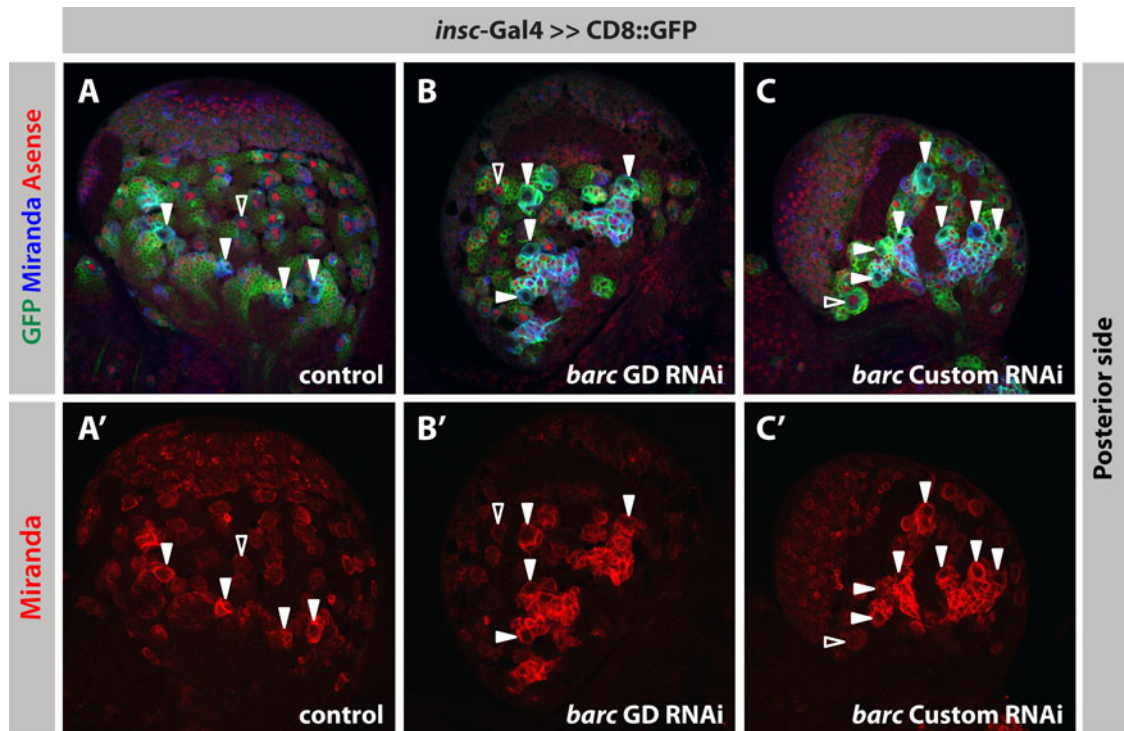


Figure 17. The accumulation of Mira⁺ cells observed with *barc* RNAi originates in type 2 lineages (A-C') Third instar brains expressing *insc-Gal4>>CD8::GFP* and labeled with indicated markers. (A,A') Control brains have eight type 2 neuroblast per lobe (Mira⁺Ase⁻, closed arrowhead, not all type 2 neuroblasts are in focus) and a large number of type 1 neuroblasts (Mira⁺Ase⁺, open arrowhead). Mira⁺ cells accumulating in brains expressing either *barc GD RNAi* (B-B') or *barc Custom RNAi* (C-C') originate from type 2 neuroblasts (closed arrowhead) and not type 1 neuroblasts (open arrowhead).

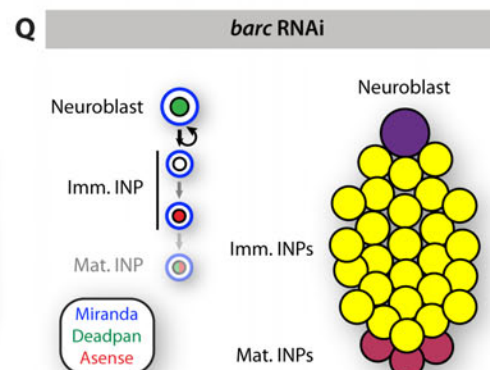
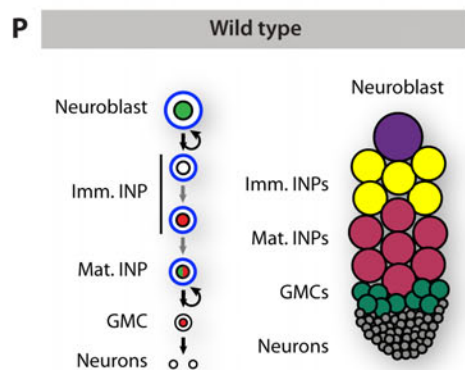
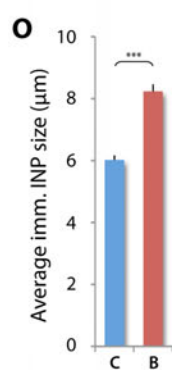
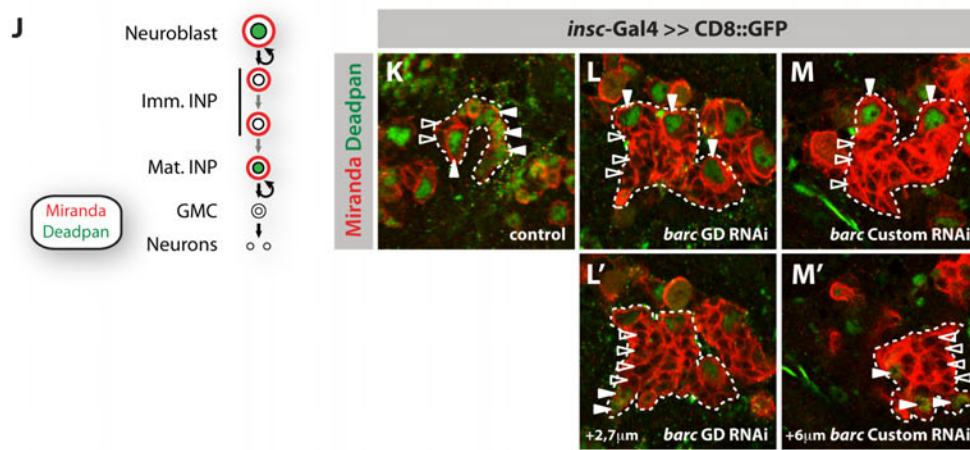
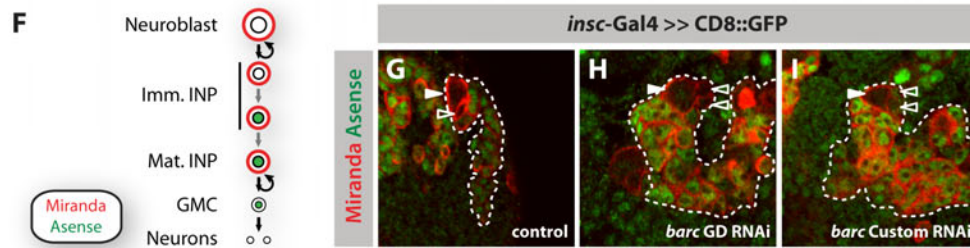
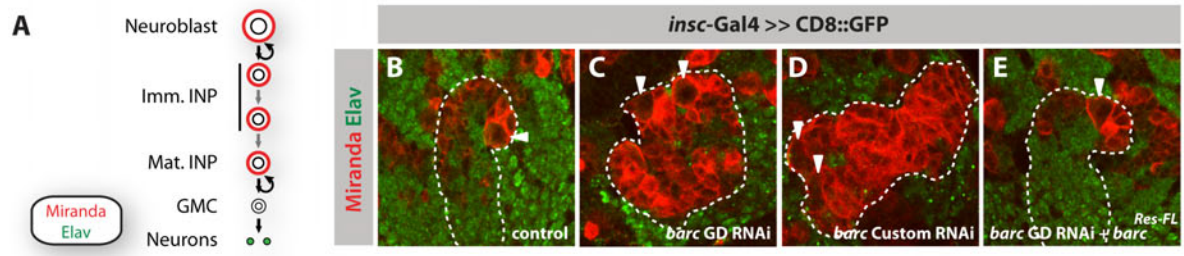


Figure 18. *barc* knock down causes defects in type 2 lineage progression

(A,F,J) Schematic representation of the expression pattern of the markers used in immunostainings (B-E,G-I,K-M') of type 2 lineages from third instar brains expressing *insc-Gal4>>CD8::GFP*. (A-E) Analysis of Mira/Elav expression. A lineage expressing no RNAi (B) is composed of a single Mira⁺Elav⁻ neuroblast (closed arrowhead), a curved chain of Mira⁺Elav⁻ INPs and a large number of Mira⁺Elav⁺ neurons. Lineages expressing either *barc* GD (C) or *barc* Custom RNAi (D) cluster in groups of 2-3 that are each composed of a single Mira⁺Elav⁻ neuroblast (closed arrowhead), a large number of Mira⁺Elav⁻ INPs and no Mira⁺Elav⁺ neurons. This phenotype can be rescued by co-expression of *barc* GD RNAi and *barc*^{Res-FL} (E). Lineages are highlighted by a dashed line. (F-I) Analysis of Mira/Ase expression. A lineage expressing no RNAi (G) is composed of a single Mira⁺Ase⁻ neuroblast (closed arrowhead), about 2 Mira⁺Ase⁻ imm. INPs (open arrowhead) and a chain of Mira⁺Ase⁺ INPs. In lineages expressing either *barc* GD (H) or *barc* Custom RNAi (I), Ase is not affected. Progenitors (Neuroblasts/INPs) are highlighted by a dashed line. (J-M') Analysis of Mira/Dpn expression. A lineage expressing no RNAi (K) is composed of a single Mira⁺Dpn⁺ neuroblast (closed arrowhead), about 4 Mira⁺Dpn⁻ imm. INPs (empty arrowhead), and a large number of Mira⁺Dpn⁺ mat. INPs. (closed arrowhead). Lineages expressing either *barc* GD (L) or *barc* Custom RNAi (M) each contain a Mira⁺Dpn⁺ neuroblast (closed arrowhead), but far too many Mira⁺Dpn⁻ imm. INPs (empty arrowhead). Deeper inside these lineages, a few Mira⁺Dpn⁺ mat. INPs. (L',M', closed arrowhead) can be observed. Progenitors (Neuroblasts/INPs) are highlighted by a dashed line. (O) Imm. INPs of lineages expressing *barc* GD RNAi (called B, n=34, from 3 brain lobes) are bigger than those of lineages expressing no RNAi (called C, n=37, from 4 brain lobes). SEM, t-test pvalue<0,001. (P-Q) In type 2 lineages expressing *barc* RNAi (Q), a large number of imm. INPs and a few mat. INPs accumulate at the expense of neurons, compared to lineages expressing no RNAi (P).

5.2.1.4. *barc* regulates INP maturation

We next wanted to determine whether INPs that accumulate in *barc* deficient type 2 lineages are immature or mature. These two different populations of cells can be distinguished based on the expression of Ase and Dpn: young immature INPs are Ase⁻Dpn⁻, old immature INPs are Ase⁺Dpn⁻ and mature INPs are Ase⁺Dpn⁺. It is important to keep in mind that the neuroblast always divides in the same orientation and that INPs do not migrate. Young INPs are therefore close to the neuroblast, whereas old INPs are far away from it.

We started our analysis by looking at Mira and Ase. A wild type lineage typically contains a single Mira⁺Ase⁻ neuroblast and two to three Mira⁺Ase⁻ INPs next to it, all other INPs being Mira⁺Ase⁺ (Fig. 18F&G). In both *barc* GD and Custom RNAi type 2 lineages, Ase had a similar expression pattern than in the wild type situation (Fig. 18H&I). This result indicates that Ase expression is not affected by loss of *barc* and that INPs that accumulate in these lineages are not young immature INPs.

To determine whether these INPs are old immature or mature INPs, we then stained these lineages with Mira and Dpn. A wild type lineage typically contains a single Mira⁺Dpn⁺ neuroblast, about four to five Mira⁺Dpn⁻ immature INPs, and more Mira⁺Dpn⁺ mature INPs farther away from the neuroblast (Fig. 18J&K). Upon *barc* knock down with either the GD or the Custom RNAi construct, we observed that although the neuroblast still expresses Dpn, the majority of Mira⁺ cells are Dpn⁻ indicating that they are immature INPs (Fig. 18L&M). It is important however, to note that a few cells located far away from the neuroblast do re-express Dpn, indicating that these few cells eventually manage to reach a mature INP state (Fig. 18L'&M').

Another interesting observation made based on these stainings, is that *barc* RNAi immature INPs (8,23µm ±0,23µm, n=34 from 3 brain lobes; SEM) are significantly larger than wild-type immature INPs (6,02µm ±0,14µm, n=37 from 4 brain lobes; SEM) (Fig. 18O).

Taken together, these data demonstrate that upon *barc* knock down, immature INPs grow and most of them remain in an immature INP state, failing to re-express Dpn (Fig. 18P&Q). This suggests that Barc is a novel regulator of INP maturation.

5.2.1.5. Quantification of the *barc* RNAi phenotype in type 2 lineages

We next wanted to quantify the accumulation of immature INPs in *barc* RNAi lineages. When we induce *barc* RNAi with *insc*-Gal4, all lineages express GFP and type 2 lineages cluster together, making it very hard to confidently count cells. To circumvent this problem, we decided to use the type 2 specific driver line *worniu*-Gal4, *asense*-Gal80 (*wor*-Gal4, *ase*-Gal80, Fig. 19A) (Neumuller et al., 2011). RNAi-mediated knock down of *barc* with this driver line resulted in lineages that mainly consist of *Mira*⁺ cells, similarly to what we observed with *insc*-Gal4 (Fig. 19B). We then stained these lineages with *Mira* and *Dpn* and observed that *barc* RNAi lineages have more *Mira*⁺*Dpn*⁻ immature INPs than wild type lineages (Fig. 19C-C',D-D').

When counting *Mira*⁺ cells of wild type lineages, we noticed that type 2 lineages are heterogeneous in terms of the amount of INPs they each produce. Indeed, the two dorsal lineages systematically generate less INPs than the six medial lineages (dorsal: 9,66 ±2,99 INPs/lineage; medial: 32,08 ±4,90 INPs/lineage; n=6 lobes; SD; Fig. 19A,E). All wild type medial lineages, however, seem to generate a similar number of INPs. For that reason, we decided to count INPs generated by the six medial lineages, solely.

Upon *barc* RNAi knock down, we observed a significant accumulation of INPs in type 2 lineages (Control: 32,08 ±0,81 INPs/lineage; *barc*: 42,19 ±0,92 INPs/lineage; n=36 lineages each; SEM; Fig. 19F). The effect of losing *barc* was much stronger on immature INPs, than on mature INPs (Control: 4,72 ±0,11 *Mira*⁺*Dpn*⁻ cells and 27,36 ±0,80 *Mira*⁺*Dpn*⁺ cells; *barc*: 9,52 ±0,34 *Mira*⁺*Dpn*⁻ cells and 32,66 ±0,89 *Mira*⁺*Dpn*⁺ cells; n=36 lineages from 6 brain lobes each; SEM; Fig. 19F). This quantification confirms our previous observation that *barc* regulates INPs (Fig. 19G). However, the number of INPs that reach a mature stage is much higher when knocking down *barc* with *wor*-Gal4, *ase*-Gal80 than with *insc*-Gal4. This observation might first seem a bit surprising. However, it is important to remember that *barc* knock down does not affect *Ase*. This means that as soon as an immature INP turns on *Ase*, Gal80 is expressed, represses Gal4 and turns off expression of the RNAi construct. In other words, with this driver line *barc* RNAi is only expressed in the neuroblast and the two to three youngest immature INPs. The very transient activity of *wor*-Gal4, *ase*-Gal80 in a *barc* RNAi background is probably responsible for the weaker phenotype observed with this driver line compared to *insc*-Gal4 (Fig. 19H).

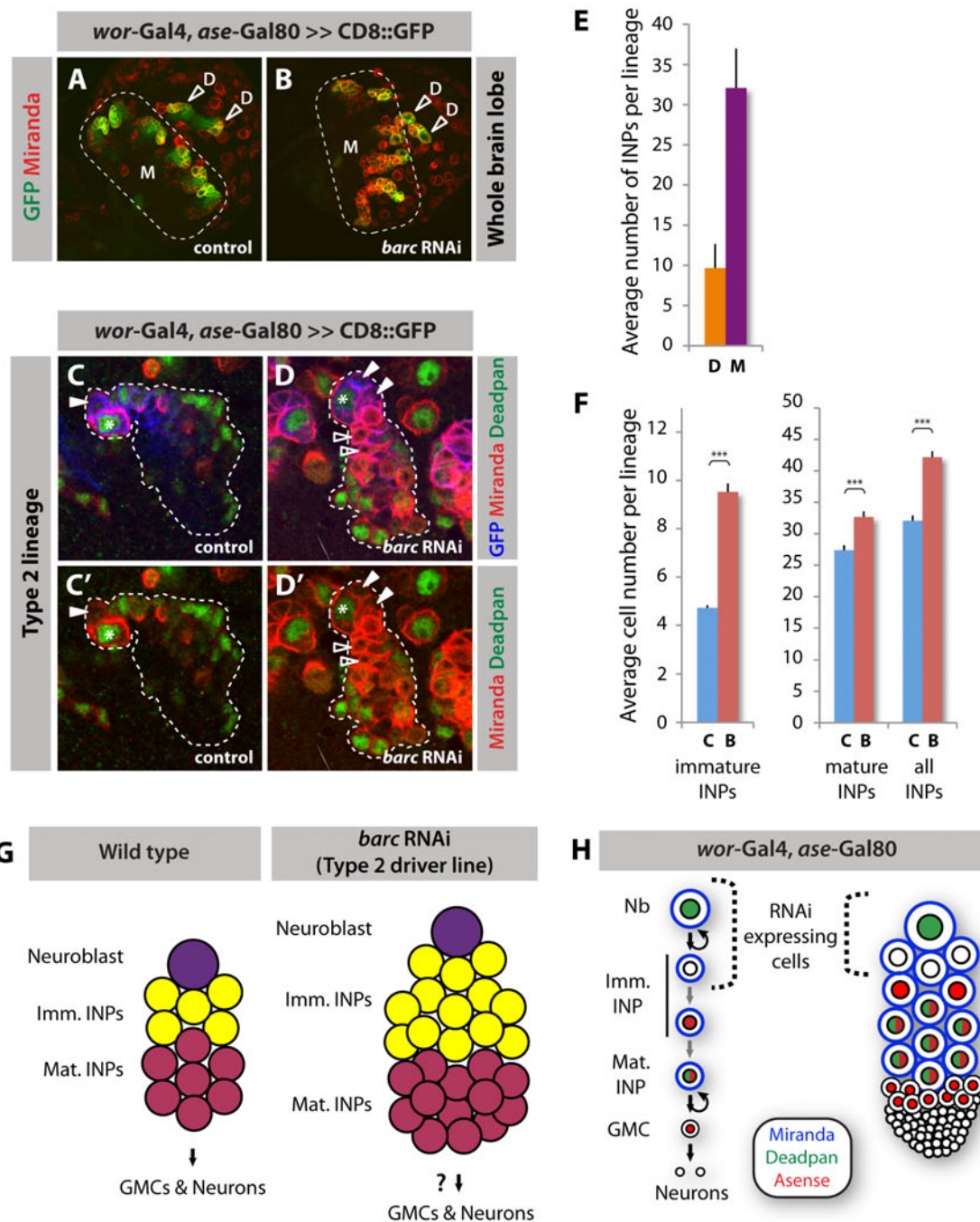


Figure 19. Quantification of the *barc* RNAi phenotype using a type 2 lineage specific driver line

Overview (**A,B**) and close-ups (**C-D'**) of third instar brains expressing *wor-Gal4,ase-Gal80>>CD8::GFP* in the 8 type 2 lineages (**A,B**: 6 medial lineages (called M, dashed line) and 2 dorsal lineages (called D, empty arrowhead). Lineages expressing *barc* GD RNAi (**B,D,D'**) have more *Mira*⁺*Dpn*⁻ imm. INPs (open arrowhead, **D,D'**) than lineages expressing no RNAi (**A,C,C'**). Asterisk: *Mira*⁺*Dpn*⁺ neuroblast. Closed arrowhead: regular *Mira*⁺*Dpn*⁻ imm. INPs. Lineages are marked with a dashed line. (**E**) Wild type dorsal lineages (called D) produce much less INPs/lineage than medial lineages (called C). SD, n=6 lobes. (**F**) Quantification of imm. INPs (*Mira*⁺*Dpn*⁻), mature INPs (*Mira*⁺*Dpn*⁺) and total INPs per medial lineages expressing *barc* GD RNAi (called B) or no RNAi (called C). n=6 lobes, SEM, t-test pvalue<0,001. (**G**) Type 2 lineages expressing *barc* GD RNAi have more imm. and mature INPs. (**H**) The weaker phenotype observed with *wor-Gal4,ase-Gal80>>CD8::GFP* is probably due to the fact that with this driver line, the RNAi is only expressed in 3-4 cells, until *Ase* turns on.

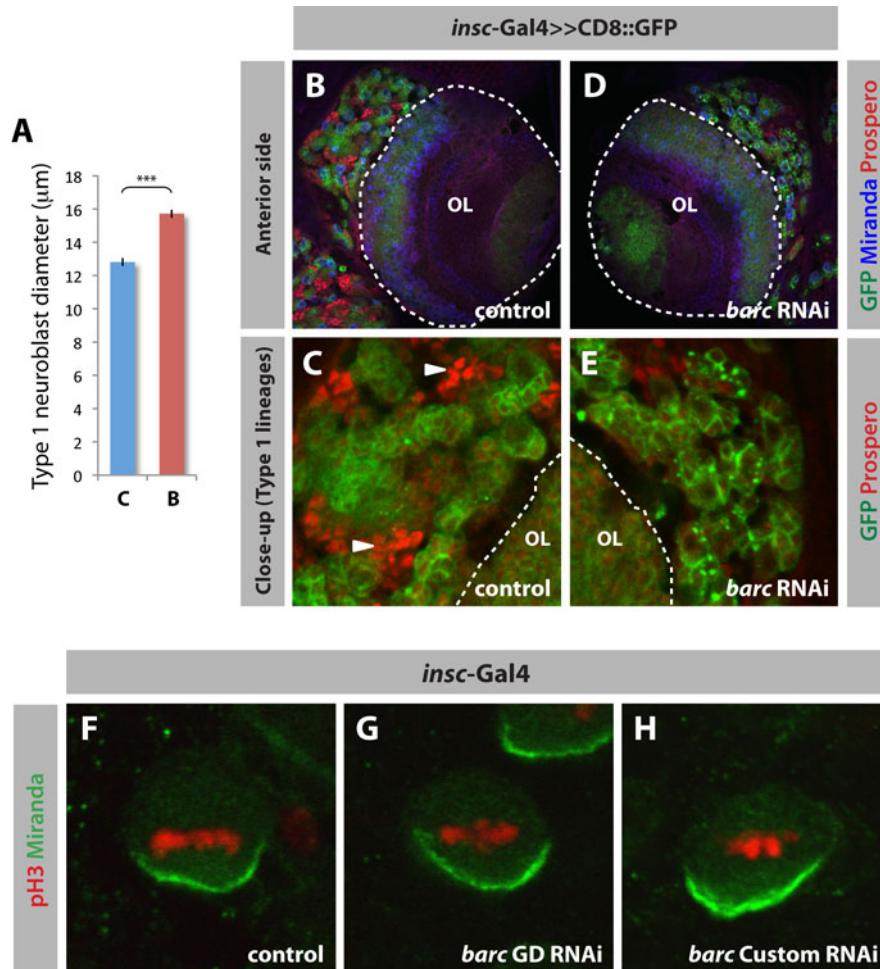


Figure 20. *barc* is also important in type 1 lineages.

(A) Type 1 neuroblasts expressing *barc* GD RNAi (called B, n=72, from 8 lobes) are bigger than those expressing no RNAi (called C, n=55, from 8 lobes). SEM, t-test, pvalue<0,001. Overview (A,D) and close-ups (C,E) of the anterior side of third instar brains expressing *insc-Gal4>>CD8::GFP* and labeled with indicated markers. Wild-type type1 neuroblasts (C) produce GMCs/neurons (Pros⁺, closed arrowhead) that are largely missing upon expression of *barc* GD RNAi (E). OL: Optic lobe. (F-H) Close-up on dividing type 1 neuroblasts. Asymmetric localization of Mira in metaphase (F) is not affected by expression of either *barc* GD (G) or *barc* Custom RNAi (H).

5.2.1.6. *barc* also plays a role in type 1 lineages

We then wanted to test whether *barc* is also required in type 1 lineages. We therefore looked at these lineages on the anterior side of the brain, using Mira to mark neuroblasts and Pros to visualize GMCs and neurons. Our first observation was that *barc* RNAi type 1 neuroblasts are significantly larger than their wild-type counterparts (wild type: $12,81\mu\text{m} \pm 0,23\mu\text{m}$ diameter, $n=55$ from 8 brain lobes; *barc*: $15,71\mu\text{m} \pm 0,23\mu\text{m}$ diameter, $n=72$ from 8 brain lobes; SEM; Fig. 20A). Since larval neuroblasts regrow between each division, an increase of their size upon *barc* knock down suggests that Barc affects either growth or cell cycle. Strikingly, we observed less Pros⁺ cells in *barc* type 1 lineages, compared to wild type lineages (Fig. 20B-E). This suggests that in *barc* RNAi brains, type 1 neuroblasts or GMCs fail to produce a proper amount of neurons. Although we could not precisely quantify a potential effect of *barc* on cell cycle using *insc*-Gal4, we did observe that *barc* RNAi type 1 neuroblast do divide in an asymmetric way (Fig. 20F-H).

Taken together, these data demonstrate that *barc* is also required in type 1 lineages, where it affects growth and possibly cell cycle, and is ultimately required to produce neurons.

5.2.2. Characterization of Barc expression pattern

Having shown that Barc plays a role in both type 1 and type 2 lineages, we became interested in determining in which cell types is Barc expressed, and whether it could play a role in other tissues as well. For that, we raised antibodies against the C-terminus of the protein, in both rabbits (Neumuller et al., 2011) and guinea pigs (this study).

5.2.2.1. Barc is strongly expressed in larval neuroblasts

Since we know Barc is important in neuroblast lineages, we decided to test our antibodies in larval brains first.

Western blots of larval brain protein extracts, revealed that our purified rabbit antibody recognizes a single band that runs around 75kDa (Fig. 21A). Barc is predicted to be 64kDa, however, just like it has been reported for human Tat-SF1, its very acidic sequence is probably responsible for the fact that it runs higher in SDS-PAGE (Zhou and Sharp, 1996). This antibody additionally recognized overexpressed Myc::*Barc* in western blots (Fig. 21A).

When we stained larval brains with our antibodies, we observed a very strong nuclear signal in both type 1 and type 2 neuroblasts and to a lesser extend in INPs and differentiated cells

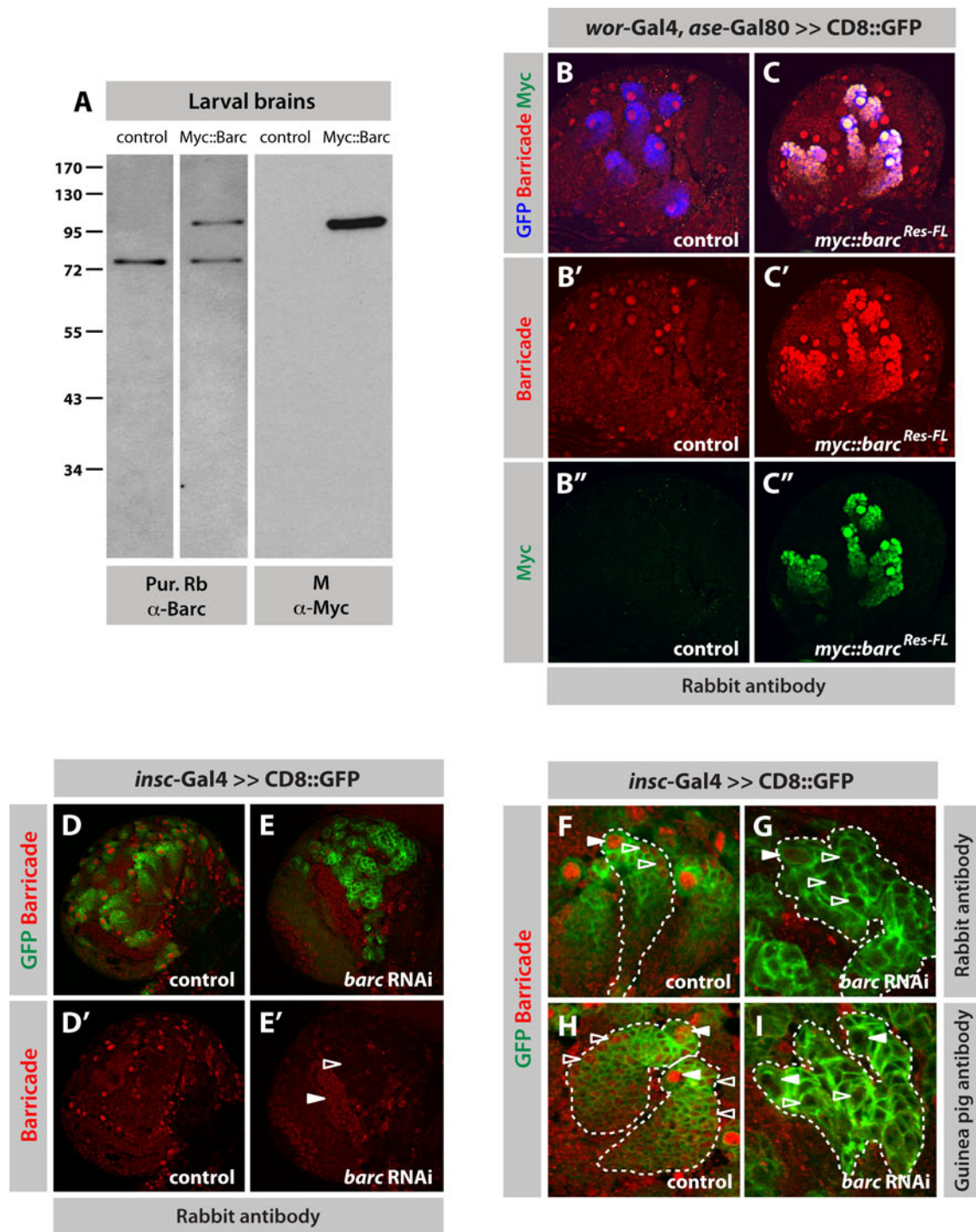


Figure 21. Barc expression pattern in the larval brain

(A) Western blot of larval brain extracts. Purified rabbit α -Barc recognizes a single band that runs at about 75kDa as well as overexpressed Myc::Barc. (B-I) Third instar brains expressing *wor-Gal4, ase-Gal80 >> CD8::GFP* or *insc-Gal4 >> CD8::GFP*. Barc is a widely expressed nuclear protein (B, B', D, D') that shows a prominent signal in all neuroblasts (F, H, closed arrowhead) and to a lesser extent in INPs (F, H, empty arrowhead) and differentiated cells. Our antibodies are specific to Barc since they recognize overexpressed Myc::Barc^{Res-FL} (C-C'') and that their signal is lost upon *barc RNAi* expression (E, E', G, I). In (E') compare areas where *barc RNAi* is expressed (empty arrowhead), to areas where *barc RNAi* is not expressed (closed arrowhead).

(Fig. 21B-B'', D-D', F&H). This signal is specific to Barc because our antibodies recognize overexpressed Myc::Barc and this signal is lost upon RNAi knock down (Fig. 21C-C'', E-E', G&I).

Taken together these data show that our antibodies are specific and reveal that Barc is strongly expressed in neuroblasts but is also present in all other cells.

5.2.2.2. Barc is also expressed in embryos and germline stem cell lineages

Having good antibodies in hand, we next wanted to ask whether Barc is specifically expressed in larval brains or whether it is also present in developing embryos and other stem cell lineages, such as the ovaries and testes.

We first tested our antibodies in western blot on embryo extracts. Just like for larval brain, our antibodies recognized a 75kDa band, suggesting Barc is also expressed in embryos (Fig. 22A). We therefore stained embryos of different age to determine which cells or tissues express Barc. In early embryos, prior to cellularization, somatic nuclei are located at the periphery of the embryo, whereas nuclei of pole cells, the germline precursors, are found at the posterior end of the embryo. At this stage, we found that Barc localizes to all nuclei (Fig. 22B,B',C,C'). In late embryos, we found Barc to be also expressed in all nuclei (Fig. 22D,D').

We then wanted to test whether Barc is expressed in stem cell lineages of the ovaries and the testes. In both these lineages, stem cells are in contact with a niche, composed of somatic cells – Cap cells (CCs) for ovaries and Hub for testes, that maintains them in a self-renewing state. Germline stem cells (GSCs) of both tissues produce cells – Cystoblasts (CBs) for ovaries and Gonialblasts (GBs) for testes – that are not in contact with the niche anymore, differentiate and divide to ultimately produce gametes (Fig. 22E&H). Interestingly, Barc seems to be expressed in virtually all cells that populate ovaries and testes (Fig. 22F,F',G,G',I,I',J,J').

Taken together, these data show that Barc is broadly expressed during embryonic development as well as in ovaries and testes. This favors the idea that Barc is a nuclear regulator that plays a role in a variety of tissues and organs in *Drosophila*.

5.2.3. Generation of a *barc* mutant and of rescue constructs

Using an inducible mutant is an optimal way to confirm an RNAi phenotype, precisely quantify an effect on cell fate and cell cycle, and circumvent possible early lethality caused

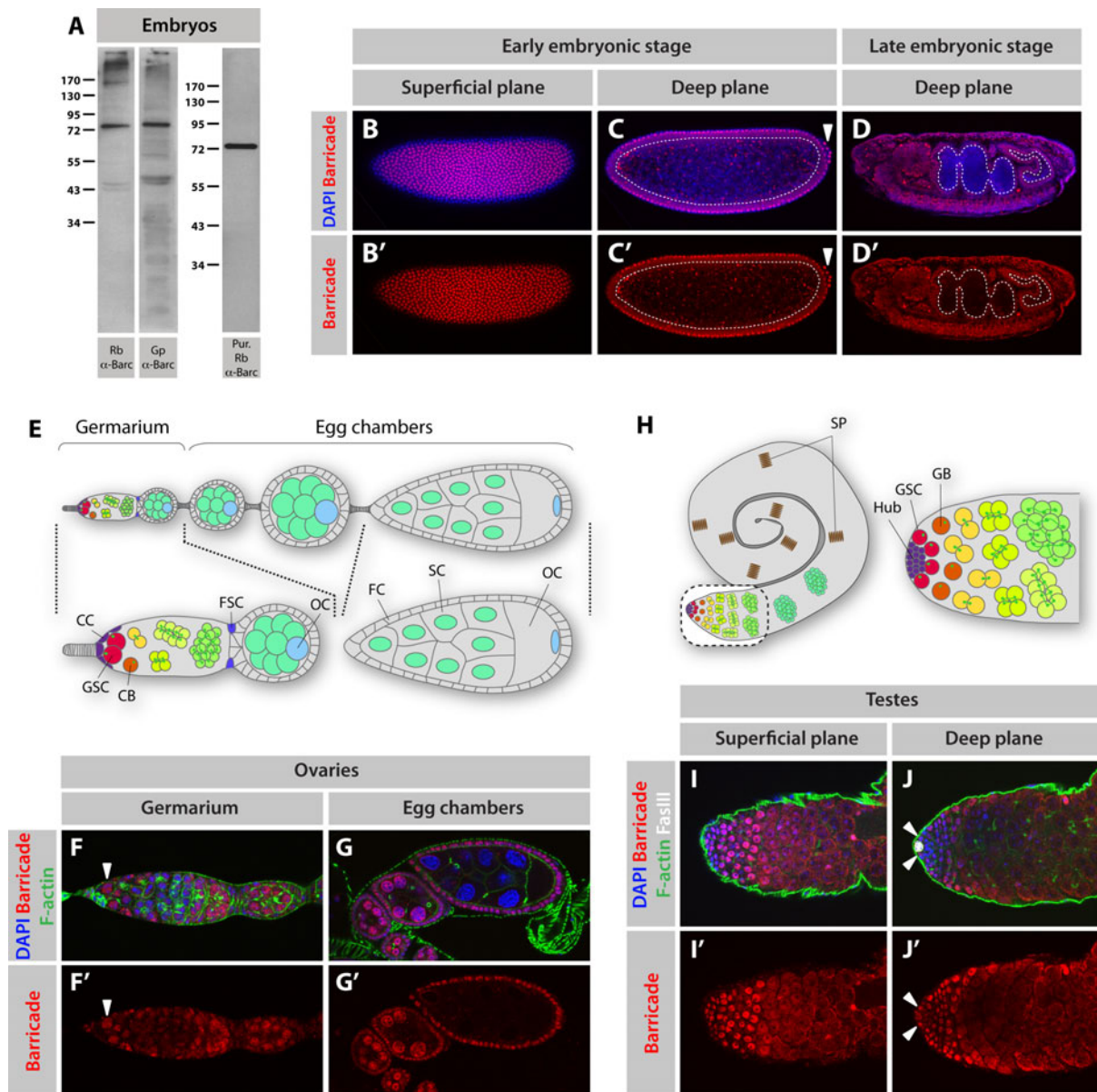


Figure 22. Expression pattern of Barc in embryos, ovaries and testes

(A) Western blot showing that Barc is expressed in embryos. (B-D') Immunostainings of embryos. Barc localizes to the nucleus of all cells both in early (B-C') and late (D,D') embryos. Dashed lines in (C,C') highlight the yolk mass found in the center of early embryos. Closed arrowheads indicate pole cells. Dashed lines in (D,D') highlight the digestive tract. (E) *Drosophila* ovaries are composed of a germarium, where germline stem cells (GSCs) are located, and of egg chambers, where eggs develop. GSCs are in contact with a niche (cap cells, CC). When they divide, they generate a cystoblast (CB) that differentiates and divides to form the future egg. A developing egg is composed of an oocyte (OC) and support cells (SC) that are surrounded by somatic cells (follicular cells, FCs) produced by follicular stem cells (FSCs) (F-G') Immunostainings of ovaries. Barc is expressed in GSCs (closed arrowhead) as well as in most other cells of the ovaries. (H) In *Drosophila* testes, germline stem cells (GSCs) are also in contact with a niche (Hub). They generate gonialblasts (GBs) that differentiate and divide to form the future spermatids (SPs). (I-J') Immunostainings of testes. Barc is expressed in GSCs (closed arrowhead) as well as in most other cells of the testes.

by broad expression of the gene of interest. Because there was no *barc* mutant available, we decided to design our own, together with two different rescue constructs.

5.2.3.1. Choice of the method to generate a *barc* mutant

There are several well-established methods that allow generating mutants in *Drosophila*. However, most of them rely on the presence of transposable elements around the gene *locus*. In addition to lacking such element insertions, the *barc locus* is very complex. Indeed, *barc* overlaps with two other genes, on the opposite strand (*rgn* & *CG33288*, Fig. 23A). We therefore decided to use Ends-out homologous recombination, an elegant and versatile method based on the recognition of homologous sequences that allows removal and replacement of any part of a *locus*. The next few paragraphs resume the method used here but for details please refer to the “Experimental Procedures” section of this chapter and to (Rong and Golic, 2000; Huang et al., 2009).

Ends-out homologous recombination requires cloning of DNA sequences flanking the region that one wishes to delete – called “homology arms”. These arms are placed on each side of a cassette that contains the selection marker *white* flanked by LoxP sites, which allow to remove the *white* gene if necessary. This construct is inserted in a *white* deficient fly on a different chromosome than the one carrying the gene of interest – this line is called “Donor” fly line. The construct is then artificially excised, and in rare cases homology arms recognize their endogenous counterparts and recombine. This leads to the replacement of the endogenous area of interest, with the *white* cassette and generates a mutant allele (Rong and Golic, 2000).

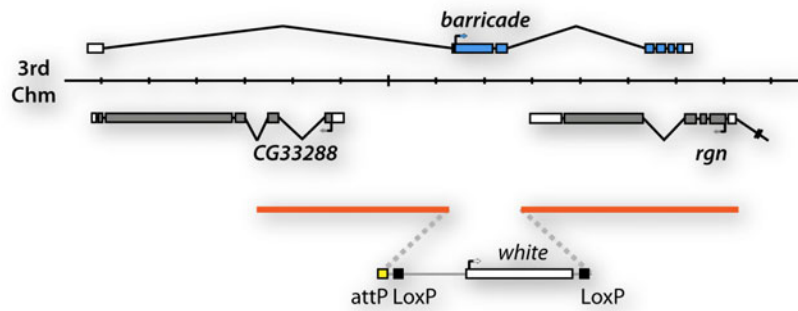
5.2.3.2. Making a *barc* mutant by homologous recombination: design of the strategy

To maximize chances that our mutant is a null allele, we decided to delete all coding sequences that do not overlap with any other gene, namely exons 2 and 3, which contain the end of the 5’UTR, the unique ATG and about 60% of the *barc* coding sequence (Fig. 23A&B). The region to be deleted encodes the N-terminus, the BTS domain and 2/3rd of the first RRM of the protein. The deletion of this 1.4 kb region of the *barc locus* should therefore result a null mutant allele.

We ultimately would like to replace this fragment with a cassette containing the selection marker *white* and a so-called minimal attP phage sequence (50bp) (Fig. 23A). This minimal attP sequence can specifically and efficiently recombine in *Drosophila* with the minimal

A

wild type (*w*-)



B

barc knock out (*w*+)



Figure 23. Generation of a *barc* mutant allele by ends out homologous recombination

Schematic of the wild type *barc* (A) and *barc*^{attKO} mutant (B) loci. We used an upstream homology arm (orange) of about 4 kb and a downstream homology arm (orange) of about 4.7 kb, to delete a 1,4kb fragment that contains the ATG of *barc* and about 60% of its coding sequence. We replaced it with a cassette containing an *attP* site and the selection marker *white*. *barc* is encoded by the minus strand and for sake of clarity the chromosome has been flipped over.

bacterial attB sequence (53bp), upon expression of the ϕ 31 recombinase (Huang et al., 2009). From a theoretical point of view, having an attP sequence in the mutant *locus* enables to rescue the mutant with an attB-*barc* construct (for details about rescue constructs, see section 5.2.3.4). From a technical point of view, however, one has to keep in mind that the insertion of attB-*barc* in the attP site would result in the formation of an attR and an attL sequence on each side of the insertion. To make sure that the attR formed upstream of the *barc* rescue coding sequence (*barc* CDS) would not interfere with splicing between exon 1 and *barc* CDS – as this could result in a failure to rescue the mutant – we decided to place the attP sequence in intron 1 rather than at the beginning of exon 2. Finally, the attP can also not be placed randomly in intron 1. Indeed, its insertion in the branch point sequence would also abolish splicing and prevent rescue of the mutant. The branch point is usually located 18 to 40 bp upstream of the 3' splice site (ss) (Will and Luhrmann, 2011). We therefore decided to place the attP site about 140bp upstream of the 3' ss. To ensure rescue, this deleted fragment of intron 1 would be inserted in the rescue constructs to ensure correct splicing between intron 1 and *barc* CDS.

In order to generate a *barc* mutant allele lacking the 1.4kb fragment described above, and having considered splicing issues, we cloned an upstream homology arm of about 4 kb that starts in intron 1, and a downstream homology arm of about 4.7 kb that starts a bit downstream of exon 3 (Fig. 23A&B).

Finally, since *Barc* could have a role in a variety of tissues and that we would like to quantify its effect on cell fate and cell cycle, we wanted this mutant to be compatible with the MARCM system (Lee and Luo, 1999). This system, widely used in chapter I, allows the generation of traceable mutant clones in an otherwise heterozygous background. This method requires the mutant allele to possess an FRT sequence on the same chromosomal arm – in this case, FRT80B. This is usually achieved by recombining the FRT sequence with the mutant arm. However, *barc* is extremely close to FRT80B, rendering recombination very difficult. We therefore decided to generate our mutant allele directly on a chromosome carrying FRT80B.

5.2.3.3. Screening for mutant candidates

To look for correct mutant, we first screened candidates for restored *white* function, located on the right chromosome, and lethal before adulthood. We then screened candidates by PCR, using primers in the *white* cassette, combined with primers that either bind the homology arm or the genomic sequence surrounding it (Data not shown). Finally, we used southern blots to

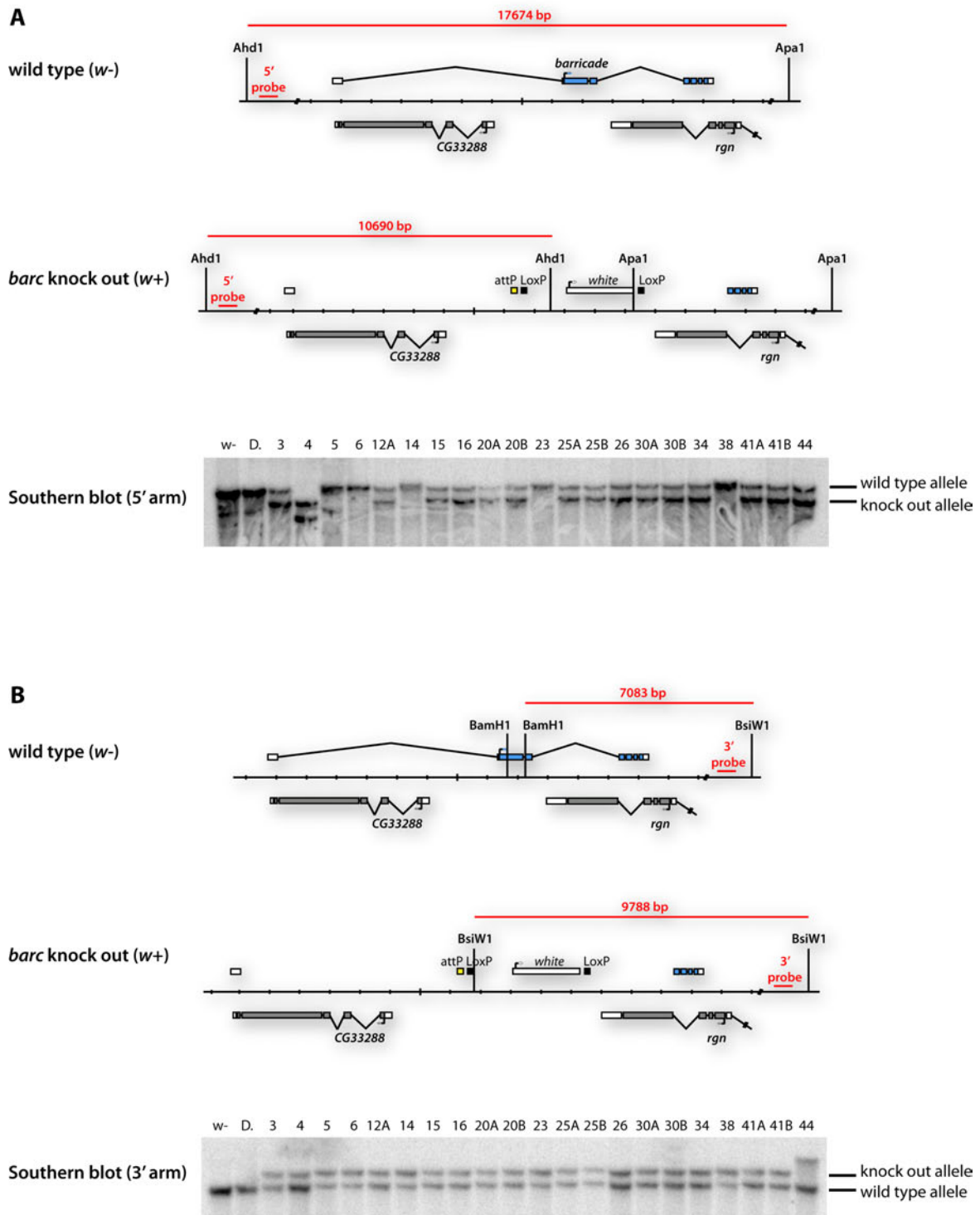


Figure 24. Screening of *barc*^{attKO} mutant candidates by Southern blot

The 5' (A) and the 3' (B) arms of *barc*^{attKO} mutant candidates were tested by southern blot. Restriction enzymes used in each case and expected fragment sizes are as indicated on the schematics. Mutants are expected to have both a knock out allele and a wild type allele since the *barc*^{attKO} should be homozygous lethal. Stocks for which both 5' and 3' arm were correct were selected for further analysis.

confirm candidates (Fig. 24A&B). The presence of the FRT sequence on the same chromosome as our mutant allele was confirmed by testing the ability of candidates to generate clones in the eye using *ey-flp* (Data not shown). Confirmed mutant candidates are called *barc*^{attPKO}.

We have generated a total of 11 *barc*^{attPKO} mutant fly lines. Preliminary analysis of these mutants revealed that homozygous *barc*^{attPKO} flies die prior to third instar larval stage, confirming that Barc is an essential protein for development.

5.2.3.4. Design of two different rescue constructs

In order to rule out that the lethality of homozygous *barc*^{attPKO} flies is directly caused by the loss of *barc* and not a second site mutation, we generated attB-*barc* rescue constructs (Fig. 25A&B). As mentioned earlier, the use of attP/attB sequences enables re-expression of Barc under the control of its own promoter (Fig. 25C-E). Having here the chance to generate useful tools for the analysis of *barc*, we have designed and prepared two different rescue constructs.

barc^{RescueA} contains a minimal attB sequence, non coding sequences deleted in the mutant (fragment of intron 1 + end of 5'UTR), and the coding sequence of *barc* fused to its 3'UTR (Fig. 25A). This construct will be used to test whether *barc*^{attPKO} can be rescued.

barc^{RescueB} is similar to *barc*^{RescueA} with the exception that the coding sequence of *barc* is tagged at its 3' end with GFP, two cleavage sites (PreScission & TEV) and a BioTag, followed by the 3'UTR of the SV40 virus (Fig. 25B, for details refer to "Experimental Procedures"). BioTag is a motif that can be biotinylated by the *E. coli* biotin ligase BirA, allowing for protein pull-down using streptavidin beads (Schatz, 1993). The *barc*^{RescueB} construct will be particularly useful to carry out biochemical experiments such as protein and chromatin immunoprecipitations since, so far, our antibodies have proven unsuccessful at doing so.

5.2.4. Study of the molecular function of Barc

In parallel to making a mutant allele and two rescue constructs for *barc*, we started investigating the possible molecular functions of the protein.

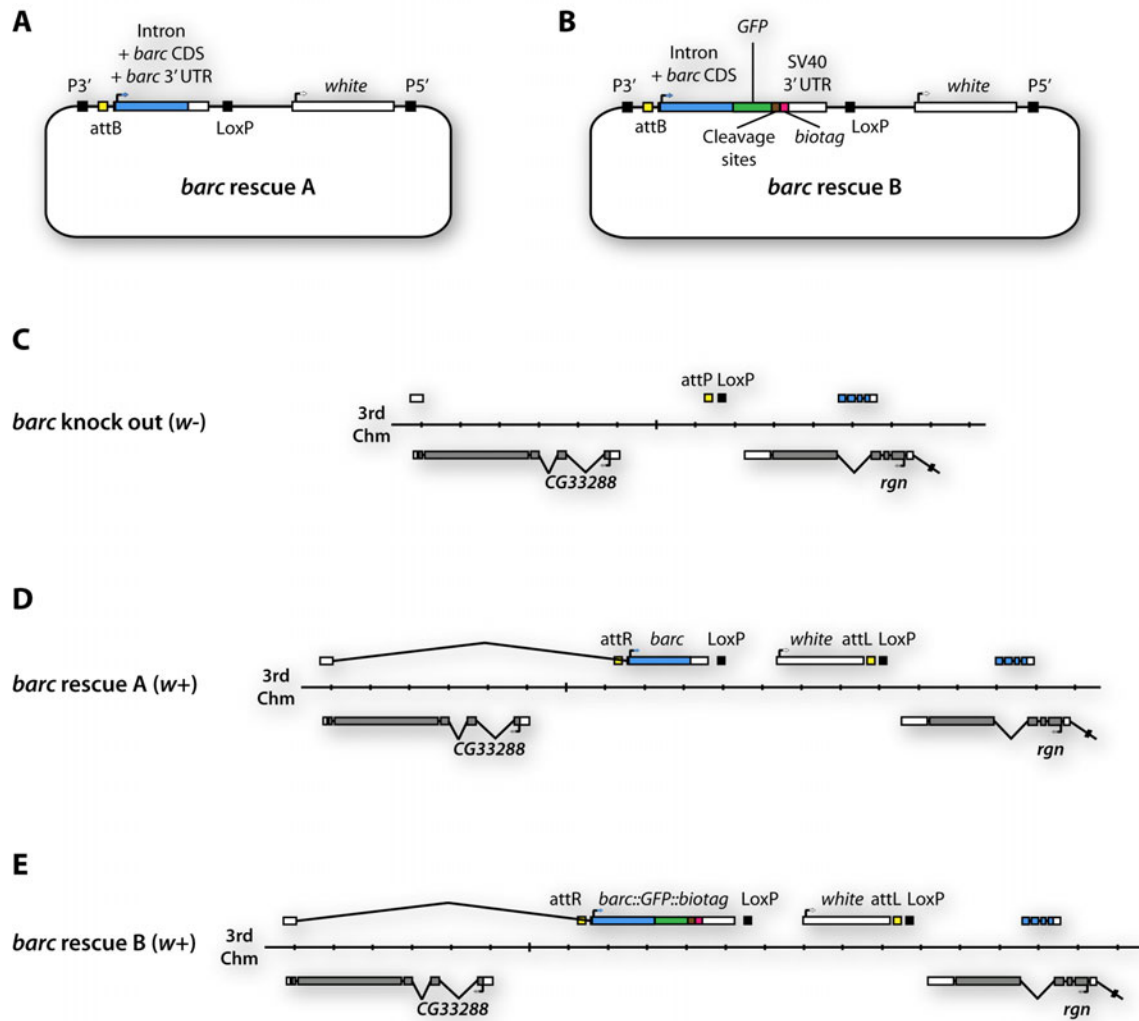


Figure 25. Rescue constructs designed to rescue *barc*^{attKO} mutants

barc^{RescueA} (**A**) contains the non coding sequences deleted in *barc*^{attKO} (fragment of intron 1 + end of 5'UTR), and the coding sequence of Barc fused to its 3'UTR. In *barc*^{RescueB} (**B**), Barc is tagged with GFP, two cleavage sites, a BioTag, and is followed by the SV40 3'UTR. These rescue constructs are designed to rescue *barc*^{attKO} mutants (**C**) via attB/attP recombination (**D,E**), and *white* is used as a selection marker.

5.2.4.1. The function of Barc does not require its second RRM

We started our analysis by testing the importance of single domains of the protein in mediating its function. For that, we generated a series of six RNAi resistant constructs, lacking different parts of the protein (Fig. 26A). We have previously shown that *Drosophila* expressing UAS-*barc*RNAi^{GD} under the control of *insc*-Gal4 die prior to adulthood, and that co-expression of UAS-*barc*^{Res-FL} rescues this lethality (Fig. 26A). We therefore decided to test our Barc deletion constructs for their ability to rescue the lethality associated with RNAi expression in neuroblast lineages. We reasoned that a construct lacking an essential domain of Barc would fail to rescue this lethality.

We first tested constructs lacking fragments of the C-terminus. Surprisingly, *barc*^{Res-ARRM2}, a construct in which the second RRM and the very C-terminus are missing, was able to rescue the RNAi lethality, indicating that these two domains are dispensable for the function of Barc (Fig. 26A). However, *barc*^{Res-ARRM1&2}, in which both RRMs, the NLS and the very C-terminus have been removed, was unable to rescue lethality (Fig. 26A). This result is in agreement with our previous observation that this construct is unable to rescue the RNAi phenotype in larval brains (Fig. 16). However, because Barc^{Res-ARRM1&2} lacks the NLS, the overexpressed truncated protein is mislocalized and can be found throughout the cell, when the endogenous protein is exclusively nuclear (Fig. 26B,B',C,C'). To rule out that the inability of Barc^{Res-ARRM1&2} to rescue *barc* RNAi-associated lethality, we used *barc*^{Res-nls-ARRM1&2}, a construct lacking the same domains as Barc^{Res-ARRM1&2} but to which we added the SV40 NLS (Fig. 26A). We first tested the intracellular localization of Barc^{Res-nls-ARRM1&2} and found that it localizes predominantly to the nucleus (Fig. 26D&D'). However, this construct was also unable to rescue *barc* RNAi lethality, indicating that Barc needs its first RRM to carry out its function. We then tested constructs lacking fragments of the N-terminus. Interestingly, all deletions affecting this part of the protein – as in *barc*^{Res-ΔN}, *barc*^{Res-ΔBTS} and *barc*^{Res-ΔRRM1} – disrupted the function of Barc (Fig. 26A). This result indicates that the N-terminus of Barc is important for the function of the protein.

Taken together, these data suggest that the second RRM and the very C-terminus of Barc are dispensable for the main function of the protein, whereas all other domains are important, either because of a direct activity or because they allow the protein to adopt its appropriate 3D structure.

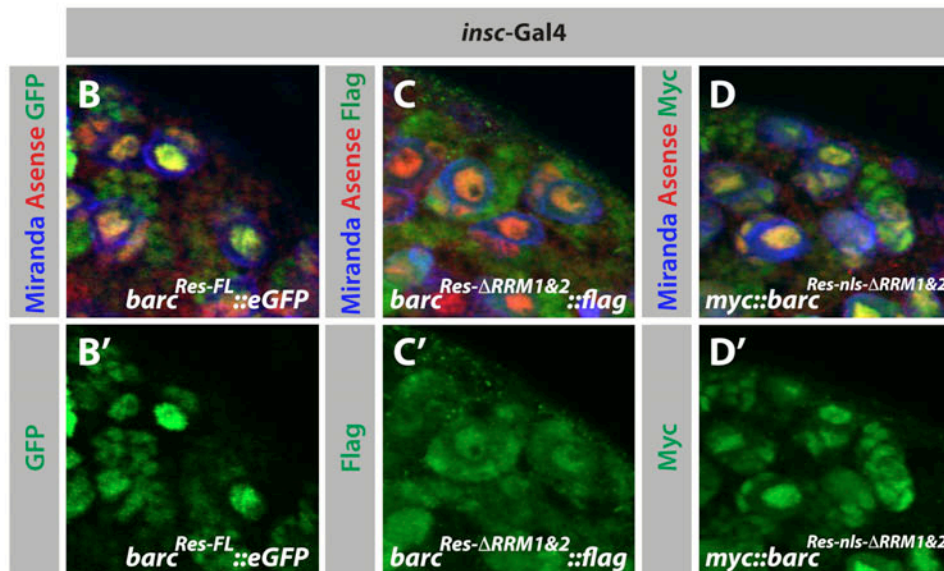
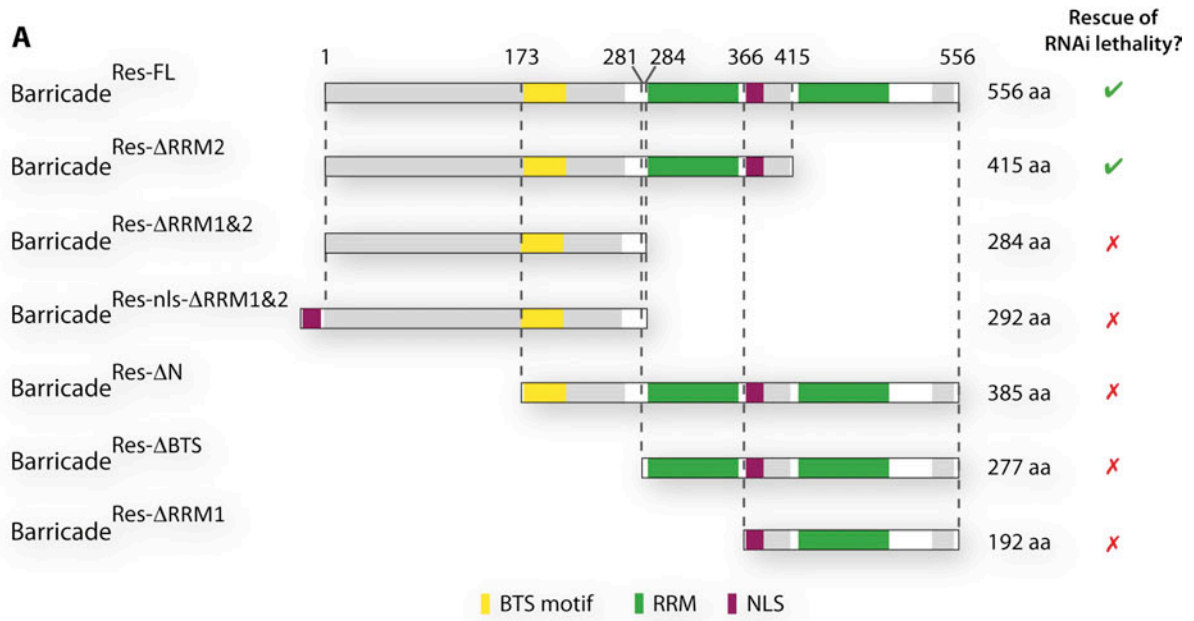


Figure 26. Analysis of Barc domains

(A) Scheme of the deletion constructs tested for their ability to rescue lethality associated with expression of *barc* GD RNAI with *insc-Gal4*>>CD8::GFP. Only the 2nd RRM of Barc is dispensable. (B-D') Close-up on neuroblasts expressing different *barc* constructs under the control of *insc-Gal4*: *barc*^{Res-FL}::GFP (B,B') is nuclear, *barc*^{Res-ΔRRM1&2}::flag (C,C') is mislocalized and *myc::barc*^{Res-nls-ΔRRM1&2} (D,D') is largely nuclear.

5.2.4.2. **Barc associates with DNA**

The presence of RRM domains in Barc as well as the function of human Tat-SF1 in transcription elongation, prompted us to determine whether Barc can associate with DNA *in vivo*.

To test this, we decided to use larval salivary glands, a well-established model to test association of proteins with DNA *in vivo*. These glands are located in the vicinity of the larval brain, and their cells undergo several rounds of endoreplication to become polyploid (Fig. 27A). Their polytene chromosomes show a reproducible, banded pattern when stained with DAPI (Fig. 27B&B'). DAPI weak bands, called interbands, correspond to open chromatin, and bright bands to packed chromatin. Most *Drosophila* genes have been mapped to a precise band or interband and conversely each band can be identified, allowing mapping protein binding on DNA.

When we stained polytene chromosomes for Barc, we observed that the protein localizes in a specific pattern, colocalizing with most interbands and suggesting that it associates with decondensed DNA regions (Fig. 27C-D'). We then wanted to ask whether Barc is found in transcribed regions that undergo active elongation. To test this, we co-stained polytene chromosomes for Barc and for elongating polymerase II (Phospho-Serine 2 of its Carboxy-terminal repeat), with a commercial antibody. Interestingly, we found that Barc largely overlaps with elongating polymerase II (Fig. 26E-H'). This expression pattern is very similar to the one of Spt5, a subunit of the DSIF complex, and of Spt6, another protein involved in transcription elongation (Kaplan et al., 2000; Andrulis et al., 2000; Ardehali et al., 2009).

These observations suggest that Barc associates with DNA *in vivo* and that it could play a role in transcription elongation.

5.2.4.3. **Testing the function of Barc in elongation and splicing**

Given that Barc seems to associate with DNA and that its homologues Tat-SF1 and CUS2 have been involved in transcription elongation and/or splicing, we wanted to test whether Barc regulates any of these two processes. To circumvent the difficulty of isolating a large number of neuroblasts from larval brains, we decided to use S2 cells, the best-established *Drosophila* cell culture model.

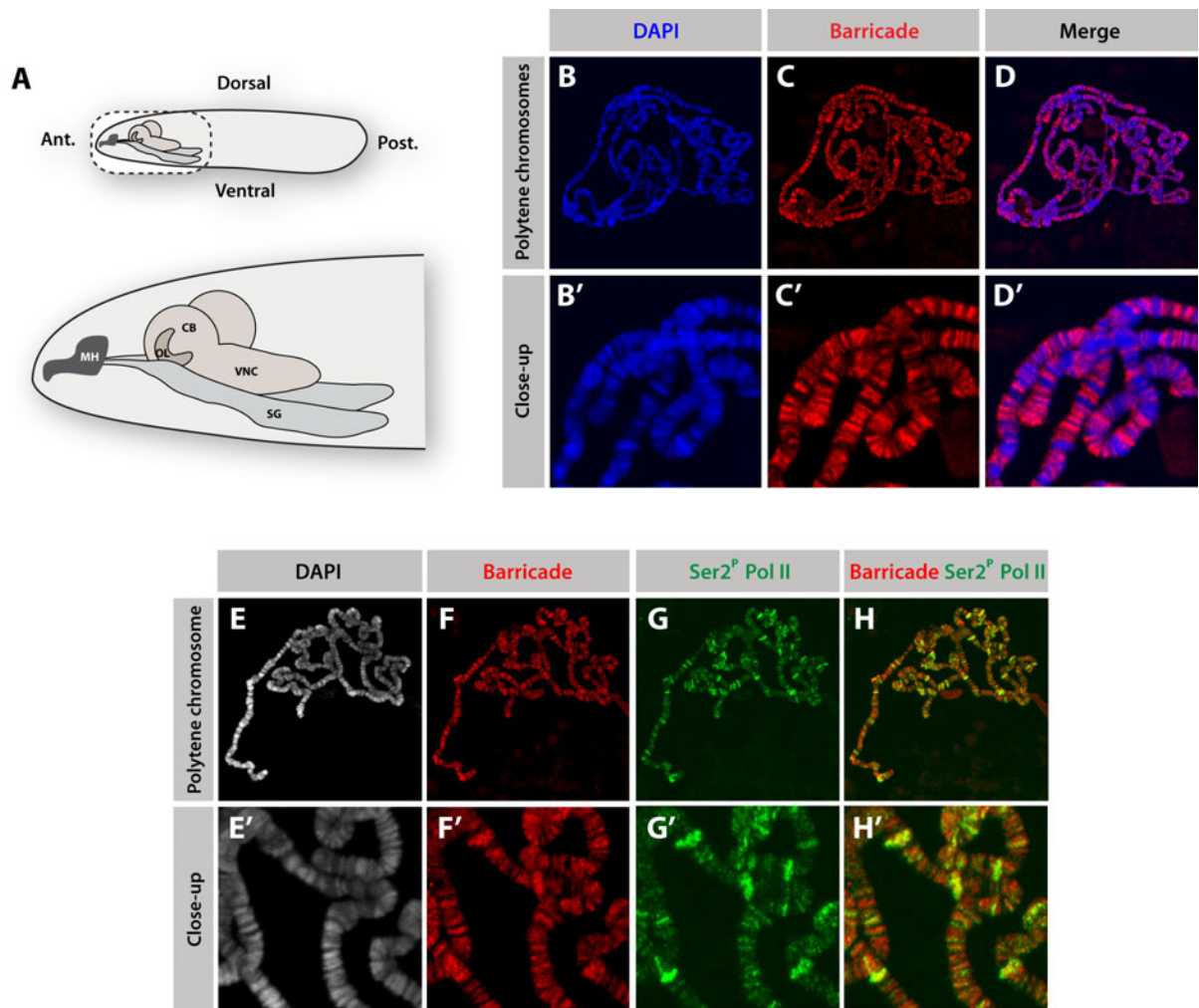


Figure 27. Barc associates with polytene chromosome

(A) Schematic displaying the localization of salivary glands (SG) in *Drosophila* larvae. Polytene chromosomes are found in the cells of these glands. MH: Mouth hooks. OL: Optic lobe. CB: Central brain. VNC: Ventral nerve cord. (B-H') Polytene chromosomes labeled with indicated markers. DAPI (B, B', D, D') marks areas corresponding to condensed DNA (bands) whereas Barc (C-D') associates with decondensed regions (interbands). (E-H') Barc (F, F', H, H') largely overlaps with elongating RNA polymerase II (phosphorylated on Serine 2 of its carboxyterminal domain, G-H').

- **Optimization of RNAi conditions in S2 cells**

After confirming that *Barc* is expressed in S2 cells, we worked on establishing optimal RNAi knock down conditions in this system (Fig. 28). A classical way to induce RNAi in S2 cells, is to serum-deprive cells and incubate them together with a double stranded fragment of RNA (dsRNA) of the gene of interest. This dsRNA enters the cells and is processed to trigger RNAi against this gene.

As a control, we decided to use untreated cells and cells incubated with dsRNA against *eGFP*, a gene that is not expressed in S2 cells. *eGFP* dsRNA serves as a control for a possible effect of activating the S2 cell dsRNA-processing machinery. To target *barc*, we tested two different fragments of dsRNA: *barc* SD dsRNA and *barc* GD dsRNA (Fig. 28A). At the time we designed these constructs, *barc* SD dsRNA was predicted to be the most efficient dsRNA fragment by SnapDragon, a program dedicated to the generation of dsRNAs to induce RNAi in S2 cells (for details, see Experimental Procedures). The *barc* GD dsRNA corresponds to the fragment of *barc* mRNA that is targeted by the GD RNAi line.

We first wanted to determine which of the two *barc* dsRNAs was more efficient. For that, we tested expression levels of *barc* relative to tubulin, three days after incubation with either no dsRNA or 15µg (per well of 6-well plates) of each dsRNA (Fig. 28B&C). As we expected, *eGFP* dsRNA had very little effect on *Barc*. However, SD and GD dsRNAs decreased *Barc* levels from 41% and 84%, respectively, compared to untreated cells. We then wanted to test whether incubating cells with 30µg of each dsRNA would increase the knock down efficiency (Fig. 28D&E). Similarly as when 15µg were used, *eGFP* dsRNA did not affect *Barc*. Interestingly, using 30µg of dsRNA did significantly increase the effect of the SD construct (from 41% with 15µg to 60% knock down with 30µg). However, doubling the amount of dsRNA, only slightly improved the GD-mediated knockdown (from 84% with 15µg, to 90% knock down with 30µg). Given these results, we decided to use the 20µg of *barc* GD dsRNA for our next experiments.

To finalize the optimization of our S2 RNAi conditions, we wanted to test whether our GD dsRNA would be more efficient if cells were given more time to degrade *Barc*. For that, we incubated cells with 20µg of GD dsRNA, collected them after three, four or five days, and quantified relative levels of *Barc* compared to untreated cells that had been prepared in parallel (Fig. 28F&G). The result of this experiment was that waiting longer before collecting

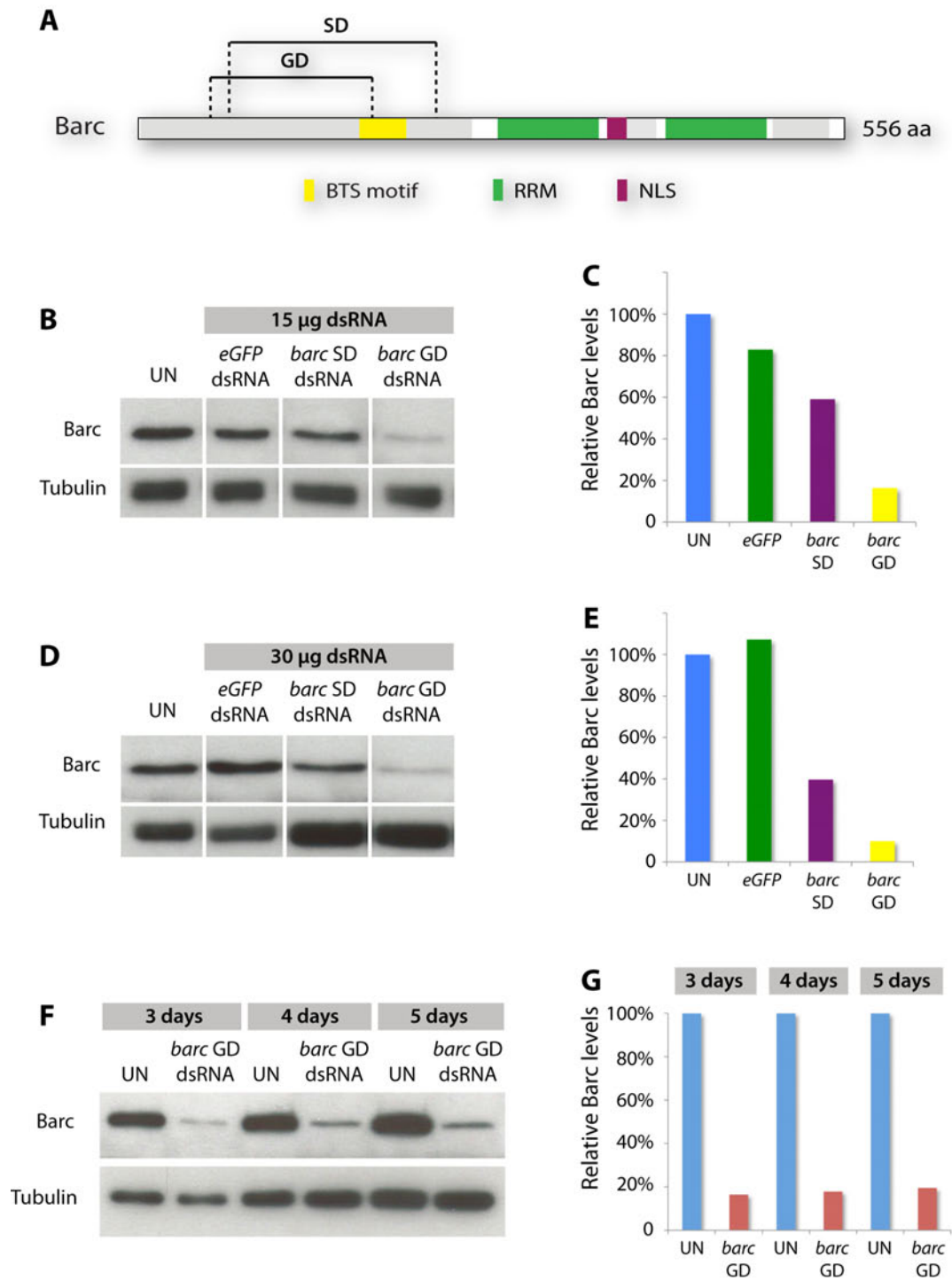


Figure 28. Optimization of *barc* RNAi knock down in S2 cells

(A) Schematic of the regions targeted by *barc* GD and SD dsRNAs. (B,D) Expression of Barc and Tubulin after a 3 days incubation with no dsRNA (UN: untreated cells), 15 μ g/well of 6-well plate (B), or 30 μ g/well of 6-well plate (D) of either dsRNA. (F) Expression of Barc and Tubulin after a 3,4 or 5 days incubation with no dsRNA (UN: untreated cells) or 20 μ g/well of 6-well plate of *barc* GD dsRNA. (C,E,G) is the quantification of the western blots presented in (B,D,F) respectively. Expression of Barc relative to Tubulin. Values for cells treated with eGFP dsRNA, *barc* GD dsRNA and *barc* SD dsRNA are normalized to the value measured in untreated cells grown in parallel.

cells does not improve the efficiency of our GD dsRNA and that knock down is optimal after three days, at which point *Barc* is only expressed at about 16% of its level in untreated cells.

- **GRO-seq versus shcRNA-seq: Choice of the method and sample preparation**

Having established optimal *barc* RNAi conditions in S2 cells, we then had to choose the best method to test the role of *barc* in elongation and splicing.

Two methods have recently been developed that enable to visualize PolIII promoter-proximal pausing (PPP) and/or elongation at a genome-wide level: global run-on sequencing (GRO-seq) and sequencing of short capped RNAs (shcRNA-seq) (Core et al., 2008; Nechaev et al., 2010).

GRO-seq is a method that requires incorporation of Br-UTP into newly synthesized RNAs by polymerase molecules engaged in transcription. Br-UTP-labeled mRNAs can then be purified using an antibody, and sequenced. The main advantage of this method is that it enables to compare the abundance of PPP polymerase compared to actively elongating polymerase, and that at each *locus*. However, because this technique involves isolation of nuclei, it requires a lot of starting material – about 5 million cells (Core et al., 2008). This is not a problem when working with S2 cells, but we were interested in using a method that could subsequently be used in neuroblasts.

We therefore decided to use shcRNA-seq, which can be performed from less than a million cells. This method relies on isolation and sequencing of short capped RNAs associated with paused polymerases (Fig. 29). Additionally, if these shcRNAs are sequenced from their 3' end, using specific adapters, it is possible to obtain resolution of polymerase PPP at the base pair level. To generate shcRNA libraries, we first isolated short RNAs from total RNAs. Because pausing happens in average around 35nt downstream from the transcription start site, we purified RNAs ranging from 25 to 120nt. We then 5'-digested uncapped RNAs – mRNAs being protected from digestion by their 7-methylguanylate cap (m^7G). Short capped RNAs were then ligated to a 3' ssRNA/DNA adapter, purified, decapped and ligated to a 5' ssRNA/DNA adapter. Finally, a cDNA library was prepared from these purified shcRNAs. The disadvantage of this method, however, is that it only provides information about transcription state around the promoter. To circumvent that, and to be able to additionally test the role of *Barc* in splicing, we decided to prepare mRNA libraries in parallel to our shcRNA libraries.

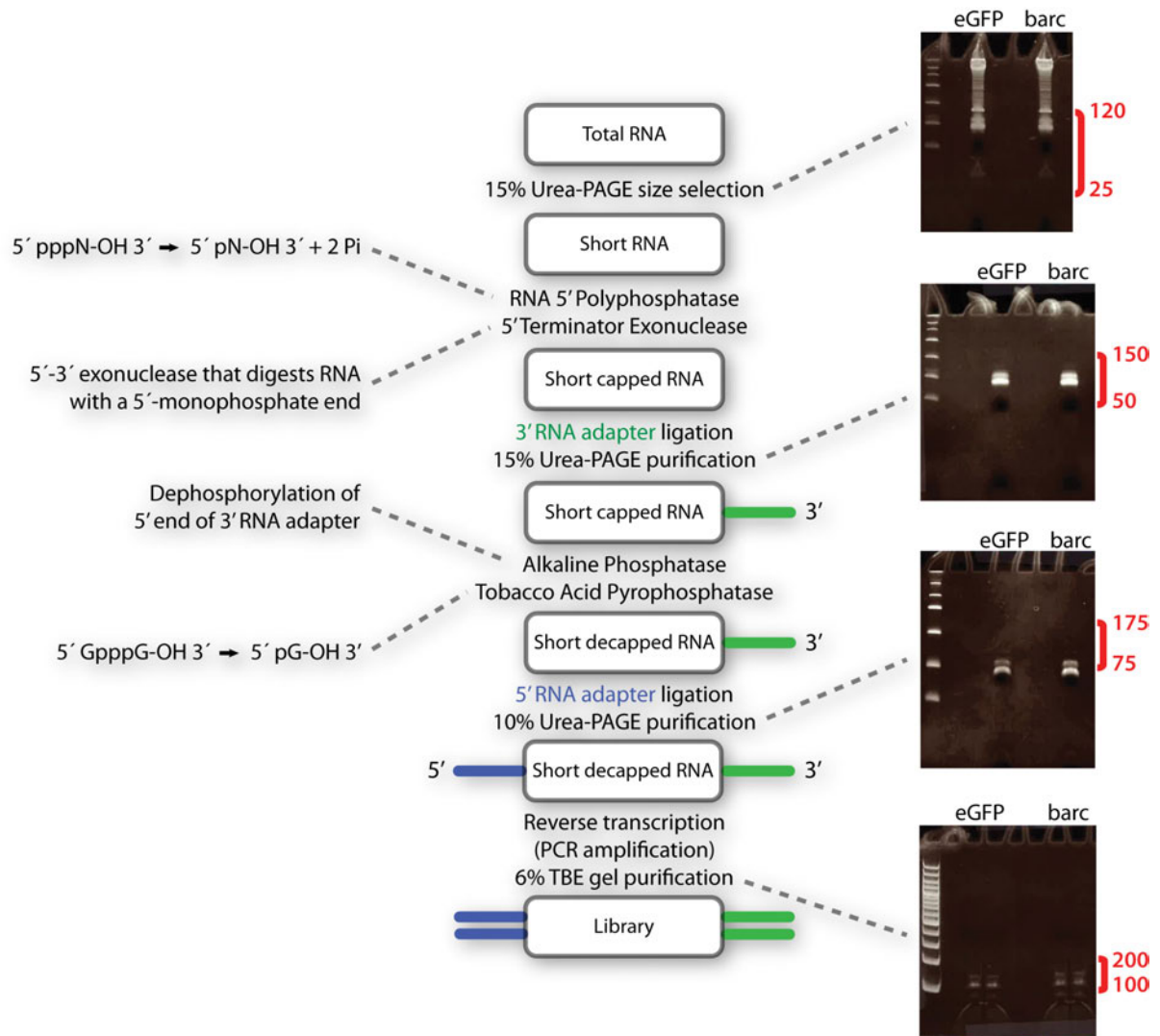


Figure 29. Protocol used to prepare libraries of short capped RNAs from S2 cells

Small RNAs are first selected from total RNAs by size. Then, uncapped RNAs are degraded and a 3' adapter is ligated to small capped RNAs. After decapping, a 5' adapter is ligated to small decapped RNAs and cDNA are prepared. Adapted from (Nechaev et al., 2010).

In summary, we treated S2 cells with either *eGFP* or *barc* GD dsRNA, collected cells after 3 days, extracted total RNAs, and prepared an mRNA and a shcRNA library from each sample (Fig. 30). We repeated this whole experiment a second time to prepare a second set of libraries and we hope that sequencing them will enable us to determine the molecular function of Barc.

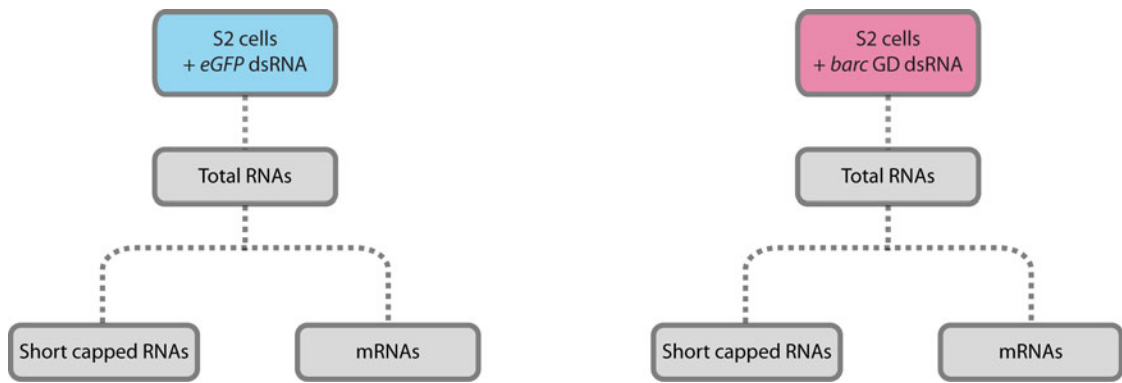


Figure 30. Scheme of the experiment to prepare short capped RNA and mRNA libraries.

S2 cells were incubated with either *eGFP* dsRNA or *barc GD* dsRNA. After a few days growth, total RNAs were isolated and served to prepare libraries of short capped RNAs and mRNAs. The whole experiment was done in duplicates.

5.3. DISCUSSION

5.3.1. Summary

CG6049/barc was originally identified as an overproliferation gene in a recent neuroblast genome-wide RNAi screen (Neumuller et al., 2011). In this study, we have shown that *barc* encodes a broadly expressed nuclear protein that plays an important role in larval neuroblast lineages, and possibly other tissues as well. In type 2 lineages, Barc regulates maturation of INPs and seems to be especially important for re-expression of the transcription factor Dpn in immature INPs. In type 1 lineages, Barc is required to produce neurons. Additionally, Barc seems to regulate growth in both lineages. Given the fact that larval neuroblasts regrow between each division, it is possible that the growth defect observed upon loss of *barc* is connected to an alteration of the cell cycle. We have presented here how we generated a *barc* mutant allele that will allow us to precisely test effects of Barc on cell fate and cell cycle.

We also designed experiments to determine how Barc regulates neuroblast lineages at the molecular level. We have for example shown that the main function of Barc is not mediated by its second RRM. Additionally, we have demonstrated that Barc associates with DNA *in vivo*. This observation, combined with the role of Tat-SF1 in regulating elongation, suggests that Barc could regulate neuroblast lineages by controlling transcription, possibly at the level of elongation. To test this and to assess a potential role of Barc in splicing, we have prepared shcRNA and mRNA libraries whose analysis should allow us to establish the molecular function of Barc. Additionally, we designed a tagged rescue construct that should enable the identification of binding partners of Barc as well as its binding pattern on DNA. It would be particularly interesting, for example, to determine whether Barc associates with all or a subset of actively transcribed *loci*. At the gene level, it would also be interesting to establish whether Barc is predominantly found around the promoter, where polymerase molecules pause, or whether it associates with elongating polymerases.

5.3.2. Making INPs: Step by step

Our data suggest that Barc is a novel regulator of INPs. We have shown that it is particularly important for immature INPs to progress to a mature INP stage. Interestingly, two transcription factors, PointedP1 (PntP1) and Earmuff (Erm), were recently shown to also affect INPs (Zhu et al., 2011; Weng et al., 2010). PntP1 is specifically expressed in type 2 lineages and its knock down leads to less INPs. This is probably due to the fact that it upregulates *Ase* in type 2 neuroblasts. Conversely, ectopic expression of PntP1 in type 1 neuroblasts, triggers formation

of INPs in lineages that normally do not produce transit amplifying cells (Zhu et al., 2011). In *erm* mutants, INPs are correctly generated, progress to a mature Ase^+Dpn^+ state, and start producing GMCs. However, these mature INPs eventually dedifferentiate and revert back to neuroblast-like cells. These ectopic neuroblasts continue to proliferate and undergo ACD to produce INPs, resulting in an overproliferation situation. *Erm* has been proposed to control INP fate by regulating *Pros* and Notch signaling via a mechanism that remains elusive (Weng et al., 2010).

It is interesting to note that although *PntP1*, *Barc* and *Erm* have an effect on INP fate, they all play different roles and a regulatory cascade can be reconstituted where *PntP1* determines type 2 neuroblast identity, *Barc* regulates the progression from immature to mature INP stages, and *Erm* is required to maintain mature INP fate.

5.3.3. Loss of *Barc* and tumor formation

Knock down of *barc* in larval brains results, in type 2 lineages, in an accumulation of INPs at the expense of neurons. Most of these INPs are Ase^+Dpn^- , a stage at which cells are normally not dividing (Boone and Doe, 2008; Weng et al., 2010; Bayraktar et al., 2010).

Interestingly, when pieces of *barc* RNAi brains are transplanted into the abdomen of wild-type flies, they proliferate and are able to form tumors in about 30% of cases, whereas wild-type brains never do so (Nidhi Saini & Heinrich Reichert, unpublished). Additionally, tumor cells from *barc* RNAi transplanted brains (traceable with GFP) can invade healthy tissues like ovaries, similarly to what has been described for mutants of several genes involved in ACD or affecting centrosomes (Nidhi Saini & Heinrich Reichert, unpublished) (Castellanos et al., 2008; Woodhouse et al., 1998; Caussinus and Gonzalez, 2005). It would be interesting to determine whether *barc* tumors display chromosomal defects, like in *mira*, *numb* and *pros* tumor cells (Caussinus and Gonzalez, 2005). The frequency of tumor-formation with *barc* RNAi is lower than with *brat* RNAi, which leads to massive overproliferation in larval brains and to tumor formation in 90% of transplantation experiments. It is surprising, however, that although *barc* knock down does not trigger a clear neuroblast overproliferation *in situ* it is able to generate tumors upon allograft transplantation. The exact mechanism behind this observation remains unclear, but three possibilities seem particularly likely.

First of all, *barc* deficient cells could require a latency phase, prior to undergoing massive proliferation. The larval brain is a rapidly evolving tissue and larval neuroblasts stop dividing

and disappear in early pupal stages. It is possible that transplantation into the abdomen of an adult fly offers *barc* RNAi cells the time to bypass the developmental constraints of the larval brain and to achieve their transformation into tumor cells. Secondly, it is possible that tumor formation upon *barc* knock down is prevented in the larval brain by the glial sheath that surrounds each neuroblast lineage (Doe, 2008). The contact between the glial sheath and neuroblasts is important for proliferation. In fact, its disruption by overexpression in glia of a dominant negative form of the adhesion protein E-cadherin results in reduced proliferation of neuroblasts (Dumstrei et al., 2003). This could be caused by the alteration of either the brain/hemolymph barrier or direct signaling between glia and neuroblasts. Glial cells are also able to inhibit the proliferation of neuroblasts during early larval stages, by secreting Anachronism (Ana) (Ebens et al., 1993). Given the fact that glial cells play a dual role in the regulation of proliferation, it is possible to conceive that alteration of the glial sheath upon transplantation is responsible for the *barc* tumor formation. Finally, it is possible that signals present in the abdomen of the host are responsible for the ultimate transformation of *barc* deficient cells into tumor cells.

The discrepancy between the *barc* RNAi phenotype in larval brains and the capacity of these brains to form tumors upon transplantation is not unprecedented. In fact, *pins*, which regulates spindle orientation in neuroblasts follows the same pattern as *barc*. Larval brains mutants for *pins* have fewer and smaller neuroblasts, however, upon transplantation they form large, invasive tumors that present chromosomal defects (Lee et al., 2006b; Caussinus and Gonzalez, 2005). A recent study demonstrated that *pins* mutant brains can form tumors in larval brains upon either food deprivation, inhibition of target of rapamycin (TOR) or reduced phosphatidylinositol 3-kinase (PI3K) activity (Rossi and Gonzalez, 2011). Interestingly, these three conditions enhanced the efficiency of *pins* mutant brains to form tumors in the abdomen of host flies, whereas they were unable to trigger tumor formation in a wild-type background. This study suggests that a set of signals acts in the larval brain to suppress overgrowth of compromised cells. A similar mechanism could explain why *barc* RNAi brains are able to form tumors upon allograft transplantation even though their neuroblasts do not overproliferate *in situ*.

5.3.4. The Barc/Tat-SF1/CUS2 family of proteins: functional evolution?

As mentioned earlier, the human protein Tat-SF1 plays a role in splicing and transcription elongation, whereas its yeast homologue, CUS2, is only known to be involved in splicing. This observation, taken together with the structural differences between CUS2 and Tat-SF1,

raises the interesting hypothesis that the structure and the function of members of this family of proteins evolved in parallel.

CUS2 and Tat-SF1 share a core structure composed of two RRM domains and a NLS. The first RRM of both proteins has been shown to be essential for their function (Fong and Zhou, 2001; Yan et al., 1998). Compared to CUS2, Tat-SF1 has two additional domains: a short N-terminus and long C-terminus. The short N-terminus, contains a BTS motif that has been shown to bind CA150, a protein that bridges transcription and splicing, and that could play a role in recruiting Tat-SF1 to elongating polymerase (Smith et al., 2004). The long acidic C-terminus is essential for binding to CyclinT1, a subunit of P-TEFb (Fong and Zhou, 2001). Additionally, Tat-SF1 has been shown to interact with the DSIF complex and the Paf1 complex (Paf1C); Tat-SF1/DSIF/Paf1C binding cooperatively to RNA Pol II to stimulate transcription elongation (Chen et al., 2009; Kim et al., 1999). However, the protein domain of Tat-SF1 engaged in these interactions remains unknown.

Structural evolution of Tat-SF1 seems to have enabled acquisition of novel functions in transcription elongation. In this context, it is particularly interesting to note that RNA pol II promoter-proximal pausing has not been observed in *S. cerevisiae* where complexes involved in pausing, such as NELF, have not been identified (Radonjic et al., 2005; Nechaev and Adelman, 2010). It is tempting to think that the structure of Tat-SF1 is adapted to the regulatory mechanism controlling elongation.

In terms of structural evolution, Barc seems to be an intermediate step between CUS2 and Tat-SF1. Indeed, Barc has a longer N-terminus than Tat-SF1 but does not have a long C-terminal extension. Similarly to Tat-SF1, the N-terminus of Barc contains a BTS motif that could allow it to interact with polymerase. The fact that the BTS domain is also present in *Arabidopsis thaliana* suggests that it was lost in yeast rather than gained in all other eukaryotes. Interestingly, the N-terminus of Barc is longer than that of Tat-SF1 and we have shown in this study that this extension is important for the function of the protein. Its precise role is yet unknown and could be of two kinds: It could be the functional equivalent of the C-terminus domain of Tat-SF1, or alternatively, it could have taken on a novel role.

5.3.5. Transcriptional elongation and regulation of neuroblast lineages

Over the last couple of years, mounting evidence has accumulated demonstrating that polymerase pausing is important for development in higher eukaryotes. Indeed, a very large

fraction of genes regulating development harbor paused polymerases, both in *Drosophila* embryos and in mouse ES cells (Rahl et al., 2010; Zeitlinger et al., 2007). Supporting this, NELF knock down-mediated abrogation of pausing leads to developmental defects in mouse ES cells, as well as in *Drosophila* (Amleh et al., 2009; Haley et al., 2008; Wang et al., 2010). Additionally, presence of paused polymerases has been recently shown to maintain an open chromatin state and prevent from these promoters to be occupied by nucleosomes (Gilchrist et al., 2010). Conceptually, polymerase pausing is now considered to maintain a “ready to go state” that would allow for tight regulation of genes that need to be rapidly activated or repressed, either during development or in response to a stimulus.

RNA Pol II promoter-proximal pausing and its release should be considered as a multilayered process. The first layer is composed of the core pausing/elongating machinery. Protein complexes such as NELF, DSIF, P-TEFb and Paf1C would fall in this category and their knock down in neuroblast lineages would be expected to affect most genes. In fact, in the neuroblast RNAi screen, knock down of subunits of DSIF, NELF, Paf1C or P-TEFb, led to underproliferation (Neumuller et al., 2011). Although the specificity of each RNAi line has not been specifically assessed, it seems that affecting these protein complexes inhibits cell cycle and/or promotes apoptosis. The second layer is composed of genes that release pausing at specific *loci* and/or under certain conditions. In *Drosophila*, such genes have not yet been identified, and in vertebrates only few examples have been described. For example, it was recently shown that in mouse ES cells c-Myc acts on its target genes by interacting with P-TEFb and releasing polymerase pausing, rather than by recruiting polymerase to their promoter (Rahl et al., 2010). Additionally, in the Zebrafish *Danio rerio*, *moonshine* – the orthologue of human Tif1 γ – has been shown to regulate hematopoiesis by controlling transcription elongation at genes required to specify erythroid cell fate (Bai et al., 2010). A model has been proposed, in which blood-specific transcription complexes interact with Tif1 γ that, in turn, recruits positive elongation factors, such as P-TEFb and the FACT complex, to blood genes.

It remains to be clearly demonstrated that *Drosophila barc* acts on elongation, and whether it plays a role at a large number of *loci* or if it regulates a restricted number of genes. Interestingly, the phenotype observed upon *barc* RNAi knock down is different from the one observed for components of the core pausing/elongating machinery. Remarkably, four other genes play a role in transcription elongation and lead to a phenotype similar to *barc* RNAi knock down in larval brains: *ssrp*, a subunit of the FACT complex, and *brm/osa/mor*, three

members the Brm complex (Neumuller et al., 2011). Both complexes have been shown to promote transcription elongation by destabilizing nucleosomes (Schwabish and Struhl, 2007; Belotserkovskaya et al., 2004). Further studies should enable to determine whether *barc* regulates transcription elongation in a general or a specific manner, and whether *barc* regulates larval neuroblast lineages via a similar or a different mechanism than *ssrp/brm/osa/mor*.

5.4. EXPERIMENTAL PROCEDURES

Fly stocks

UAS-*Dicer-2*; *insc*-Gal4, UAS-*CD8::GFP*/CyO (Neumuller et al., 2011)

UAS-*Dicer-2*; *wor*-Gal4, *ase*-Gal80; UAS-*CD8::GFP* (Neumuller et al., 2011)

UAS-*barcRNAi*^{GD} (TID25497, Vienna *Drosophila* Stock Center)

UAS*t-barricade*^{Res-FL}; UAS-*barcRNAi*^{Custom} (Neumuller et al., 2011)

UAS*t-barricade*^{Res-FL}::eGFP; UAS*t-eGFP*::*barricade*^{Res-FL}; UAS*t-6xMyc*::*barricade*^{Res-FL};

UAS*t-barricade*^{Res-FL}::6xMyc; UAS*t-3xFLAG*::*barricade*^{Res-FL}; UAS*t-barricade*^{Res-FL}::3xFLAG;

UAS*t-3xFLAG*::*barricade*^{Res-ΔRRM2}; UAS*t-barricade*^{Res-ΔRRM2}::3xFLAG;

UAS*t-barricade*^{Res-ΔRRM1&2}; UAS*t-barricade*^{Res-ΔRRM1&2}::3xFLAG;

UAS*t-barricade*^{Res-nls-ΔRRM1&2}; UAS*t-3xFLAG*::*barricade*^{Res-nls-ΔRRM1&2};

UAS*t-6xMyc*::*barricade*^{Res-nls-ΔRRM1&2}; UAS*t-barricade*^{Res-ΔN};

UAS*t-barricade*^{Res-ΔBTS}; UAS*t-barricade*^{Res-ΔRRM1}.

Cloning of UAS constructs

All UAS*t-barricade* constructs were cloned from a plasmid containing the coding sequence of *barricade* that is resistant to UAS-*barcRNAi*^{GD} and was published in (Neumuller et al., 2011). We used the Gateway system to clone the following DNA fragments in pDONOR221. Gateway attB sequences are underlined.

Full length (amino acids 1 to 556):

Upstream: 5'-GGGGACAAGTTTGTACAAAAAAGCAGGCTTCATGAGCGACGAAGGTGGCTG-3'

Downstream: 5'-GGGGACCACTTTGTACAAGAAAGCTGGGICCTAAGGGGTGGCGTCTCCTG-3' (Stop) or 5'-GGGGACCACTTTGTACAAGAAAGCTGGGICAGGGGTGGCGTCTCCTGGCA-3' (No Stop).

ΔRRM2 (amino acids 1 to 415):

Upstream: 5'-GGGGACAAGTTTGTACAAAAAAGCAGGCTTCATGAGCGACGAAGGTGGCTG-3'

Downstream: 5'-GGGGACCACTTTGTACAAGAAAGCTGGGICCTATTTCTCATTCTTTGACCGTTCCG-3' (Stop) or 5'-GGGGACCACTTTGTACAAGAAAGCTGGGICTTTCTCATTCTTTGACCGTTCCG-3' (No Stop).

ΔRRM1&2 (amino acids 1 to 284):

Upstream: 5'-GGGGACAAGTTTGTACAAAAAAGCAGGCTTCATGAGCGACGAAGGTGGCTG-3'

Downstream:

5'-GGGGACCACTTTGTACAAGAAAGCTGGGICCTAGGTGTTCTGCAATGGATCCATTTCCG-3' (Stop) or

5'-GGGGACCACTTTGTACAAGAAAGCTGGGTCGGTGTCTGCAATGGATCCATTTTCG-3' (No Stop).

nls- Δ RRM1&2 (nls sequence from SV40, followed by amino acids 1 to 284):

Upstream: 5'-

GGGGACAAGTTTGTACAAAAAAGCAGGCTTCATGACTGCTCCAAAGAAGAAGCGTAAGAGCGACGAAGGTGG
CTG-3' (SV40.nls)

Downstream:

5'-GGGGACCACTTTGTACAAGAAAGCTGGGTCCTAGGTGTCTGCAATGGATCCATTTTCG-3' (Stop).

Δ N (amino acids 173 to 556):

Upstream: 5'-GGGGACAAGTTTGTACAAAAAAGCAGGCTTCATGGAACACGGGGAACGAACCTATAC-3'

Downstream: 5'-GGGGACCACTTTGTACAAGAAAGCTGGGTCCTAAGGGGTGGCGTCTCCTG-3' (Stop).

Δ BTS (amino acids 281 to 556):

Upstream: 5'-GGGGACAAGTTTGTACAAAAAAGCAGGCTTCATGTTGCAGAACACCAAGGTGTATG-3'

Downstream: 5'-GGGGACCACTTTGTACAAGAAAGCTGGGTCCTAAGGGGTGGCGTCTCCTG-3' (Stop).

Δ RRM1 (amino acids 366 to 556):

Upstream: 5'-GGGGACAAGTTTGTACAAAAAAGCAGGCTTCATGAGGGCTCAGTTCCAAATGCCGTG-3'

Downstream: 5'-GGGGACCACTTTGTACAAGAAAGCTGGGTCCTAAGGGGTGGCGTCTCCTG-3' (Stop).

Donor vectors containing the above fragments were recombined onto the appropriate destination vectors. Final destination vectors were used to generate transgenic flies using standard P-element transformation.

Generation of an attP *barricade* knock-out

A deletion of 1424bp containing the first two coding exons of *barricade* and a part of each flanking intron was generated by ends-out homologous recombination (for description of the general method and vectors, see (Huang et al., 2009)).

The upstream homology arm (with respect to the orientation of the gene) of 4015bp was amplified using the following primers: 5'-GATCGCGGCCGCTACCCATTTTATAGACTTCC-3' (NotI) and 5'-GATCGGTACCCGTGAAACAACAAAACTAAATTGC-3' (KpnI).

The downstream homology arm of 4777bp was amplified using the following primers:

5'-GATCGCGCGCCTTTAGTTTTATTCGCTTTTCATTTC-3' (AscI)

and 5'-GATCCTGCAGCTTGTTAGAGGCTTCTCCGACAT-3' (PstI).

These DNA fragments were amplified from a pNB61 vector containing a longer upstream arm and the same downstream arm than the ones described above (donated by Ralph Neumueller and Constance Richter).

Both arms were cloned in pGX-attP using NotI/KpnI for the upstream arm and AscI/PstI for the downstream arm, to generate pGX-*barc*^{attP} (final mutants are called *barc*^{attPKO}). Subsequent fly work was done essentially as described in (Huang et al., 2009).

Correct recombination of the homology arms was screened by PCR and by Southern blot using a standard protocol. Restriction enzymes used to digest DNA fragments were AhdI and ApaI (Upstream arm) or BsiWI and BamHI (Downstream arm).

Primers used to amplify the upstream probe (also called 5' probe): 5'-CACGACATGCTCATCTTGGG-3' and 5'-CGCAAGAATATTGCTTTGAACGCT-3'

Primers used to amplify the downstream probe (also called 3' probe): 5'-TGGGCCCAATACACGGGAAAATACTTT-3' and 5'-AAGTTCATATCTACCGGCA-3'

Generation of attB *barricade* rescue constructs

Rescue A (*barc*^{RescueA})

The end of the first intron (deleted in *barc*^{attPKO}) and the beginning of the first coding exon were cloned from genomic DNA using 5'-GATCGCATGCTGGTGATTATTTGTTGTCCTG-3' (SphI) and 5'-CAGCCACCTTCGTCGCTCATTTTGC GTTCTGTAATTAAGC-3'.

The coding sequence of *barc* was cloned from a vector containing *barc* cDNA using 5'-GCTTAATTACAGAACGCAAAATGAGCGACGAAGGTGGCTG-3' and 5'-GATCACTAGICTAAGGGGTGGCGTCTCCTG-3' (SpeI).

These two fragments were mixed and a PCR was done using:

5'-GATCGCATGCTGGTGATTATTTGTTGTCCTG-3' (SphI)

and 5'-GATCACTAGICTAAGGGGTGGCGTCTCCTG-3' (SpeI).

barc 3'UTR was cloned from pGX-*barc*^{attP} using:

5'-GATCACTAGITTTTTCATTTACCTGCGATCGTTTTTC-3' (SpeI)

and 5'-GATCGGTACCGACAAAAACGCCAATCTTACAGAGC-3' (KpnI).

This fragment was ligated with the previous one after digestion with SpeI. This rescue construct was cloned in pGE-attB-GMR using SphI/KpnI to generate pGE-*barc*^{RescueA}.

Rescue B (*barc*^{RescueB})

The end of the first intron and the coding sequence of *barc* was cloned from pGE-*barc*^{RescueA} using 5'-GATCGCATGCTGGTGATTATTTGTTGTCCTGG-3' (SphI) and 5'-GATCACTAGTAGGGGTGGCGTCTCCTGGCAA-3' (SpeI).

A DNA fragment containing the coding sequence of GFP, a PreScission cleavage site, a TEV cleavage site, a Biotin acceptor tag (Schatz, 1993) and the SV40 3'UTR was amplified from a vector donated by the Brennecke Lab using:

5'-GATCACTAGTGGCGGGCGGCGTGAGCAAGGGCGA-3' (SpeI)
and 5'-GATCCGGTACCGGATCCAGACATGATAAGATAC-3' (KpnI).

These two fragments were ligated together after digestion with SpeI. This rescue construct was cloned in pGE-attB-GMR using SphI/KpnI to generate pGE-*barc*^{RescueB}.

Antibodies and immunohistochemistry

Antibodies used in this study are rabbit anti-Mira (1:100, (Betschinger et al., 2006)), rat anti-Mira (1:100), mouse anti-Pros (1:10, Developmental Studies Hybridoma Bank, University of Iowa [DSHB]), guinea pig anti-Ase (1:100, (Bhalerao et al., 2005)), guinea pig anti-Dpn (1:1000, gift from J. Skeath), mouse anti-PhosphoH3 (1:1000 Cell Signaling Technology), mouse anti-Ser2-phosphorylated CTD of Pol II (1:50 H5 monoclonal, Covance), rat anti-Elav (1:300 [DSHB]), mouse anti-Elav (1:100, Developmental Studies Hybridoma Bank, University of Iowa [DSHB]), mouse anti-FasIII (1:10, Developmental Studies Hybridoma Bank, University of Iowa [DSHB]), mouse anti-c-Myc (1:1000, Santa Cruz Bio- technology). Barc specific antisera were generated in rabbits (Neumuller et al., 2011) and guinea pigs (this study) against the C-terminal peptide: MKEEDVDSPENQLLPGDATP. Cortical actin was visualized using rhodamine Phalloidin (Molecular Probes) or Alexa 488 Phalloidin (Molecular Probes). Secondary antibodies were conjugated to Alexa 405, Alexa 488, Alexa 568 and Alexa 633 (Molecular Probes) or Cy5 (Jackson Immunofluorescence).

Larval brains were dissected in PBS and fixed in 5% PFA, 0,1% Triton-X100 in PBS for 20 minutes at room temperature. Embryos of the appropriate stage were collected and dechorionated using a standard protocol and fixed in 5% FA for 20 minutes at room temperature. Ovaries and testes were dissected in PBS and fixed in 4% FA, 0.2% Triton X-100 in PBS for 20 minutes at room temperature. Stainings of larval brains, ovaries and testes were

done following a standard protocol. Polytene stainings were done using third instar female larvae grown at 18°C. Preparation and staining of polytene chromosomes were done essentially as described in (Paro, 2008). All samples were mounted in Vectashield (with or without DAPI), and imaged using a ZEISS LSM confocal microscope.

dsRNA generation

eGFP: A DNA fragment of 495bp (base pairs 65 to 569 of the coding sequence of eGFP) flanked by T7 promoter sequences was generated using the following primers:

5'-TAATACGACTCACTATAGGGACGTAACGGCCACAAGTTC-3'

and 5'-TAATACGACTCACTATAGGGTGTCTGCTGGTAGTGGTTCG-3' (T7 promoter).

Barc_GD: A DNA fragment of 342bp (base pairs 173 to 514 of the coding sequence of *barricade*) flanked by T7 promoter sequences, was generated using the following primers:

5'-TAATACGACTCACTATAGGGCGGACAAAACGGACGAAACTCCA-3'

and 5'-TAATACGACTCACTATAGGGCCACACCGCAAACCCCTTCC-3' (T7 promoter).

This fragment corresponds to the one used to generate the VDRC TID25497.

Barricade SD: A DNA fragment of 491bp (base pairs 224 to 714 of the coding sequence of *barricade*) flanked by T7 promoter sequences, was generated using the following primers:

5'-TAATACGACTCACTATAGGGACATGACCTATGGAGCGGAC-3'

and 5'-TAATACGACTCACTATAGGGCTCCTCCTTTCTCTTGGCCT-3' (T7 promoter).

This fragment corresponded to the first prediction of the dsRNA design program SnapDragon when we designed it. SnapDragon: http://www.flyrnai.org/cgi-bin/RNAi_find_primers.pl. RNAi efficiency was tested by western blots, which were quantified using Image J.

S2 cells culture conditions

Drosophila S2 cells were cultured at 27°C in M3+BPYE media (Shields and Sang's M3 media, 0,25% bactopectone, 0,1% Yeast extract) supplemented with 10% heat-inactivated bovine serum (HBS).

RNAi in S2 cells

Cells were grown to a density of 3 to 5×10^6 cells/ml at 27°C in 75cm³ flasks. They were then centrifuged for 4 minutes at 400g and resuspended at $1,5 \times 10^6$ cells/ml in M3+BPYE media without serum. 5ml of cells were placed in a 75cm³ flask with the appropriate amount of dsRNA and incubated for 45 minutes at room temperature. 5ml of M3+BPYE media supplemented with 20% HBS was then added to each flask and cells were incubated at 27°C. After the appropriate amount of days, proteins were extracted with laemmli buffer using standard conditions and total RNAs were extracted using a standard Trizol extraction protocol.

Preparation of short capped RNA (shcRNA) libraries

Short-capped RNA libraries were prepared from 15 to 20µg of total RNA (10µl). Total RNAs were mixed with 10µl of formamide loading buffer, heated for 5 minutes at 65°C and separated on a 15% Urea-PAGE gel that had pre-run for 15-30 min in TBE at 200V. A ssRNA ladder and a miRNA ladder were used to estimate the size of RNAs. The gel was run at 200V for 1 hour and stained with ethidium bromide.

The portion of the gel containing RNAs ranging from 25 to 120 bases was cut and placed in a 0,5ml tube pierced several times with a 22-gauge needle and placed in a 2ml tube. Gel fragments were crushed by centrifugation for 2 minutes at maximum speed. 400µl of 300mM NaCl were added on the gel slurry and samples were incubated for 4 hours at room temperature on a rapidly rotating wheel. Samples were then transferred to a 0,22µm spin filter column and centrifuged for 2 minutes at 1000g. One microliter of glycoblu and 2,5 volumes of ethanol were added to the eluate and RNA was precipitated at -80°C for at least 30 minutes. After centrifugation for 30 minutes at maximum speed, pellets were washed with 70% ethanol and resuspended in 17µl of DEPC-treated water.

The 5' end of uncapped transcripts was dephosphorylated by adding 2µl of 10X buffer for 5' polyphosphatase, 1µl of 5' polyphosphatase enzyme and incubating reactions at 37°C for 30 minutes. Reactions were stopped by adding 80µl of phenol/chloroform/isoamyl alcohol and 80µl of DEPC-treated water, extracted with 60µl of chloroform and RNA in the water phase was precipitated for 30 minutes at -80°C after adding 1/10 volume of 5M NaCl, 1µl of glycoblu, and 2,5 volumes of ethanol. After pellet centrifugation and washing as described above, RNA was resuspended in 17µl of DEPC-treated water.

Uncapped transcripts were degraded by adding 2µl of 10x buffer for 5' Terminator exonuclease, 1µl of 5' Terminator nuclease and incubating the reaction at 30°C for 1 hour. Reactions were stopped with phenol/choloroform, extracted with chloroform and precipitated with ethanol as described above and resuspended in 6,4µl of DEPC-treated water.

3' adaptor ligation was done by adding 0,6µl of a 1/150 dilution of LLi3' adaptor (Stock solution: 1mM in TE pH 7,0), 1µl of RNase inhibitor, 1µl of 10x buffer for ssRNA ligase 1, 1µl of T4 ssRNA ligase 1 and incubating reactions for 6 hours at 20°C.

RNA fragments were prepared and separated on a 15% Urea-PAGE gel as described above. Gel fragments containing RNA molecules between 50 and 150 bases were cut and RNA was extracted from these fragments and precipitated as described above. RNA was resuspended in 17µl of DEPC-treated water.

Excess 3' adaptors were dephosphorylated by adding 2 µl of 10x Heat Labile Alkaline Phosphatase buffer, 1 µl of Heat Labile Alkaline Phosphatase and incubation at 37°C for 10 minutes. Reactions were stopped and RNA precipitated as described above. RNA was resuspended in 44µl of DEPC-treated water.

Decapping of RNA fragments was done by adding 5µl of 10x buffer for Tobacco Acid Pyrophosphatase, 1ul Tobacco Acid Pyrophosphatase and incubation at 37°C for 1,5 hours. Reactions were stopped and RNA precipitated as described above. RNA was resuspended in 5,7µl of DEPC-treated water.

5' adaptor ligation was done by adding 1,3µl of a 1/150 dilution of LLi5' adaptor (Stock solution: 1mM in TE pH 7,0), 1µl of RNase inhibitor, 1µl of 10x buffer for ssRNA ligase 1, 1µl of T4 ssRNA ligase 1 and incubating reactions for 6 hours at 20°C.

RNA fragments were prepared and separated on a 10% Urea-PAGE gel as described above. Gel fragments containing RNA molecules between 75 and 175 bases were cut and RNA was extracted from these fragments and precipitated as described above. RNA was resuspended in 4,5µl of DEPC-treated water.

Prior to performing the RT reaction, samples were mixed with 0.5 µl of GX1 primer, incubated at 65°C for 10 minutes and placed immediately on ice. Then, 4µl of RT mix (2 µl of

5xSSRT buffer, 1 µl of DTT, 0.5 µl of RNase inhibitor, 0.5 µl of 12.5mM dNTP mix) was added, samples were incubated at 3 minutes at 48°C and 1µl of SSRT II enzyme was added before incubation at 44°C for 1 hour.

PCR reaction was performed by adding 40 µl of PCR mix (10 µl of 5x Phusion PCR buffer HF, 0.5 µl of 25mM dNTP mix, 0.5 µl of GX1, 0.5 µl of GX2, 0.5 µl Phusion DNA polymerase) and using the following PCR program:

1 cycle of: 98°C – 30s

16-17 cycles of: 98°C - 12s; 60°C - 30s; 72°C – 15s

1 cycle of: 72°C – 10 min

DNA fragments were mixed with 6x DNA loading dye and separated on a 6% TBE gel, alongside 10µl of Gene Ruler 100bp DNA ladder. The gel was run in 1xTBE at 200V for 20-30 minutes. Gel fragments containing DNA molecules between 100 and 200 bp were cut and DNA was extracted from these fragments with 400µl of elution buffer supplemented with 50mM of NaCl at room temperature for 2 hours. The supernatant was filtered as described above and DNA was precipitated with 40µl of 3M NaAcetate, 1 µl of glycoblue and 1ml of ethanol. The DNA was immediately centrifuged for 30 minutes at maximum speed. Pellets were washed with 70% ethanol and resuspended in 100µl of elution buffer. DNA libraries were purified using Qiagen MinElute kit, eluted with 17µl of elution buffer and their concentration measured with Nanodrop spectrophotometer or Picogreen. These libraries will be sequenced using a HiSeq2000 or a GAllx machine and a standard protocol.

Primers and adapters for shcRNA libraries:

LLi3' 5'-/5Phos/rGrArUCGTCGGACTGTAGAACTCTGAACT/3InvdT/-3'

LLi5' 5'-ACAAGCAGAAGACGGCATArCrGrA-3'

GX1 5'-AATGATACGGCGACCACCGACAGGTTTCAGAGTTCTACAGTCCGA-3'

GX2 5'-CAAGCAGAAGACGGCATArCrGrA-3'

Preparation of messenger RNA libraries

mRNA libraries were prepared from 7 to 10µg of total RNA (5µl). Total RNAs were mixed with 20µl of DEPC-treated water, heated for 5 minutes at 65°C and immediately placed on ice. To remove rRNAs, total RNAs were purified using Dynabeads oligo(dT)25 beads as follow. Prior to purification, an aliquot of 50µl of Dynabeads oligo(dT)25 beads was washed twice with 50µl of binding buffer. Beads were pelleted using a magnet and resuspended is

25µl of binding buffer. Samples were incubated together with these beads for 5 minutes at room temperature. After discarding the supernatant, the beads were washed twice with 50µl of washing buffer, resuspended in 10µl of 10mM Tris-HCl and incubated 2 minutes at 80°C. After this incubation, the supernatant was immediately transferred to 40µl of binding buffer and the beads were discarded. mRNAs were purified a second time using another aliquot of 50µl of Dynabeads oligo(dT)25 beads as described above except that this time, the final supernatant was mixed with 30µl of DEPC-treated water and 10µl of 5x fragmentation buffer. Samples were then heated for 2,5 minutes at 94°C and mixed with 50µl of DEPC-treated water, 10µl NaAc, 1µl Glycoblue, 250µl of 100% EtOH and incubated overnight at -20°C. After centrifugation for 1 hour at maximum speed, pellets were washed with 70% ethanol and resuspended in 8µl of DEPC-treated water.

The first strand of cDNA was synthesized as follow. Samples were mixed with 1µl of random primers (3µg/µl) and 1µl of dNTP mix (10mM each) and heated for 5 minutes at 65°C. After chilling on ice, samples were mixed with 2µl of 10x RT buffer, 4µl 25mM MgCl₂, 2µl 0,1 M DTT, 1µl RNase OUT, 1µl of Superscript III and were incubated 10 minutes at 25°C, 50 minutes at 50°C and 5 minutes at 85°C. After chilling on ice, samples were mixed with 10µl DEPC-treated water, 3µl 4M NaCl, 90µl 100% EtOH and were incubated overnight at -20°C.

The second strand of cDNA was synthesized as follow. After centrifugation for 1 hour at maximum speed, pellets were washed twice with 70% ethanol and resuspended in 50µl of water. Samples were then mixed with 20µl 5x second strand buffer, 1µl random primers (3µg/µl), 0,2µl 100mM dATP, 0,2µl 100mM dCTP, 0,2µl 100mM dGTP, 0,2µl 100mM dUTP, 2,66µl DNA PolI, 0,66µl DNA ligase, 0,66µl RNase H and 24,22µl water. These samples were then incubated 2 hours at 16°C. cDNA libraries were purified using Qiagen MinElute kit and their concentration was measured with Nanodrop spectrophotometer or Picogreen. Adaptors compatible with Illumina paired-end sequencing were ligated following a standard protocol and these libraries will be sequenced using a HiSeq2000 or a GAIIx machine.

5.5. CONTRIBUTIONS

The genome-wide RNAi screen that identified *CG6049/barricade* and briefly described its RNAi phenotype was designed, conducted and analyzed by Ralph Neumueller, Constance Richter, Anja Fischer, Maria Novatchkova, Klaus Neumueller and Juergen Knoblich. Results from this screen were published as (Neumuller et al., 2011) and are publicly available at <http://neuroblasts.imba.oeaw.ac.at/>. All transgenic constructs were injected into fly embryos by Sara Farina-Lopez. The plasmid from which *barc* knock out homology arms were cloned was donated by Ralph Neumueller and Constance Richter. Generation of the *barc* knock out and screening of candidates was done with assistance from Peter Duchek. Southern blots presented in figure 24 were done by Elke Kleiner. The rest of this chapter was contributed by the author of this thesis.

6. REFERENCES

- Adelman, K., Wei, W., Ardehali, M. B., Werner, J., Zhu, B., Reinberg, D., and Lis, J. T. (2006). *Drosophila* Paf1 modulates chromatin structure at actively transcribed genes. *Mol Cell Biol* 26, 250-260.
- Albertson, R., and Doe, C. Q. (2003). Dlg, Scrib and Lgl regulate neuroblast cell size and mitotic spindle asymmetry. *Nat Cell Biol* 5, 166-170.
- Almeida, M. S., and Bray, S. J. (2005). Regulation of post-embryonic neuroblasts by *Drosophila* Grainyhead. *Mech Dev*
- Amleh, A., Nair, S. J., Sun, J., Sutherland, A., Hasty, P., and Li, R. (2009). Mouse cofactor of BRCA1 (Cobra1) is required for early embryogenesis. *PLoS One* 4, e5034.
- Andrulis, E. D., Guzman, E., Doring, P., Werner, J., and Lis, J. T. (2000). High-resolution localization of *Drosophila* Spt5 and Spt6 at heat shock genes in vivo: roles in promoter proximal pausing and transcription elongation. *Genes Dev* 14, 2635-2649.
- Ardehali, M. B., Yao, J., Adelman, K., Fuda, N. J., Petesch, S. J., Webb, W. W., and Lis, J. T. (2009). Spt6 enhances the elongation rate of RNA polymerase II in vivo. *EMBO J* 28, 1067-1077.
- Atwood, S. X., and Prehoda, K. E. (2009). aPKC Phosphorylates Miranda to Polarize Fate Determinants during Neuroblast Asymmetric Cell Division. *Curr Biol* 19, 723-729.
- Badenhorst, P., Finch, J. T., and Travers, A. A. (2002). Tramtrack co-operates to prevent inappropriate neural development in *Drosophila*. *Mech Dev* 117, 87-101.
- Bai, X., Kim, J., Yang, Z., Jurynek, M. J., Akie, T. E., Lee, J., LeBlanc, J., Sessa, A., Jiang, H., DiBiase, A., Zhou, Y., Grunwald, D. J., Lin, S., Cantor, A. B., Orkin, S. H., and Zon, L. I. (2010). TIF1gamma controls erythroid cell fate by regulating transcription elongation. *Cell* 142, 133-143.
- Basto, R., Brunk, K., Vinadogrova, T., Peel, N., Franz, A., Khodjakov, A., and Raff, J. W. (2008). Centrosome amplification can initiate tumorigenesis in flies. *Cell* 133, 1032-1042.
- Bayraktar, O. A., Boone, J. Q., Drummond, M. L., and Doe, C. Q. (2010). *Drosophila* type II neuroblast lineages keep Prospero levels low to generate large clones that contribute to the adult brain central complex. *Neural Dev* 5, 26.
- Bello, B., Reichert, H., and Hirth, F. (2006). The brain tumor gene negatively regulates neural progenitor cell proliferation in the larval central brain of *Drosophila*. *Development* 133, 2639-2648.
- Bello, B. C., Izergina, N., Caussinus, E., and Reichert, H. (2008). Amplification of neural stem cell proliferation by intermediate progenitor cells in *Drosophila* brain development. *Neural Dev* 3, 5.

Belotserkovskaya, R., Saunders, A., Lis, J. T., and Reinberg, D. (2004). Transcription through chromatin: understanding a complex FACT. *Biochim Biophys Acta* 1677, 87-99.

Bentley, D. L., and Groudine, M. (1986). A block to elongation is largely responsible for decreased transcription of c-myc in differentiated HL60 cells. *Nature* 321, 702-706.

Berdnik, D., and Knoblich, J. A. (2002). Drosophila Aurora-A is required for centrosome maturation and actin-dependent asymmetric protein localization during mitosis. *Curr Biol* 12, 640-647.

Berdnik, D., Torok, T., Gonzalez-Gaitan, M., and Knoblich, J. A. (2002). The endocytic protein alpha-Adaptin is required for numb-mediated asymmetric cell division in Drosophila. *Dev Cell* 3, 221-231.

Betschinger, J., Mechtler, K., and Knoblich, J. A. (2006). Asymmetric segregation of the tumor suppressor brat regulates self-renewal in Drosophila neural stem cells. *Cell* 124, 1241-1253.

Betschinger, J., Mechtler, K., and Knoblich, J. A. (2003). The Par complex directs asymmetric cell division by phosphorylating the cytoskeletal protein Lgl. *Nature* 422, 326-330.

Bhalerao, S., Berdnik, D., Torok, T., and Knoblich, J. A. (2005). Localization-dependent and -independent roles of numb contribute to cell-fate specification in Drosophila. *Curr Biol* 15, 1583-1590.

Boone, J. Q., and Doe, C. Q. (2008). Identification of Drosophila type II neuroblast lineages containing transit amplifying ganglion mother cells. *Dev Neurobiol* 68, 1185-1195.

Bowman, S. K., Neumuller, R. A., Novatchkova, M., Du, Q., and Knoblich, J. A. (2006). The Drosophila NuMA Homolog Mud Regulates Spindle Orientation in Asymmetric Cell Division. *Dev Cell* 10, 731-742.

Bowman, S. K., Rolland, V., Betschinger, J., Kinsey, K. A., Emery, G., and Knoblich, J. A. (2008). The tumor suppressors Brat and Numb regulate transit-amplifying neuroblast lineages in Drosophila. *Dev Cell* 14, 535-546.

Brand, A. H., and Perrimon, N. (1993). Targeted gene expression as a means of altering cell fates and generating dominant phenotypes. *Development* 118, 401-415.

Brand, M., Jarman, A. P., Jan, L. Y., and Jan, Y. N. (1993). asense is a Drosophila neural precursor gene and is capable of initiating sense organ formation. *Development* 119, 1-17.

Burge, C. B., Tuschl, T., and Sharp, P. A. (1999). 20 Splicing of Precursors to mRNAs by the Spliceosomes. *Cold Spring Harbor Monograph Archive; Volume 37 (1999): The RNA World, 2nd Ed.: The Nature of Modern RNA Suggests a Prebiotic RNA World*

Cabernard, C., and Doe, C. Q. (2009). Apical/basal spindle orientation is required for neuroblast homeostasis and neuronal differentiation in Drosophila. *Dev Cell* 17, 134-141.

Castellanos, E., Dominguez, P., and Gonzalez, C. (2008). Centrosome Dysfunction in *Drosophila* Neural Stem Cells Causes Tumors that Are Not due to Genome Instability. *Curr Biol* 18, 1209-1214.

Caussinus, E., and Gonzalez, C. (2005). Induction of tumor growth by altered stem-cell asymmetric division in *Drosophila melanogaster*. *Nat Genet* 37, 1125-1129.

Chen, Y., Yamaguchi, Y., Tsugeno, Y., Yamamoto, J., Yamada, T., Nakamura, M., Hisatake, K., and Handa, H. (2009). DSIF, the Paf1 complex, and Tat-SF1 have nonredundant, cooperative roles in RNA polymerase II elongation. *Genes Dev* 23, 2765-2777.

Chia, W., Somers, W. G., and Wang, H. (2008). *Drosophila* neuroblast asymmetric divisions: cell cycle regulators, asymmetric protein localization, and tumorigenesis. *J Cell Biol* 180, 267-272.

Chien, C. T., Wang, S., Rothenberg, M., Jan, L. Y., and Jan, Y. N. (1998). Numb-associated kinase interacts with the phosphotyrosine binding domain of Numb and antagonizes the function of Numb in vivo. *Mol Cell Biol* 18, 598-607.

Choksi, S. P., Southall, T. D., Bossing, T., Edoff, K., de Wit, E., Fischer, B. E., van Steensel, B., Micklem, G., and Brand, A. H. (2006). Prospero Acts as a Binary Switch between Self-Renewal and Differentiation in *Drosophila* Neural Stem Cells. *Dev Cell* 11, 775-789.

Core, L. J., Waterfall, J. J., and Lis, J. T. (2008). Nascent RNA sequencing reveals widespread pausing and divergent initiation at human promoters. *Science* 322, 1845-1848.

Crozat, A., Aman, P., Mandahl, N., and Ron, D. (1993). Fusion of CHOP to a novel RNA-binding protein in human myxoid liposarcoma. *Nature* 363, 640-644.

Delattre, O., Zucman, J., Plougastel, B., Desmaze, C., Melot, T., Peter, M., Kovar, H., Joubert, I., de Jong, P., Rouleau, G., and et, a. (1992). Gene fusion with an ETS DNA-binding domain caused by chromosome translocation in human tumours. *Nature* 359, 162-165.

Dietzl, G., Chen, D., Schnorrer, F., Su, K. C., Barinova, Y., Fellner, M., Gasser, B., Kinsey, K., Opel, S., Scheiblauer, S., Couto, A., Marra, V., Keleman, K., and Dickson, B. J. (2007). A genome-wide transgenic RNAi library for conditional gene inactivation in *Drosophila*. *Nature* 448, 151-156.

Doe, C. Q. (2008). Neural stem cells: balancing self-renewal with differentiation. *Development* 135, 1575-1587.

Doe, C. Q., Chu-LaGraff, Q., Wright, D. M., and Scott, M. P. (1991). The prospero gene specifies cell fates in the *Drosophila* central nervous system. *Cell* 65, 451-464.

Dominguez, M., and Campuzano, S. (1993). *asense*, a member of the *Drosophila* achaete-scute complex, is a proneural and neural differentiation gene. *EMBO J* 12, 2049-2060.

Dumstrei, K., Wang, F., and Hartenstein, V. (2003). Role of DE-Cadherin in Neuroblast Proliferation, Neural Morphogenesis, and Axon Tract Formation in *Drosophila* Larval Brain Development. *J Neurosci* 23, 3325-3335.

Ebens, A. J., Garren, H., Cheyette, B. N., and Zipursky, S. L. (1993). The *Drosophila* anachronism locus: a glycoprotein secreted by glia inhibits neuroblast proliferation. *Cell* 74, 15-27.

Egger, B., Boone, J. Q., Stevens, N. R., Brand, A. H., and Doe, C. Q. (2007). Regulation of spindle orientation and neural stem cell fate in the *Drosophila* optic lobe. *Neural Dev* 2, 1.

Fong, Y. W., and Zhou, Q. (2001). Stimulatory effect of splicing factors on transcriptional elongation. *Nature* 414, 929-933.

Frank, D. J., Edgar, B. A., and Roth, M. B. (2002). The *Drosophila melanogaster* gene brain tumor negatively regulates cell growth and ribosomal RNA synthesis. *Development* 129, 399-407.

Furriols, M., and Bray, S. (2001). A model Notch response element detects Suppressor of Hairless-dependent molecular switch. *Curr Biol* 11, 60-64.

Gallagher, C. M., and Knoblich, J. A. (2006). The conserved c2 domain protein lethal (2) giant discs regulates protein trafficking in *Drosophila*. *Dev Cell* 11, 641-653.

Gateff, E. (1994). Tumor suppressor and overgrowth suppressor genes of *Drosophila melanogaster*: developmental aspects. *Int J Dev Biol* 38, 565-590.

Gilchrist, D. A., Dos Santos, G., Fargo, D. C., Xie, B., Gao, Y., Li, L., and Adelman, K. (2010). Pausing of RNA polymerase II disrupts DNA-specified nucleosome organization to enable precise gene regulation. *Cell* 143, 540-551.

Gilmour, D. S., and Lis, J. T. (1986). RNA polymerase II interacts with the promoter region of the noninduced hsp70 gene in *Drosophila melanogaster* cells. *Mol Cell Biol* 6, 3984-3989.

Goldstein, B., and Macara, I. G. (2007). The par proteins: fundamental players in animal cell polarization. *Dev Cell* 13, 609-622.

Guo, M., Jan, L. Y., and Jan, Y. N. (1996). Control of daughter cell fates during asymmetric division: interaction of Numb and Notch. *Neuron* 17, 27-41.

Haley, B., Hendrix, D., Trang, V., and Levine, M. (2008). A simplified miRNA-based gene silencing method for *Drosophila melanogaster*. *Dev Biol* 321, 482-490.

Heitzler, P., Bourouis, M., Ruel, L., Carteret, C., and Simpson, P. (1996). Genes of the Enhancer of split and achaete-scute complexes are required for a regulatory loop between Notch and Delta during lateral signalling in *Drosophila*. *Development* 122, 161-171.

Hirata, J., Nakagoshi, H., Nabeshima, Y., and Matsuzaki, F. (1995). Asymmetric segregation of the homeodomain protein Prospero during *Drosophila* development. *Nature* 377, 627-630.

Huang, J., Zhou, W., Dong, W., Watson, A. M., and Hong, Y. (2009). From the Cover: Directed, efficient, and versatile modifications of the *Drosophila* genome by genomic engineering. *Proc Natl Acad Sci U S A* *106*, 8284-8289.

Ikeshima-Kataoka, H., Skeath, J. B., Nabeshima, Y., Doe, C. Q., and Matsuzaki, F. (1997). Miranda directs Prospero to a daughter cell during *Drosophila* asymmetric divisions. *Nature* *390*, 625-629.

Ito, K., Awano, W., Suzuki, K., Hiromi, Y., and Yamamoto, D. (1997). The *Drosophila* mushroom body is a quadruple structure of clonal units each of which contains a virtually identical set of neurones and glial cells. *Development* *124*, 761-771.

Ito, K., and Hotta, Y. (1992). Proliferation pattern of postembryonic neuroblasts in the brain of *Drosophila melanogaster*. *Dev Biol* *149*, 134-148.

Izergina, N., Balmer, J., Bello, B., and Reichert, H. (2009). Postembryonic development of transit amplifying neuroblast lineages in the *Drosophila* brain. *Neural Dev* *4*, 44.

Izumi, Y., Ohta, N., Hisata, K., Raabe, T., and Matsuzaki, F. (2006). *Drosophila* Pins-binding protein Mud regulates spindle-polarity coupling and centrosome organization. *Nat Cell Biol* *8*, 586-593.

Jaekel, R., and Klein, T. (2006). The *Drosophila* Notch Inhibitor and Tumor Suppressor Gene lethal (2) giant discs Encodes a Conserved Regulator of Endosomal Trafficking. *Dev Cell* *11*, 655-669.

Jarman, A. P., Brand, M., Jan, L. Y., and Jan, Y. N. (1993). The regulation and function of the helix-loop-helix gene, *asense*, in *Drosophila* neural precursors. *Development* *119*, 19-29.

Kao, S. Y., Calman, A. F., Luciw, P. A., and Peterlin, B. M. (1987). Anti-termination of transcription within the long terminal repeat of HIV-1 by *tat* gene product. *Nature* *330*, 489-493.

Kaplan, C. D., Morris, J. R., Wu, C., and Winston, F. (2000). Spt5 and spt6 are associated with active transcription and have characteristics of general elongation factors in *D. melanogaster*. *Genes Dev* *14*, 2623-2634.

Kielkopf, C. L., Lucke, S., and Green, M. R. (2004). U2AF homology motifs: protein recognition in the RRM world. *Genes Dev* *18*, 1513-1526.

Kim, J. B., Yamaguchi, Y., Wada, T., Handa, H., and Sharp, P. A. (1999). Tat-SF1 protein associates with RAP30 and human SPT5 proteins. *Mol Cell Biol* *19*, 5960-5968.

Kitajima, A., Fuse, N., Isshiki, T., and Matsuzaki, F. (2010). Progenitor properties of symmetrically dividing *Drosophila* neuroblasts during embryonic and larval development. *Dev Biol* *347*, 9-23.

Knoblich, J. A., Jan, L. Y., and Jan, Y. N. (1995). Asymmetric segregation of Numb and Prospero during cell division. *Nature* 377, 624-627.

Knoblich, J. A. (2008). Mechanisms of asymmetric stem cell division. *Cell* 132, 583-597.

Knoblich, J. A. (2010). Asymmetric cell division: recent developments and their implications for tumour biology. *Nat Rev Mol Cell Biol* 11, 849-860.

Kraut, R., Chia, W., Jan, L. Y., Jan, Y. N., and Knoblich, J. A. (1996). Role of inscuteable in orienting asymmetric cell divisions in *Drosophila*. *Nature* 383, 50-55.

Krumm, A., Meulia, T., Brunvand, M., and Groudine, M. (1992). The block to transcriptional elongation within the human c-myc gene is determined in the promoter-proximal region. *Genes Dev* 6, 2201-2213.

Kulkarni, M. M., Booker, M., Silver, S. J., Friedman, A., Hong, P., Perrimon, N., and Mathey-Prevot, B. (2006). Evidence of off-target effects associated with long dsRNAs in *Drosophila melanogaster* cell-based assays. *Nat Methods* 3, 833-838.

Ladanyi, M. (1995). The emerging molecular genetics of sarcoma translocations. *Diagn Mol Pathol* 4, 162-173.

Lai, Z. C., Harrison, S. D., Karim, F., Li, Y., and Rubin, G. M. (1996). Loss of tramtrack gene activity results in ectopic R7 cell formation, even in a sina mutant background. *Proc Natl Acad Sci U S A* 93, 5025-5030.

Lee, C., Li, X., Hechmer, A., Eisen, M., Biggin, M. D., Venters, B. J., Jiang, C., Li, J., Pugh, B. F., and Gilmour, D. S. (2008). NELF and GAGA factor are linked to promoter-proximal pausing at many genes in *Drosophila*. *Mol Cell Biol* 28, 3290-3300.

Lee, C. Y., Andersen, R. O., Cabernard, C., Manning, L., Tran, K. D., Lanskey, M. J., Bashirullah, A., and Doe, C. Q. (2006a). *Drosophila* Aurora-A kinase inhibits neuroblast self-renewal by regulating aPKC/Numb cortical polarity and spindle orientation. *Genes Dev* 20, 3464-3474.

Lee, C. Y., Robinson, K. J., and Doe, C. Q. (2006b). Lgl, Pins and aPKC regulate neuroblast self-renewal versus differentiation. *Nature* 439, 594-598.

Lee, C. Y., Wilkinson, B. D., Siegrist, S. E., Wharton, R. P., and Doe, C. Q. (2006c). Brat Is a Miranda Cargo Protein that Promotes Neuronal Differentiation and Inhibits Neuroblast Self-Renewal. *Dev Cell* 10, 441-449.

Lee, T., Lee, A., and Luo, L. (1999). Development of the *Drosophila* mushroom bodies: sequential generation of three distinct types of neurons from a neuroblast. *Development* 126, 4065-4076.

Lee, T., and Luo, L. (1999). Mosaic analysis with a repressible cell marker for studies of gene function in neuronal morphogenesis. *Neuron* 22, 451-461.

- Levine, M. (2011). Paused RNA Polymerase II as a Developmental Checkpoint. *Cell* 145, 502-511.
- Li, L., and Vaessin, H. (2000). Pan-neural Prospero terminates cell proliferation during *Drosophila* neurogenesis. *Genes Dev* 14, 147-151.
- Li, X. Y., and Green, M. R. (1998). The HIV-1 Tat cellular coactivator Tat-SF1 is a general transcription elongation factor. *Genes Dev* 12, 2992-2996.
- Lu, B., Rothenberg, M., Jan, L. Y., and Jan, Y. N. (1998). Partner of Numb colocalizes with Numb during mitosis and directs Numb asymmetric localization in *Drosophila* neural and muscle progenitors. *Cell* 95, 225-235.
- Mancebo, H. S., Lee, G., Flygare, J., Tomassini, J., Luu, P., Zhu, Y., Peng, J., Blau, C., Hazuda, D., Price, D., and Flores, O. (1997). P-TEFb kinase is required for HIV Tat transcriptional activation in vivo and in vitro. *Genes Dev* 11, 2633-2644.
- Maris, C., Dominguez, C., and Allain, F. H. (2005). The RNA recognition motif, a plastic RNA-binding platform to regulate post-transcriptional gene expression. *FEBS J* 272, 2118-2131.
- Matsuzaki, F., Ohshiro, T., Ikeshima-Kataoka, H., and Izumi, H. (1998). *miranda* localizes *staufer* and *prospero* asymmetrically in mitotic neuroblasts and epithelial cells in early *Drosophila* embryogenesis. *Development* 125, 4089-4098.
- Miller, H. B., Robinson, T. J., Gordan, R., Hartemink, A. J., and Garcia-Blanco, M. A. (2011). Identification of Tat-SF1 cellular targets by exon array analysis reveals dual roles in transcription and splicing. *RNA*
- Miller, H. B., Saunders, K. O., Tomaras, G. D., and Garcia-Blanco, M. A. (2009). Tat-SF1 is not required for Tat transactivation but does regulate the relative levels of unspliced and spliced HIV-1 RNAs. *PLoS One* 4, e5710.
- Muse, G. W., Gilchrist, D. A., Nechaev, S., Shah, R., Parker, J. S., Grissom, S. F., Zeitlinger, J., and Adelman, K. (2007). RNA polymerase is poised for activation across the genome. *Nat Genet* 39, 1507-1511.
- Nechaev, S., and Adelman, K. (2010). Pol II waiting in the starting gates: Regulating the transition from transcription initiation into productive elongation. *Biochim Biophys Acta*
- Nechaev, S., Fargo, D. C., dos Santos, G., Liu, L., Gao, Y., and Adelman, K. (2010). Global analysis of short RNAs reveals widespread promoter-proximal stalling and arrest of Pol II in *Drosophila*. *Science* 327, 335-338.
- Neumuller, R. A., Betschinger, J., Fischer, A., Bushati, N., Poernbacher, I., Mechtler, K., Cohen, S. M., and Knoblich, J. A. (2008). *Mei-P26* regulates microRNAs and cell growth in the *Drosophila* ovarian stem cell lineage. *Nature* 454, 241-245.

- Neumuller, R. A., and Knoblich, J. A. (2009). Dividing cellular asymmetry: asymmetric cell division and its implications for stem cells and cancer. *Genes Dev* 23, 2675-2699.
- Neumuller, R. A., Richter, C., Fischer, A., Novatchkova, M., Neumuller, K. G., and Knoblich, J. A. (2011). Genome-Wide Analysis of Self-Renewal in *Drosophila* Neural Stem Cells by Transgenic RNAi. *Cell Stem Cell* 8, 580-593.
- Oellers, N., Dehio, M., and Knust, E. (1994). bHLH proteins encoded by the Enhancer of split complex of *Drosophila* negatively interfere with transcriptional activation mediated by proneural genes. *Mol Gen Genet* 244, 465-473.
- Ohno, S. (2001). Intercellular junctions and cellular polarity: the PAR-aPKC complex, a conserved core cassette playing fundamental roles in cell polarity. *Curr Opin Cell Biol* 13, 641-648.
- Ohshiro, T., Yagami, T., Zhang, C., and Matsuzaki, F. (2000). Role of cortical tumour-suppressor proteins in asymmetric division of *Drosophila* neuroblast. *Nature* 408, 593-596.
- Ott, M., Geyer, M., and Zhou, Q. (2011). The Control of HIV Transcription: Keeping RNA Polymerase II on Track. *Cell Host Microbe* 10, 426-435.
- Page, S. L., McKim, K. S., Deneen, B., Van Hook, T. L., and Hawley, R. S. (2000). Genetic studies of mei-P26 reveal a link between the processes that control germ cell proliferation in both sexes and those that control meiotic exchange in *Drosophila*. *Genetics* 155, 1757-1772.
- Papoulas, O., Beek, S. J., Moseley, S. L., McCallum, C. M., Sarte, M., Shearn, A., and Tamkun, J. W. (1998). The *Drosophila* trithorax group proteins BRM, ASH1 and ASH2 are subunits of distinct protein complexes. *Development* 125, 3955-3966.
- Parmentier, M. L., Woods, D., Greig, S., Phan, P. G., Radovic, A., Bryant, P., and O'Kane, C. J. (2000). Rapsynoid/Partner of Inscuteable Controls Asymmetric Division of Larval Neuroblasts in *Drosophila*. *J Neurosci (Online)* 20, RC84.
- Paro, R. (2008). Mapping protein distributions on polytene chromosomes by immunostaining. *CSH Protoc* 2008, pdb.prot4714.
- Peng, C. Y., Manning, L., Albertson, R., and Doe, C. Q. (2000). The tumour-suppressor genes *lgl* and *dlg* regulate basal protein targeting in *Drosophila* neuroblasts. *Nature* 408, 596-600.
- Pereanu, W., and Hartenstein, V. (2006). Neural lineages of the *Drosophila* brain: a three-dimensional digital atlas of the pattern of lineage location and projection at the late larval stage. *J Neurosci* 26, 5534-5553.
- Petronczki, M., and Knoblich, J. A. (2001). DmPAR-6 directs epithelial polarity and asymmetric cell division of neuroblasts in *Drosophila*. *Nat Cell Biol* 3, 43-49.
- Rabbitts, T. H. (1994). Chromosomal translocations in human cancer. *Nature* 372, 143-149.

Rabbitts, T. H., Forster, A., Larson, R., and Nathan, P. (1993). Fusion of the dominant negative transcription regulator CHOP with a novel gene FUS by translocation t(12;16) in malignant liposarcoma. *Nat Genet* 4, 175-180.

Radonjic, M., Andrau, J. C., Lijnzaad, P., Kemmeren, P., Kockelkorn, T. T., van Leenen, D., van Berkum, N. L., and Holstege, F. C. (2005). Genome-wide analyses reveal RNA polymerase II located upstream of genes poised for rapid response upon *S. cerevisiae* stationary phase exit. *Mol Cell* 18, 171-183.

Rahl, P. B., Lin, C. Y., Seila, A. C., Flynn, R. A., McCuine, S., Burge, C. B., Sharp, P. A., and Young, R. A. (2010). c-Myc regulates transcriptional pause release. *Cell* 141, 432-445.

Rasmussen, E. B., and Lis, J. T. (1993). In vivo transcriptional pausing and cap formation on three *Drosophila* heat shock genes. *Proc Natl Acad Sci U S A* 90, 7923-7927.

Reis, T., and Edgar, B. A. (2004). Negative regulation of dE2F1 by cyclin-dependent kinases controls cell cycle timing. *Cell* 117, 253-264.

Reisman, D., Glaros, S., and Thompson, E. A. (2009). The SWI/SNF complex and cancer. *Oncogene* 28, 1653-1668.

Reya, T., Morrison, S. J., Clarke, M. F., and Weissman, I. L. (2001). Stem cells, cancer, and cancer stem cells. *Nature* 414, 105-111.

Rhyu, M. S., Jan, L. Y., and Jan, Y. N. (1994). Asymmetric distribution of numb protein during division of the sensory organ precursor cell confers distinct fates to daughter cells. *Cell* 76, 477-491.

Rodriguez, A., Zhou, Z., Tang, M. L., Meller, S., Chen, J., Bellen, H., and Kimbrell, D. A. (1996). Identification of immune system and response genes, and novel mutations causing melanotic tumor formation in *Drosophila melanogaster*. *Genetics* 143, 929-940.

Rolls, M. M., Albertson, R., Shih, H. P., Lee, C. Y., and Doe, C. Q. (2003). *Drosophila* aPKC regulates cell polarity and cell proliferation in neuroblasts and epithelia. *J Cell Biol* 163, 1089-1098.

Rong, Y. S., and Golic, K. G. (2000). Gene targeting by homologous recombination in *Drosophila*. *Science* 288, 2013-2018.

Rossi, F., and Gonzalez, C. (2011). Synergism between altered cortical polarity and the PI3K/TOR pathway in the suppression of tumour growth. *EMBO Rep*

Rougvie, A. E., and Lis, J. T. (1988). The RNA polymerase II molecule at the 5' end of the uninduced hsp70 gene of *D. melanogaster* is transcriptionally engaged. *Cell* 54, 795-804.

Santolini, E., Puri, C., Salcini, A. E., Gagliani, M. C., Pelicci, P. G., Tacchetti, C., and Di Fiore, P. P. (2000). Numb is an endocytic protein. *J Cell Biol* 151, 1345-1352.

Schaefer, M., Shevchenko, A., Shevchenko, A., and Knoblich, J. A. (2000). A protein complex containing Inscuteable and the Galpha-binding protein Pins orients asymmetric cell divisions in *Drosophila*. *Curr Biol* 10, 353-362.

Schaefer, M., Petronczki, M., Dorner, D., Forte, M., and Knoblich, J. A. (2001). Heterotrimeric G proteins direct two modes of asymmetric cell division in the *Drosophila* nervous system. *Cell* 107, 183-194.

Schatz, P. J. (1993). Use of peptide libraries to map the substrate specificity of a peptide-modifying enzyme: a 13 residue consensus peptide specifies biotinylation in *Escherichia coli*. *Biotechnology (N Y)* 11, 1138-1143.

Schober, M., Schaefer, M., and Knoblich, J. A. (1999). Bazooka recruits Inscuteable to orient asymmetric cell divisions in *Drosophila* neuroblasts. *Nature* 402, 548-551.

Schuldt, A. J., Adams, J. H. J., Davidson, C. M., Micklem, D. R., Haseloff, J., Johnston, D. S., and Brand, A. H. (1998). Miranda mediates asymmetric protein and RNA localization in the developing nervous system. *Genes Dev* 12, 1847-1857.

Schwabish, M. A., and Struhl, K. (2007). The Swi/Snf complex is important for histone eviction during transcriptional activation and RNA polymerase II elongation in vivo. *Mol Cell Biol* 27, 6987-6995.

Shen, C. P., Jan, L. Y., and Jan, Y. N. (1997). Miranda is required for the asymmetric localization of Prospero during mitosis in *Drosophila*. *Cell* 90, 449-458.

Siller, K. H., Cabernard, C., and Doe, C. Q. (2006). The NuMA-related Mud protein binds Pins and regulates spindle orientation in *Drosophila* neuroblasts. *Nat Cell Biol* 8, 594-600.

Slack, F. J., and Ruvkun, G. (1998). A novel repeat domain that is often associated with RING finger and B-box motifs. *Trends Biochem Sci* 23, 474-475.

Smith, M. J., Kulkarni, S., and Pawson, T. (2004). FF domains of CA150 bind transcription and splicing factors through multiple weak interactions. *Mol Cell Biol* 24, 9274-9285.

Sonoda, J., and Wharton, R. P. (2001). *Drosophila* Brain Tumor is a translational repressor. *Genes Dev* 15, 762-773.

Sorensen, P. H., Lessnick, S. L., Lopez-Terrada, D., Liu, X. F., Triche, T. J., and Denny, C. T. (1994). A second Ewing's sarcoma translocation, t(21;22), fuses the EWS gene to another ETS-family transcription factor, ERG. *Nat Genet* 6, 146-151.

Sotillos, S., Diaz-Meco, M. T., Caminero, E., Moscat, J., and Campuzano, S. (2004). DaPKC-dependent phosphorylation of Crumbs is required for epithelial cell polarity in *Drosophila*. *J Cell Biol* 166, 549-557.

Sousa-Nunes, R., Chia, W., and Somers, W. G. (2009). Protein phosphatase 4 mediates localization of the Miranda complex during *Drosophila* neuroblast asymmetric divisions. *Genes Dev* 23, 359-372.

Southall, T. D., and Brand, A. H. (2009). Neural stem cell transcriptional networks highlight genes essential for nervous system development. *EMBO J*

Spana, E. P., and Doe, C. Q. (1995). The prospero transcription factor is asymmetrically localized to the cell cortex during neuroblast mitosis in *Drosophila*. *Development* 121, 3187-3195.

Spana, E. P., Kopczynski, C., Goodman, C. S., and Doe, C. Q. (1995). Asymmetric localization of numb autonomously determines sibling neuron identity in the *Drosophila* CNS. *Development* 121, 3489-3494.

Sprang, S. R. (1997). G protein mechanisms: insights from structural analysis. *Annu Rev Biochem* 66, 639-678.

Strobl, L. J., and Eick, D. (1992). Hold back of RNA polymerase II at the transcription start site mediates down-regulation of c-myc in vivo. *EMBO J* 11, 3307-3314.

Suzuki, A., and Ohno, S. (2006). The PAR-aPKC system: lessons in polarity. *J Cell Sci* 119, 979-987.

Truman, J. W., and Bate, M. (1988). Spatial and temporal patterns of neurogenesis in the central nervous system of *Drosophila melanogaster*. *Dev Biol* 125, 145-157.

Wallace, K., Liu, T. H., and Vaessin, H. (2000). The pan-neural bHLH proteins DEADPAN and ASENSE regulate mitotic activity and cdk inhibitor dacapo expression in the *Drosophila* larval optic lobes. *Genesis* 26, 77-85.

Wang, H., Ouyang, Y., Somers, W. G., Chia, W., and Lu, B. (2007). Polo inhibits progenitor self-renewal and regulates Numb asymmetry by phosphorylating Pon. *Nature* 449, 96-100.

Wang, H., Somers, G. W., Bashirullah, A., Heberlein, U., Yu, F., and Chia, W. (2006). Aurora-A acts as a tumor suppressor and regulates self-renewal of *Drosophila* neuroblasts. *Genes Dev* 20, 3453-3463.

Wang, X., Hang, S., Prazak, L., and Gergen, J. P. (2010). NELF potentiates gene transcription in the *Drosophila* embryo. *PLoS One* 5, e11498.

Wei, P., Garber, M. E., Fang, S. M., Fischer, W. H., and Jones, K. A. (1998). A novel CDK9-associated C-type cyclin interacts directly with HIV-1 Tat and mediates its high-affinity, loop-specific binding to TAR RNA. *Cell* 92, 451-462.

Weigmann, K., and Lehner, C. F. (1995). Cell fate specification by even-skipped expression in the *Drosophila* nervous system is coupled to cell cycle progression. *Development* 121, 3713-3721.

- Weng, M., Golden, K. L., and Lee, C. Y. (2010). dFezf/Earmuff maintains the restricted developmental potential of intermediate neural progenitors in *Drosophila*. *Dev Cell* *18*, 126-135.
- Wheeler, S. R., Carrico, M. L., Wilson, B. A., Brown, S. J., and Skeath, J. B. (2003). The expression and function of the achaete-scute genes in *Tribolium castaneum* reveals conservation and variation in neural pattern formation and cell fate specification. *Development* *130*, 4373-4381.
- Will, C. L., and Luhrmann, R. (2011). Spliceosome structure and function. *Cold Spring Harb Perspect Biol* *3*,
- Wilson, A., and Radtke, F. (2006). Multiple functions of Notch signaling in self-renewing organs and cancer. *FEBS Lett* *580*, 2860-2868.
- Wirtz-Peitz, F., Nishimura, T., and Knoblich, J. A. (2008). Linking cell cycle to asymmetric division: Aurora-A phosphorylates the Par complex to regulate Numb localization. *Cell* *135*, 161-173.
- Wodarz, A., Ramrath, A., Grimm, A., and Knust, E. (2000). *Drosophila* atypical protein kinase C associates with Bazooka and controls polarity of epithelia and neuroblasts. *J Cell Biol* *150*, 1361-1374.
- Wodarz, A., Ramrath, A., Kuchinke, U., and Knust, E. (1999). Bazooka provides an apical cue for Inscuteable localization in *Drosophila* neuroblasts. *Nature* *402*, 544-547.
- Woodhouse, E., Hersperger, E., and Shearn, A. (1998). Growth, metastasis, and invasiveness of *Drosophila* tumors caused by mutations in specific tumor suppressor genes. *Dev Genes Evol* *207*, 542-550.
- Wu, P. S., Egger, B., and Brand, A. H. (2008). Asymmetric stem cell division: Lessons from *Drosophila*. *Semin Cell Dev Biol*
- Yan, D., Perriman, R., Igel, H., Howe, K. J., Neville, M., and Ares, M. J. (1998). CUS2, a yeast homolog of human Tat-SF1, rescues function of misfolded U2 through an unusual RNA recognition motif. *Mol Cell Biol* *18*, 5000-5009.
- Yoo, A. S., and Crabtree, G. R. (2009). ATP-dependent chromatin remodeling in neural development. *Curr Opin Neurobiol* *19*, 120-126.
- Zeitlinger, J., Stark, A., Kellis, M., Hong, J. W., Nechaev, S., Adelman, K., Levine, M., and Young, R. A. (2007). RNA polymerase stalling at developmental control genes in the *Drosophila melanogaster* embryo. *Nat Genet* *39*, 1512-1516.
- Zhou, Q., Chen, D., Pierstorff, E., and Luo, K. (1998). Transcription elongation factor P-TEFb mediates Tat activation of HIV-1 transcription at multiple stages. *EMBO J* *17*, 3681-3691.

- Zhou, Q., and Sharp, P. A. (1996). Tat-SF1: cofactor for stimulation of transcriptional elongation by HIV-1 Tat. *Science* 274, 605-610.
- Zhou, Q., and Yik, J. H. (2006). The Yin and Yang of P-TEFb regulation: implications for human immunodeficiency virus gene expression and global control of cell growth and differentiation. *Microbiol Mol Biol Rev* 70, 646-659.
- Zhu, B., Mandal, S. S., Pham, A. D., Zheng, Y., Erdjument-Bromage, H., Batra, S. K., Tempst, P., and Reinberg, D. (2005). The human PAF complex coordinates transcription with events downstream of RNA synthesis. *Genes Dev* 19, 1668-1673.
- Zhu, S., Barshow, S., Wildonger, J., Jan, L. Y., and Jan, Y. N. (2011). Ets transcription factor Pointed promotes the generation of intermediate neural progenitors in *Drosophila* larval brains. *Proc Natl Acad Sci U S A* 108, 20615-20620.
- Zhu, S., Lin, S., Kao, C. F., Awasaki, T., Chiang, A. S., and Lee, T. (2006). Gradients of the *Drosophila* Chinmo BTB-Zinc Finger Protein Govern Neuronal Temporal Identity. *Cell* 127, 409-422.
- Zhu, Y., Pe'ery, T., Peng, J., Ramanathan, Y., Marshall, N., Marshall, T., Amendt, B., Mathews, M. B., and Price, D. H. (1997). Transcription elongation factor P-TEFb is required for HIV-1 tat transactivation in vitro. *Genes Dev* 11, 2622-2632.

7. CURRICULUM VITAE

Vivien ROLLAND

Born 25th of October 1984
in Strasbourg, FRANCE
Nationality: French

Address: IMBA GmbH, Dr. Bohrgasse 3, 1030 Vienna, AUSTRIA
Phone: +43 1 79044 4824
email: Vivien.rolland@imba.oeaw.ac.at

ACADEMIC EDUCATION & RESEARCH EXPERIENCES

- Sept. 2007-present Pre-doctoral student in the laboratory of Dr. Juergen Knoblich
Institute of Molecular Biotechnology (IMBA GmbH), Vienna, Austria
- June 2007 Master of Sciences, "Cellular & Molecular Biology, Oncology"
University Claude Bernard Lyon 1 (UCBL1), France.
- Sept. 2006-June 2007 Master thesis in the laboratory of Pr. Dr. Bénédicte Durand
Molecular and Cellular Genetic Center, UCBL1, France.
Title: Contribution to the study of dRFX target genes in Drosophila.
- June-Aug. 2006 Summer research project in the laboratory of Dr. Barry Dickson
Institute of Molecular Pathology - IMP, Austria.
Topic: Taste behaviour of Drosophila.
- Feb.-Mar. 2006 Practical work in the laboratory of Pr. Dr. Bénédicte Durand
Molecular and Cellular Genetic Center, UCBL1, France.
Topic: Ciliogenesis and signaling in Drosophila.
- June 2005 Bachelor of Sciences, "Genetics & developmental biology".
University of Ottawa, Canada & University Claude Bernard Lyon 1, France
- June-Jul. 2005 Summer practical work in the laboratory of Pr. Dr. Micheline
Paulin-Levasseur, University of Ottawa, Canada.
Topic: Laminar proteins in cell culture.
- June 2002 Scientific Baccalauréat, specialty: Biology.
Lycée Jean-Moulin, France.

SCIENTIFIC PUBLICATIONS

- 2008 Bowman SK, Rolland V, Betschinger J, Kinsey KA, Emery G and Knoblich JA. The
Tumor Suppressors Brat and Numb Regulate Transit-Amplifying Neuroblast
Lineages in *Drosophila*. *Developmental Cell*. 2008; 14(4): 535-46
- 2007 Laurençon A, Dubruille R, Efimenko E, Grenier G, Bissett R, Cortier E, Rolland V,
Swoboda P, Durand B. Identification of novel regulatory factor X (RFX) target genes
by comparative genomics in *Drosophila* species. *Genome Biology*. 2007;8(9):R195.

AWARDS

- 2011 Poster prize at the “EuroSystem 3rd annual Consortium meeting”, Czech Republic.
- 2006-2007 “Bourse du Ministère de l’Enseignement Supérieur sur critères universitaires”
fellowship given to the best Master students.

SCIENTIFIC TALKS

- 2011 Title: *Role of Barricade in the regulation of Drosophila stem cells.*
EuroSystem 3rd annual Consortium meeting, Czech Republic.
- Title: *Role of Barricade in the regulation of Drosophila stem cells.*
VBC Friday seminar, Austria.
- 2008 Title: *Asymmetric cell division and cell fate in the Drosophila peripheral nervous system*
VBC Monday seminar, Austria.

SCIENTIFIC POSTERS

- 2011 Title: *Role of barricade in the regulation of Drosophila stem cells.*
EuroSystem 3rd annual Consortium meeting, Czech Republic.
- Title: *Role of barricade in the regulation of Drosophila stem cells.*
3rd EMBO Meeting, Austria.
- Title: *Regulation of lineage progression in Drosophila stem cells.*
IMP-IMBA Annual recess, Austria.

VOLUNTEERING RESPONSABILITIES

- 2008-2009 IMBA PhD representative.
- 2009 Organizing member of the “2009 Vienna Biocenter PhD retreat” & the “1st Vienna Biocenter Career Day”.
- Host of a scientific station at the IMBA Sponsoring event “Come, See, Meet” & at the 2009 “European Researchers’ Night”.
- 2008 Organizing member of the “Vienna Biocenter PhD Symposium on Synthetic Biology”.
- Host of a scientific station at the IMBA Sponsoring event “Come, See, Meet” & at the “Long Night of Research”.

8. ACKNOWLEDGMENTS

My PhD would have been so different without the many people that supported me through these few years!...

First of all, thank you very much Juergen, for allowing me to work in your lab, for mentoring me and for always being enthusiastic about discussing science, politics and many other things. Many thanks also to Carrie and Barry, for supervision during my PhD and for interesting discussions. Big thanks, and much appreciation to Karen, Sergei, Ginger and the rest of the Adelman lab, for welcoming me in North Carolina and for being so open and generous with me!

I would also like to thank all members of the Knoblich lab, past and present, for creating a very nice atmosphere to work in! A bunch of talented and knowledgeable people! It is very difficult to thank individual people since everyone brought something to my experience in the lab. However, I would like to give a special "thank you" to Spyros, Ilka, Pedro, Federico, Ryan, Christian, Madeline, Nina, Christoph and Onur for good laughs, friday flyroom discussions, intense table soccer matches and great support! And also for digging me out of the snow after I broke my back!...

Thanks a lot to Sarah as well, for making the beginning of my PhD such a pleasant, intense and exciting experience. Thanks a lot also to Ralph, Constance and Anja for laying out the foundations of the *barc* project and for sharing reagents and ideas. Finally, many thanks to Elke, Sara and Peter, for organizing the lab, patiently injecting lots of transgenic constructs and carrying out exciting fly work.

Of course, the support I received extends far beyond lab walls. I would like to have a few words for people that are or were really close to me during these intense years:

Maman & Papa, pour toujours avoir répondu présent, chacun à votre manière!

Martin, pour être un frère fantastique! Ne change pas!

Jade, pour m'avoir aidé à trier des mouches à défaut d'éléphants!

Et tous les autres membres de ma famille pour de formidables bulles d'air! Merci!

Lisa, for having shared my life during most of my PhD. We went separate ways, but it was a great experience.

And last but not least, Ana, Maja, Bob, Daniel, Jean-Yves, Gerald and Greg, for being such great friends, for a lot of fun, sometimes tough discussions, but INCREDIBLE support! I am so glad you guys are in my life!

And to anyone who read up to here!